

**DOKUZ EYLÜL UNIVERSITY
GRADUATE SCHOOL OF NATURAL AND APPLIED
SCIENCES**

**INVESTIGATION OF THE GEOTHERMAL
SOURCES IN ÇEŞME AND URLA BY USING
REMOTE SENSING AND GEOGRAPHICAL
INFORMATION SYSTEMS TECHNIQUES**

by

Ezgi ELVEREN

May, 2013

İZMİR

**INVESTIGATION OF THE GEOTHERMAL
SOURCES IN ÇEŞME AND URLA BY USING
REMOTE SENSING AND GEOGRAPHICAL
INFORMATION SYSTEMS TECHNIQUES**

**A Thesis Submitted to the
Graduate School of Natural and Applied Sciences of Dokuz Eylül University in
Partial Fulfillment of the Requirements for the Degree of Master of Science in
Geographical Information Systems, Geographical Information Systems
Program**

by

Ezgi ELVEREN

May, 2013

İZMİR

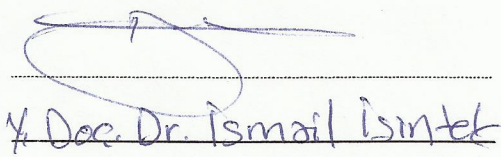
M.Sc THESIS EXAMINATION RESULT FORM

We have read the thesis entitled “**INVESTIGATION OF THE GEOTHERMAL SOURCES IN ÇEŞME AND URLA BY USING REMOTE SENSING AND GEOGRAPHICAL INFORMATION SYSTEMS TECHNIQUES**” completed by **EZGİ ELVEREN** under supervision of **Prof. Dr. GÜLTEKİN TARCAN** and we certify that in our opinion it is fully adequate, in scope and in quality, as a thesis for the degree of Master of Science.

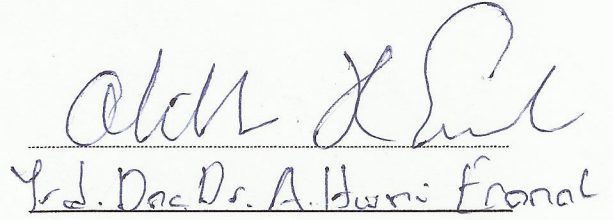
Prof. Dr. GÜLTEKİN TARCAN



Supervisor



(Jury Member)



(Jury Member)



Prof. Dr. Ayşe OKUR

Director

Graduate School of Natural and Applied Sciences

ACKNOWLEDGEMENTS

I would like to thank my supervisor, Prof. Dr. Gültekin TARCAN and Assist. Prof. Dr. A. Hüsnü ERONAT for their invaluable support and guidance.

I am also grateful to my dear friend, Research Assistant Nur Sinem ÖZCAN for the help and motivation she provided.

Finally, I am obliged to express my gratitude to my whole family, especially to my aunt, Teaching Assistant Ferda ŞAHİNBAŞ BEYDİLLİ for their love, patience, help and support throughout this study.

Ezgi ELVEREN

INVESTIGATION OF THE GEOTHERMAL SOURCES IN ÇEŞME AND URLA BY USING REMOTE SENSING AND GEOGRAPHICAL INFORMATION SYSTEMS TECHNIQUES

ABSTRACT

The concept of energy and the sustainability of energy sources has been one of the world's most important issues. Rapid depletion of energy resources, unconscious use of non-renewable resources like oil, coal, nuclear power and environmental and atmospheric pollution resulted from these sources have led people to use renewable energy sources. Many studies and projects have been carried out in order to meet the world's energy needs. The geothermal energy is the most important renewable energy source and can be used in countless areas such as power generation, medicine, tourism, agriculture and industry. There are lots of benefits of geothermal energy resources. The most important benefits are that it is a renewable source, it is easy to detect and produce, it is cheap, it provides return on investment in a very short time and it damages the environment very little.

In this study, the methods of defining the geothermal energy sources by remote sensing and geographical information systems have been analysed.

Keywords: Geothermal resource, geothermal energy, geographical information systems, remote sensing

ÇEŞME VE URLA'DAKİ JEOTERMAL KAYNAKLARIN UZAKTAN ALGILAMA VE COĞRAFI BİLGİ SİSTEMLERİ TEKNİKLERİ KULLANILARAK İNCELENMESİ

ÖZ

Enerji kavramı ve enerji kaynaklarının sürdürülebilirliği geçmişten bugüne dünyanın en önemli konularından ve sorunlarından biri olmuştur. Enerji kaynaklarının hızla tükenmesi, petrol, kömür, nükleer enerji gibi kendini yenileme durumu olmayan kaynakların bilinçsizce kullanılması, bu kaynakların çevreye ve atmosfere verdiği kirlilik gibi etkenler insanları yenilenebilir enerji kaynaklarını kullanmaya yönlendirmiştir. Dünyanın enerji ihtiyacını karşılamak amacıyla bir çok çalışma ve proje yürütülmektedir. Yenilenebilir enerji kaynaklarının en önemlilerinden olan jeotermal enerji ise günümüzde elektrik üretimi, tıp, turizm, ziraat, endüstri gibi sayısız alanda kullanılabilen bir kaynaktır. Jeotermal enerji kaynaklarının nice faydası bulunmakla birlikte, bunların başlıcaları daha önce belirtildiği gibi yenilenebilir olması yani doğru kullanımla tükenmesi zor bir enerji çeşidi olması, tespit ve üretiminin kolay olması, maliyetinin düşük olması, yatırımın çok kısa bir zamanda geri dönüş sağlaması, ayrıca diğer kaynaklara göre çevreye verilen zararın çok az olmasıdır.

Bu çalışmada jeotermal enerji kaynaklarının uzaktan algılama ve coğrafi bilgi sistemleri teknikleriyle belirleme yöntemleri incelenmiştir.

Anahtar sözcükler: Jeotermal kaynak, jeotermal enerji, coğrafi bilgi sistemleri, uzaktan algılama

CONTENTS

	Page
M. Sc. THESIS EXAMINATION RESULT FORM	ii
ACKNOWLEDGEMENTS	iii
ABSTRACT	iv
ÖZ	v
LIST OF FIGURES	ix
LIST OF TABLES	xiii
CHAPTER ONE – INTRODUCTION	1
1.1 Study Area	1
1.2 Data	1
CHAPTER TWO - GEOTHERMAL ENERGY	3
2.1 Geothermal Source; Definiton and Classification	3
2.2 Geothermal Systems and Classification	4
2.2.1 Vapor Dominated Systems	5
2.2.2 Hot Water System	6
2.2.3 Geopressed Systems	8
2.2.4 Hot Dry Rock Systems	8
2.2.5 Magma Systems	9
2.3 Usage Areas Of Geothermal Energy	9
2.4 Usage Of Geothermal Energy In The World	11
2.5 Usage Of Geothermal Energy In Turkey	16
CHAPTER THREE - GEOGRAPHICAL INFORMATION SYSTEMS AND REMOTE SENSING	23
3.1 Geographical Information Systems	23
3.1.1 The Basis Components Of GIS	23

3.2 Remote Sensing	25
3.2.1 Electromagnetic Spectrum	25
3.2.2 Remote Sensing Operations	27
3.2.3 Characteristics Of Remote Sensing Images	28
3.2.3.1 Pixel	29
3.2.3.2 Swath	30
3.2.3.3 Bands	30
3.2.3.4 Resolution	31
3.2.4 Types Of Images	33
3.2.5 Remote Sensing Systems	34
3.2.6 Satellites	35
3.2.6.1 Landsat	39
3.2.6.2 Terra Aster	40
3.2.6.3 Spot	41
3.2.6.4 Ikonos	41
3.2.7 Image Processing	43
3.2.7.1 Image Restoration	44
3.2.7.1.1 Radiometric Restoration	44
3.2.7.1.1 Geometric Restoration	46
3.2.7.2 Image Enhancement	46
3.2.7.3 Image Classification	48
3.2.7.4 Image Transformation	49
3.2.8 Usage Areas Of Remote Sensing	50
3.2.9 Remote Sensing In Turkey	50
CHAPTER FOUR – APPLICATIONS.....	55
4.1 Georeferencing	55
4.2 Remote Sensing Applications	57
4.2.1 Filtering	57
4.2.2 Digital Elevation Model	68
4.2.3 Classification	70

4.2.4 Principal Components Analysis	73
4.2.5 Band Ratioing	79
4.2.6 Determination of The Thermal Anomalies	84
CHAPTER FIVE – CONCLUSIONS	87
REFERENCES	89
APPENDICES	93
APPENDIX-1	93
APPENDIX-2	94
APPENDIX-3	95

LIST OF FIGURES

	Page
Figure 1.1 Location map of the study area (Google Earth)	2
Figure 1.2 Geological map of the study area (MTA)	3
Figure 1.3 Active fault map of the study area (MTA)	3
Figure 2.1 Geothermal system and it's components (anonymus)	5
Figure 2.2 Conceptual model of a vapor dominated system (Gupta,2006)	7
Figure 2.3 Conceptual model of a hot water system (Gupta,2006)	8
Figure 2.4 Conceptual model of a geopressed system (anonymus)	9
Figure 2.5 The Lindal diagram that shows the usage of geothermal energy	11
Figure 2.6 Plate boundaries and geothermal activity around the world (anonymus)	12
Figure 2.7 Map of geothermal resources and volcanic areas (MTA)	17
Figure 2.8 Distribution of geothermal resources (MTA)	18
Figure 2.9 Application of geothermal resources map (MTA)	19
Figure 3.1 Electromagnetic spectrum (NASA)	26
Figure 3.2 Electric and magnetic field and their motion (NASA)	26
Figure 3.3 Wavelength and frequency (NASA)	27
Figure 3.4 Remote sensing operations (İşlem GIS) A) Energy source and lightning B) Emission and atmosphere C) Prevention of earth's surface D) Sensor records the energy E) Assessment and analysis F,G) Application	28
Figure 3.5 Image structure (İşlem GIS)	29
Figure 3.6 Pixel structure (İşlem GIS)	29
Figure 3.7 Swath (İşlem GIS)	30
Figure 3.8 Bands (İşlem GIS)	30
Figure 3.9 Spatial resolution (anonymus)	31
Figure 3.10 Image of one band and image of three bands (İşlem GIS)	32
Figure 3.11 Radiometric resolution (İşlem GIS)	32
Figure 3.12 Panchromatic and multispectral images (İşlem GIS)	34
Figure 3.13 Working principle of passive sensors (İşlem GIS)	35
Figure 3.14 Working principle of active sensors (İşlem GIS)	35
Figure 3.15 Technical specificications of earth observing satellites (Nik System)...	36

Figure 3.16 Technical specifications of earth observing satellites (Nik System)....	37
Figure 3.17 Technical specifications of earth observing satellites (Nik System)....	38
Figure 3.18 Band striping error image and image after correction (IDRISI Manual)	
.....	44
Figure 3.19 Landsat TM Band 1 images before and after haze removal (IDRISI Manual)	
.....	45
Figure 3.20 TM Band 3 (visible red) and its histogram and after contrast stretching values between 12 and 60 (IDRISI Manual)	
.....	47
Figure 3.21 Several composites made with different band combinations from the same set of TM images (IDRISI Manual)	
.....	47
Figure 3.22 Panchromatic merge using Quickbird imagery-multispectral at 2.4 m, panchromatic at 0.6 m. Raw image is on the left and image on right is after the merge (IDRISI Manual)	
.....	47
Figure 3.23 Unsupervised classification image of Pensacola,FL (anonymus)	48
Figure 3.24 Supervised classification image of Pensacola,FL (anonymus)	49
Figure 3.25 Bilsat satellite (TUBITAK UZAY)	51
Figure 3.26 İstanbul, Turkey image recorded by Bilsat (TUBITAK UZAY)	51
Figure 3.27 Çoban and Gezgin (TUBITAK UZAY)	52
Figure 3.28 Rasat (TUBITAK UZAY)	53
Figure 3.29 Göktürk-2 (TUBITAK UZAY)	54
Figure 4.1 The attribute tables of formations and faults created with MapInfo	55
Figure 4.2 The geological map and active fault map of the study area after georeferencing process	56
Figure 4.3 Band 8 of Landsat 7	58
Figure 4.4 Band 8 after filtering with 3x3 kernel of high-pass filter	58
Figure 4.5 A closer look to possible fault zone	59
Figure 4.6 Actual fault overlapping the possible fault line	59
Figure 4.7 Band 8 after filtering with 7x7 kernel of Laplacian filter	61
Figure 4.8 A closer look to possible fault zone and the edge of the area	61
Figure 4.9 Actual fault overlapping the possible fault line	62
Figure 4.10 Southwest directional filter and overlapping fault	63
Figure 4.11 Southeast directional filter and overlapping fault	64

Figure 4.12 Northeast directional filter and overlapping fault	65
Figure 4.13 Northwest directional filter and overlapping fault	66
Figure 4.14 Digital Elevation Model (DEM) of the study area	67
Figure 4.15 Possible fault lines	68
Figure 4.16 Actual fault zones	68
Figure 4.17 Formation boundaries	69
Figure 4.18 Earthquake epicenters recorded between 01.01.1950 – 23.03.2013 and the square box shows the concentration of the earthquakes	69
Figure 4.19 Earthquake epicenters and actual fault lines	70
Figure 4.20 Minimum distance classification of Çeşme and Urla	71
Figure 4.21 Maximum likelihood classification of Çeşme and Urla	71
Figure 4.22 Parallelepiped classification of Çeşme and Urla	72
Figure 4.23 Linear discriminant analysis (Fisher) classification of Çeşme and Urla	72
Figure 4.24 The image created with the combinaton 2-3-1(RGB) after PCA analysis	74
Figure 4.25 The image created with the combinaton 1-2-3(RGB) after PCA analysis	74
Figure 4.26 The image created with the combinaton 3-2-1(RGB) after PCA analysis	75
Figure 4.27 The image created with the combinaton 3-7-4(RGB) after PCA analysis	75
Figure 4.28 The image created with the combinaton 4-3-7(RGB) after PCA analysis	76
Figure 4.29 The image created with the combinaton 2-3-4(RGB) after PCA analysis	76
Figure 4.30 The image created with the combinaton 7-4-2(RGB) after PCA analysis	77
Figure 4.31 The image created with the combinaton 4-3-2(RGB) after PCA analysis	77
Figure 4.32 The image created with the combinaton 7-1-4(RGB) after PCA analysis	78

Figure 4.33 The image created with the combinaton 7-3-4(RGB) after PCA analysis	78
Figure 4.34 Ratio image obtained using band ratio 5/7	80
Figure 4.35 Ratio image obtained using band ratio 5/4	80
Figure 4.36 Ratio image obtained using band ratio 4/3	81
Figure 4.37 Ratio image obtained using band ratio 2/3	81
Figure 4.38 Ratio image obtained using band ratio 4/5	82
Figure 4.39 Ratio image obtained using band ratio 3/1	82
Figure 4.40 RGB image combination of respectively (5/7), (5/4), (3/1)	83
Figure 4.41 RGB image combination of respectively (5/7), (3/1), (4/3)	83
Figure 4.42 RGB image combination of respectively (5/7), (2/3), (4/5)	84
Figure 4.43 Blackbody temperature map of the study area and the active faults, square box shows the region with high temperature	86

LIST OF TABLES

	Page
Table 2.1 Countries using geothermal energy in electricity generation and installed power capacity (Dokuzuncu Beş Yıllık Kalkınma Planı Madencilik Özel İhtisas Komisyonu Raporu, 2009)	13
Table 2.2 Direct usage of geothermal energy in the world (Dokuzuncu Beş Yıllık Kalkınma Planı Madencilik Özel İhtisas Komisyonu Raporu, 2009)	15
Table 2.3 Geothermal electricity generation projections (Dokuzuncu Beş Yıllık Kalkınma Planı Madencilik Özel İhtisas Komisyonu Raporu, 2009)	20
Table 2.5 The employment projection of geothermal applications(electricity+direct use) in 2013 (Dokuzuncu Beş Yıllık Kalkınma Planı Madencilik Özel İhtisas Komisyonu Raporu, 2009)	22
Table 3.1 Technical specification of Landsat sensors	39
Table 3.2 Technical specification of Landsat sensors	40
Table 3.3 Technical specification of Aster sensor	41
Table 3.4 Technical specification of Spot sensors	42
Table 3.5 Technical specification of Spot sensors	43
Table 3.6 Technical specification of Bilsat (TUBITAK UZAY)	51
Table 3.7 Technical specification of Rasat	53
Table 3.8 Technical specification of Göktürk-2	54
Table 4.1 Band ratios that used for RGB combinations	79
Table 4.2 Radiance values of the thermal bands that used in the study	85
Table 4.3 Emissivities of various common materials (Lillesand and Keifer, 1994)...85	85

CHAPTER ONE

INTRODUCTION

Today, the current resources directed the users to renewable and clean energy sources because of their environmental damages. Geothermal energy is at the beginning of the renewable energy sources. In our country, geothermal energy is used in many areas like electricity generation or heating and new geothermal resource exploration studies are being carried out. Geothermal resource explorations are carried out by various techniques like drilling and geophysical studies. The most inexpensive and hassle-free technique is exploration with aerial photographs and satellite images. At this stage, geographical information systems and remote sensing techniques are engaged. Remote sensing is used for obtaining the aerial photographs and satellite images. Geographical information systems allows processing the images for different purposes and obtaining meaningful data.

1.1 Study Area

The study area is the area between Çeşme And Urla district boundaries from İzmir province (Figure 1.1).

Çeşme district lies to the west of İzmir province. It is surrounded on the east by Urla, on the north by Karaburun, on the west and the south by The Aegean Sea. It has an altitude of 5 m. above sea level and a surface area of 260 km².

Urla district lies to the west of the city of İzmir. It is surrounded on the east by Güzelbahçe and Seferihisar, on the west by Çeşme, on the north-west by Karaburun, on the north and the south by The Aegean Sea. It has an altitude of 50 m. above sea level and a surface area of 728 km².

1.2 Data

For the study, geological map, geothermal resources map, digital elevation model (DEM), earthquake data and satellite images of the study area are used. Geological map and geothermal resources map were obtained from the Maden Tetkik ve Arama internet database. Satellite images of Landsat 7 were obtained from Global Land Cover Facility website. ASTER global digital elevation model (DEM) of the study

area was obtained from USGS website. Earthquake data was retrieved from AFAD Earthquake Department database in their website.

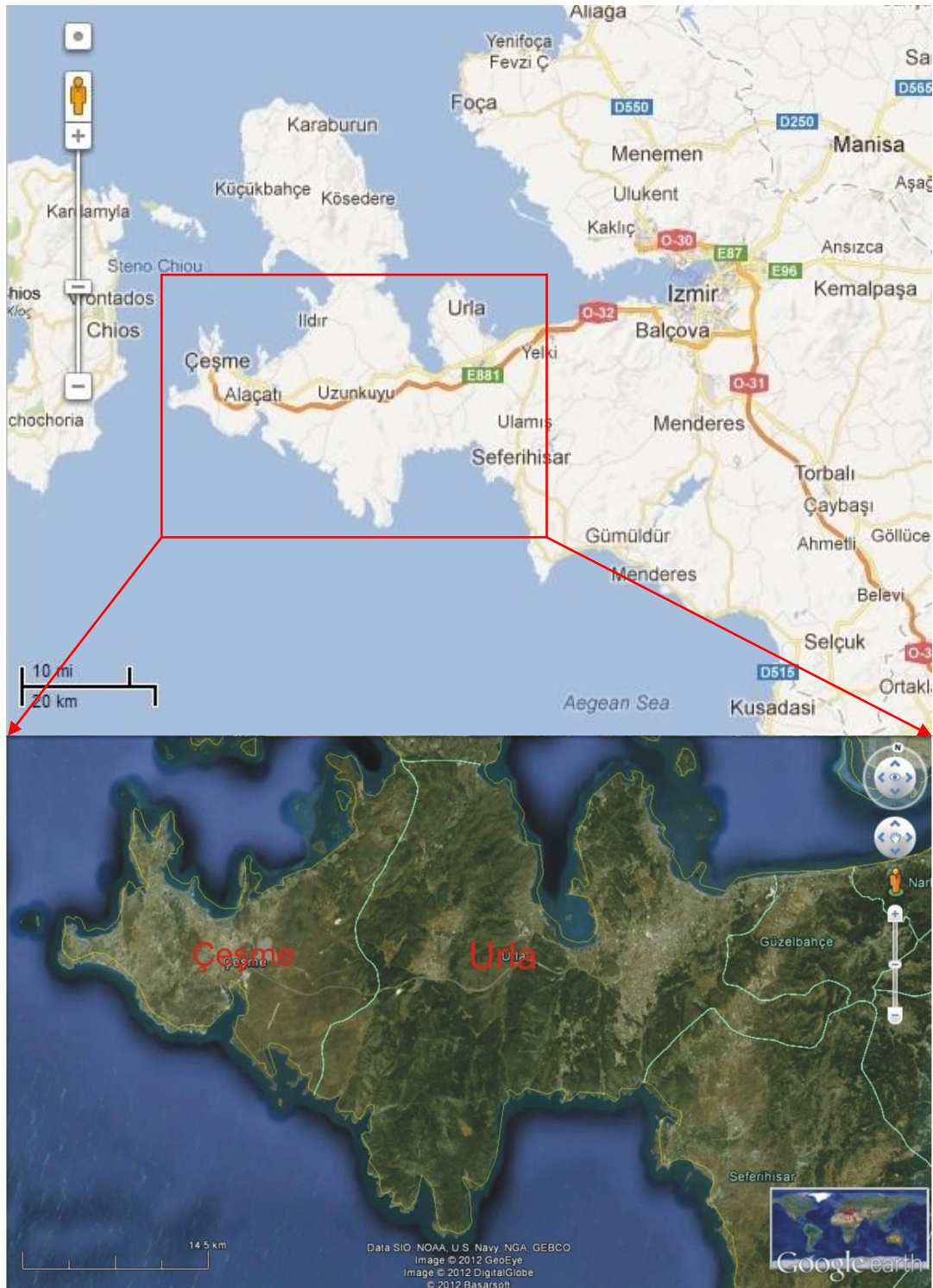


Figure 1.1 Location map of the study area (Google Earth)

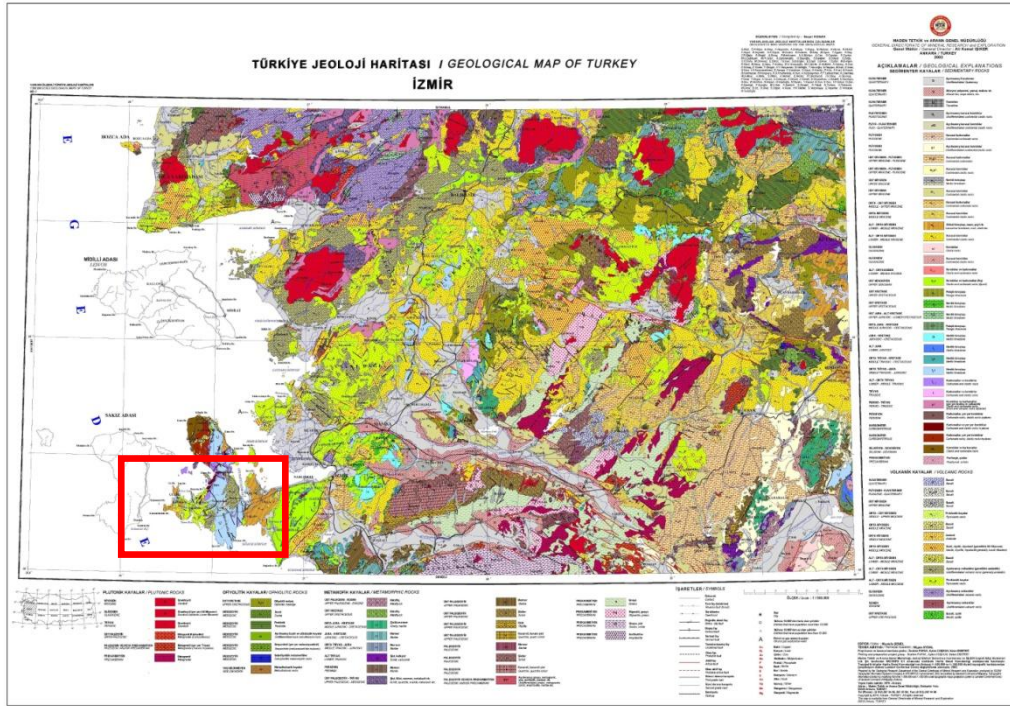


Figure 1.2 Geological map of the study area (MTA)

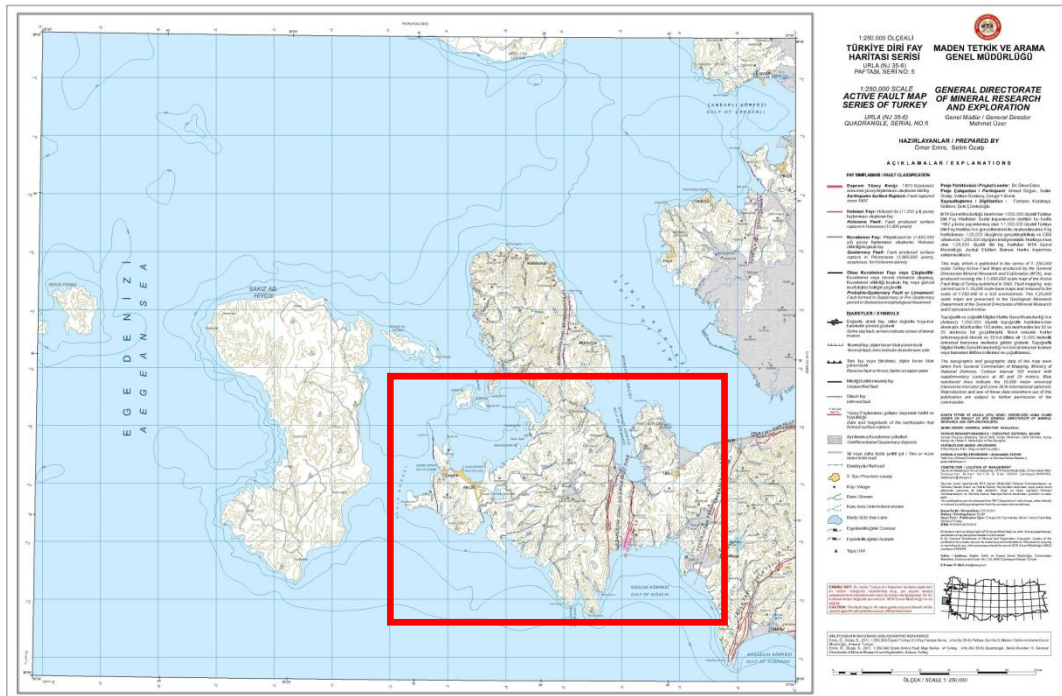


Figure 1.3 Active fault map of the study area (MTA)

CHAPTER TWO

GEOHERMAL ENERGY

2.1 Geothermal Source; Definiton and Classification

The adjective 'geothermal' originates from the Greek roots γη (ge), meaning earth and θερμος (thermos), meaning hot, so it means the 'heat of the earth'.

Geothermal source is defined as; hot water and steam that include molten minerals, various salts and gases formed by the heat accumulated in the earth's crust at various depths and temperatures above the regional average temperature of atmosphere and surface (Sekizinci Beş Yıllık Kalkınma Planı Madencilik Özel İhtisas Komisyonu Raporu, 2001).

Geothermal resources are divided into three groups according to their temperatures (Sekizinci Beş Yıllık Kalkınma Planı Madencilik Özel İhtisas Komisyonu Raporu, 2001);

- Low-temperature areas (20-70°C)
- Medium-temperature areas (70-150°C)
- High-temperature areas (Higher than 150°C)

Low and medium-temperature areas are used in building and greenhouse heating, agricultural work, industrial areas, drying food, lumbering, paper and textile industry, leather trade, the refrigeration of plants, the production of boric acid, ammonium bicarbonate, heavy water and the extraction of dry ice from CO₂ in the fluid. Moreover, technologies have been devised for producing electricity from the fluids obtained from middle and high-temperature fields.

2.2 Geothermal Systems and Classification

Geothermal systems consist of three main elements; heat source, reservoir rock and fluid carrying the heat (Figure 2.1).

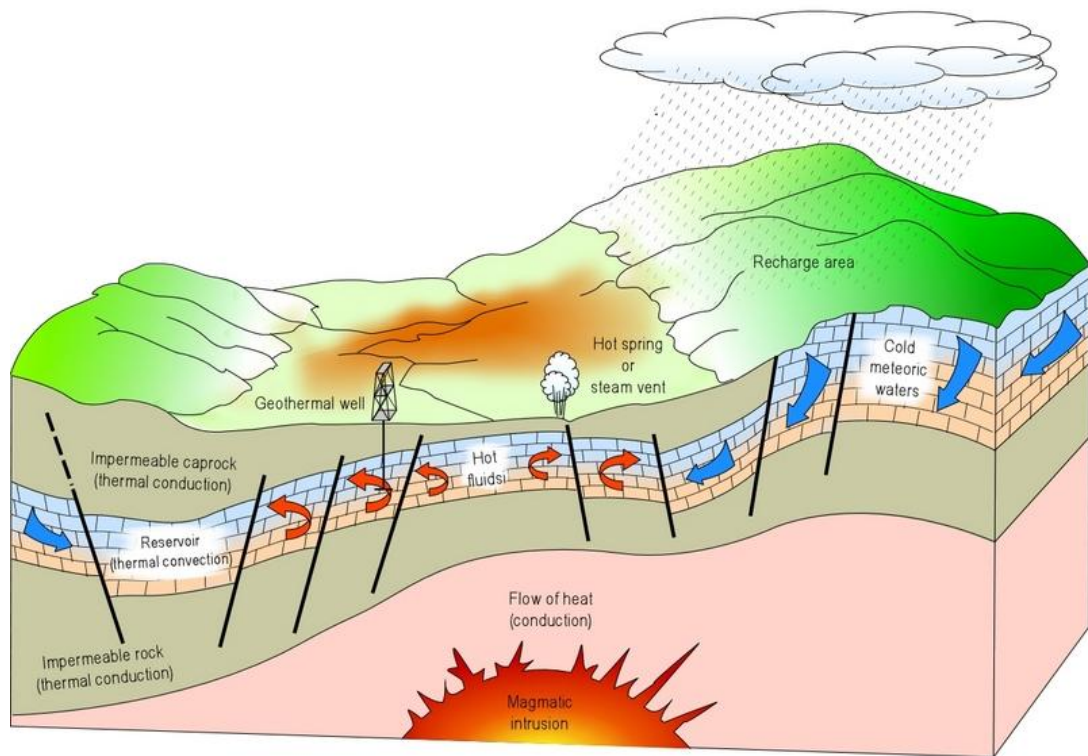


Figure 2.1 Geothermal system and it's components (anonymus)

Magmatic intrusions reaching close to the surface (5-10 km.) with temperatures higher than 600°C or the geothermal gradient increasing 2.5-3°C every 100 m. can create the heat source.

Fluid carrying the heat consists of meteoric water which contains several chemical substances and gases (CO₂, H₂S) and is usually in liquid or steam form depending on the reservoir temperature and pressure.

Reservoir is the fractured and permeable rock that fluid carrying heat moves in. Generally there are impermeable rocks above the reservoir rock.

Operating mechanism of geothermal system can be described as; meteoric water accumulates in the fractured and permeable reservoir rock and be heated by the heat source and expands. Expanded hot water moves through the fractures of the rocks.

Geothermal systems can be divided into five groups according to the conditions in which fluid and reservoir and the heat source come together conditions (Gupta, 2006).

- Vapor dominated systems
- Hot water systems
- Geopressured systems
- Hot dry rock systems
- Magma systems

2.2.1 Vapor Dominated Systems

Most of the presently used geothermal fields contain water at high pressures, and temperatures in excess of 100°C. When this water is brought to the Earth's surface, the pressure is considerably reduced, generating large quantities of steam, and a mixture of saturated steam and water is produced. The ratio of steam to water varies from one site to another (Figure 2.2). Some of the best-known geothermal fields, such as Cerro Prieto (Mexico), Wairakei (New Zealand), Reykjavik (Iceland), Salton Sea (U.S.A.) and Otake (Japan), belong to this category. There are a few other important geothermal fields such as Larderello (Italy) and The Geysers (U.S.A.) which produce superheated steam with no associated fluids (Gupta, 2006).

2.2.2 Hot Water Systems

The geology of hot water geothermal fields is quite similar to that of an ordinary groundwater system. In hot water geothermal fields, water-convection currents carry the heat from the deep source to the shallow reservoir. They differ from the earlier discussed vapor-dominated geothermal fields in the fact that the hot water geothermal fields are characterized by liquid water being the continuous pressure-controlling fluid phase. Typically, the temperature of hot-water reservoirs varies from 60°C to 100°C and they occur at depths ranging from 1500 to 3000 m. (Figure 2.3). Some of the best-known hot water system geothermal fields are; Salton Sea

(U.S.A.), Cerro Prieto (Mexico), Wairakei (New Zealand) and Yellowstone Park (U.S.A.) (Gupta, 2006).

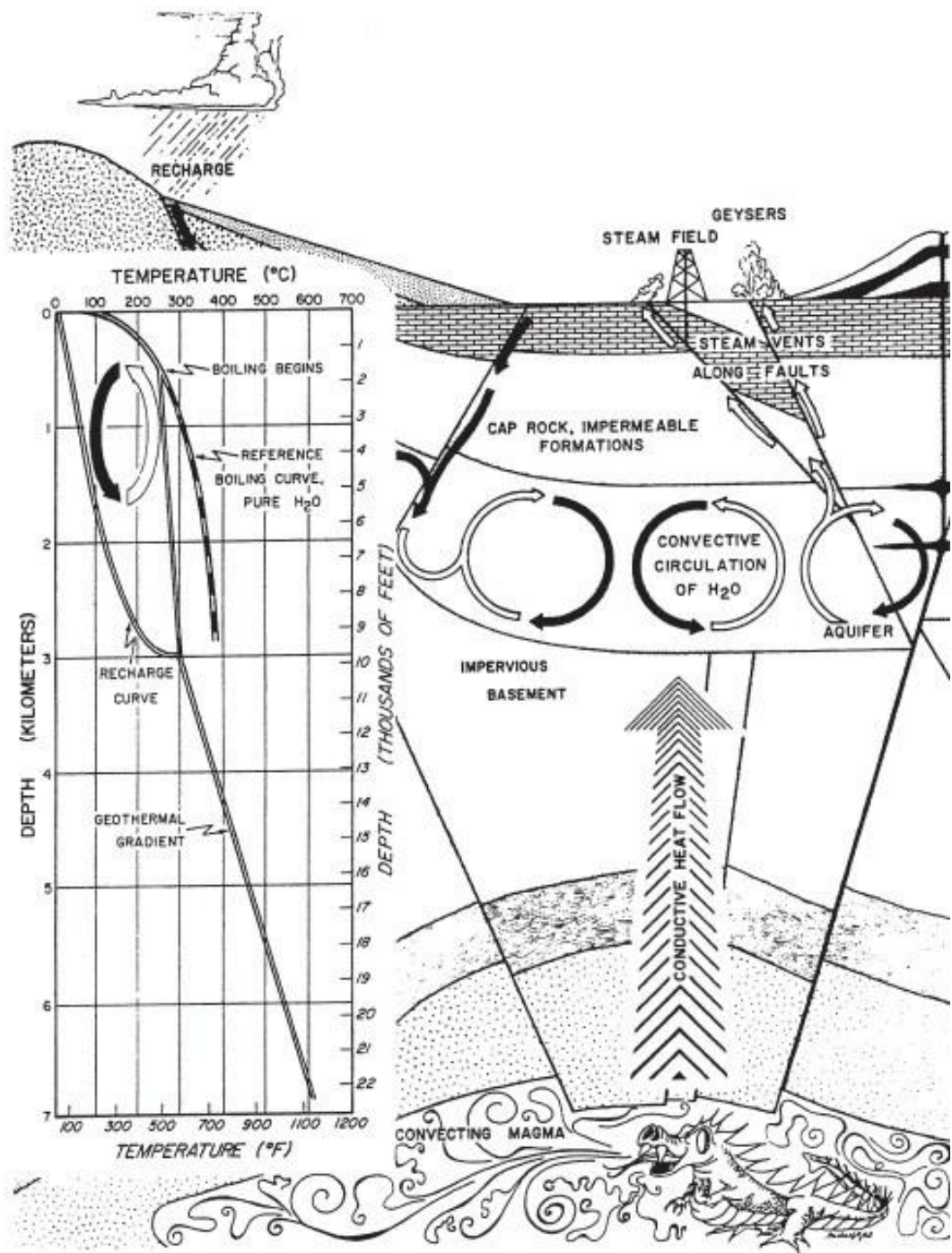


Figure 2.2 Conceptual model of a vapor dominated system (Gupta,2006)

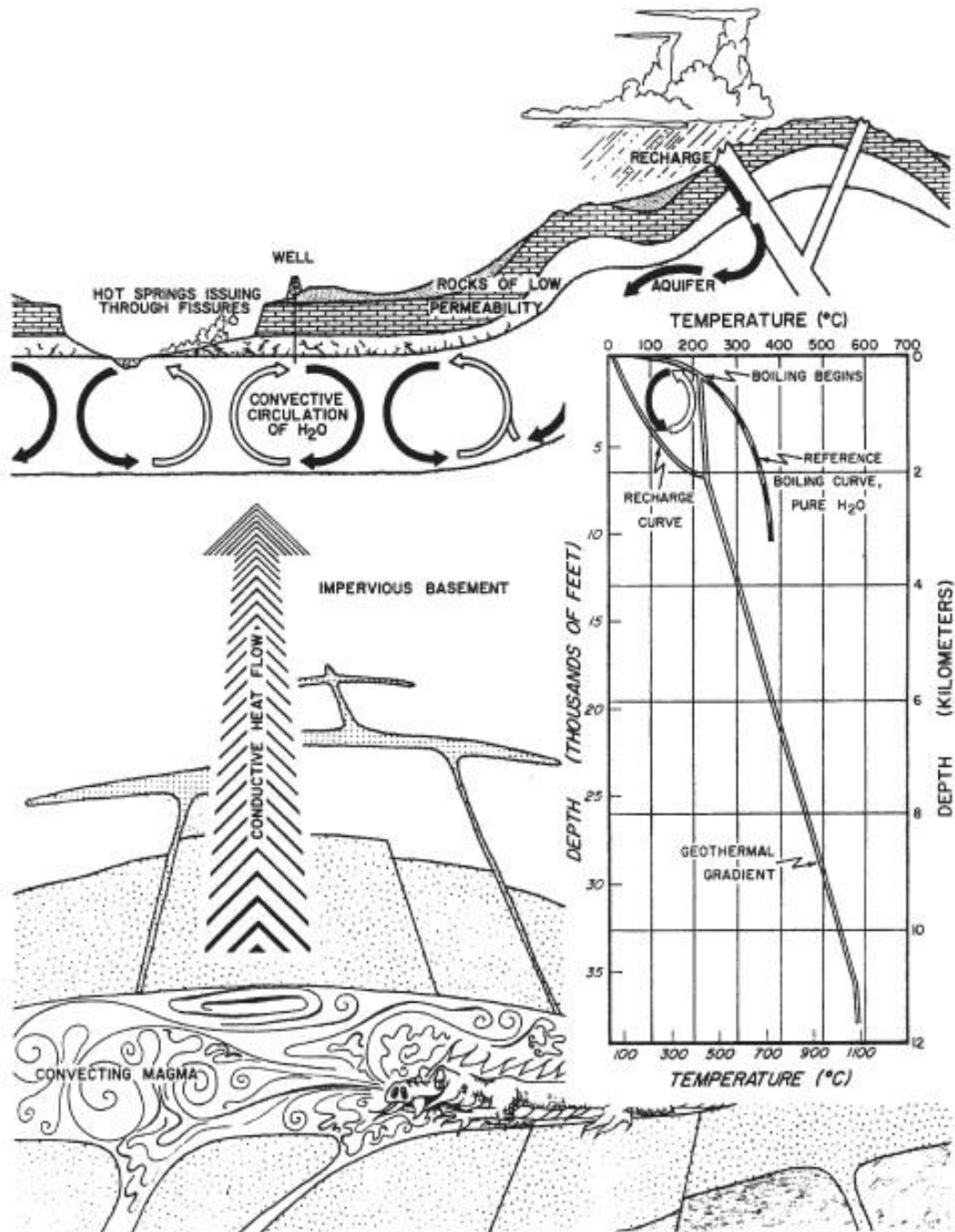


Figure 2.3 Conceptual model of a hot water system (Gupta,2006)

2.2.3 Geopressured Systems

Geopressured systems are geothermal systems in which the pressure on the reservoir is higher than the pressure of water. Less permeable rocks prevent the water from escaping up. These less permeable rocks suffers thermal metamorphism under pressure and release various hydrocarbons such as methane gas with hot water.

Production geothermal energy and dissolved methane from geopressed systems is still an emerging technology. Nowadays, this application is not economical for use of only hot water. The best known geopressed system is on the coasts of Gulf of Mexico (Figure 2.4).

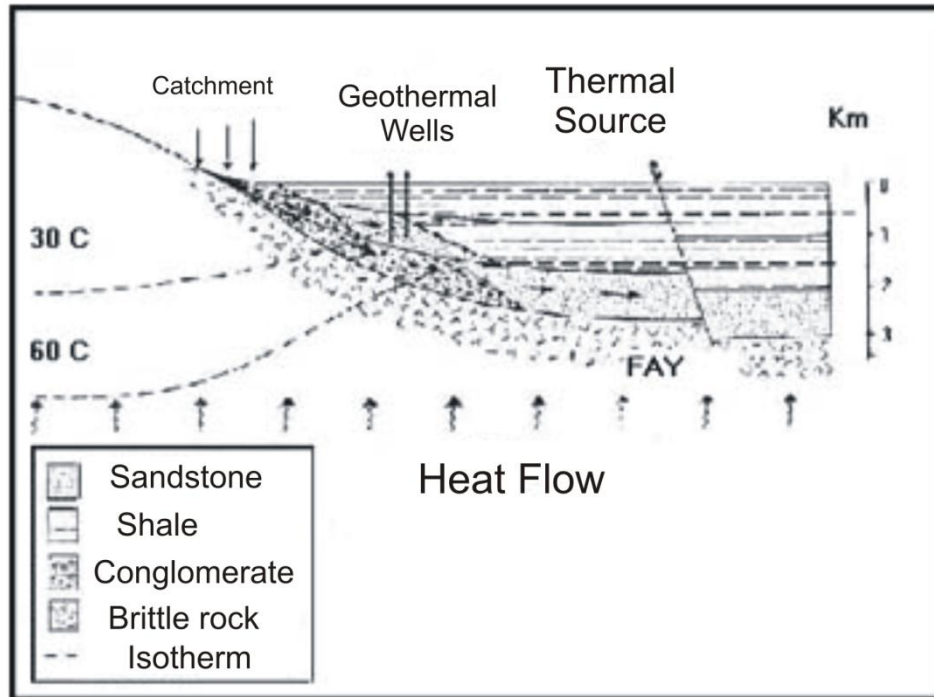


Figure 2.4 Conceptual model of a geopressed system (anonymus)

2.2.4 Hot Dry Rock Systems

Hot dry rock geothermal energy systems have no connection with any hot fluid. Geothermal energy is kept in hot and low permeable rocks in the shallow depths of the earth's crust. Those systems can occur in three ways; shallow magmatic intrusions heat the surrounding rocks, upper mantle with high temperature heats the shallow parts of the earth crust by the help of heat tranfer and radioactive minerals increase the temperature of the region by concentrating and disintegrating in certain regions of the earth's crust. In order to acquire geothermal energy from hot dry rocks artificial fracture systems can be created and hot water can be obtained by injection. This type of systems have been studied in Central Europe, Great Britain, Russia, Japan and Australia and a pilot project was carried out in Upper Rhine Graben located on the border of France and Germany (Gupta, 2006).

2.2.5 Magma Systems

Magma is the source of all high-temperature geothermal systems. The heat energy obtained from magma can provide many benefits to supply the global energy needs. But nowadays; there is no technology to provide geothermal energy from the magma. The main reasons for this are that drilling sites can not be determined, drilling costs are very high and the equipment is indurable in hot and corrosive environment. For this type of system test drillings were made in Hawaii (Gupta, 2006).

2.3 Usage Areas Of Geothermal Energy

Since ancient times geothermal resources have been utilized for health purposes and for the first time in Italy it was used for boric acid production in 1827. In 1904, power generation initiated from geothermal steam and a turbogenerator was established in 1912. In 1930's geothermal resources were used for heating in Larderello (Italy) region. In 1949, drillings started to provide hot water for a hotel in Wairakei (New Zealand) and in 1954 a power plant was established for electricity production. The usage of geothermal energy became widespread around the world in 1960's due to power plants established in U.S.A., Mexico and Japan (Sekizinci Beş Yıllık Kalkınma Planı Madencilik Özel İhtisas Komisyonu Raporu, 2001).

Usage of geothermal energy can be divided into two areas as direct and indirect use. Direct uses are; greenhouse heating, district heating, industrial use, agricultural product drying, cold and snow melting and thermal tourism. Electricity production is the only indirect use of geothermal energy (Yiğit, 1994).

The usage areas of geothermal energy varies according to the temperature of the hot fluid (Lindal,1973) (Figure 2.5).

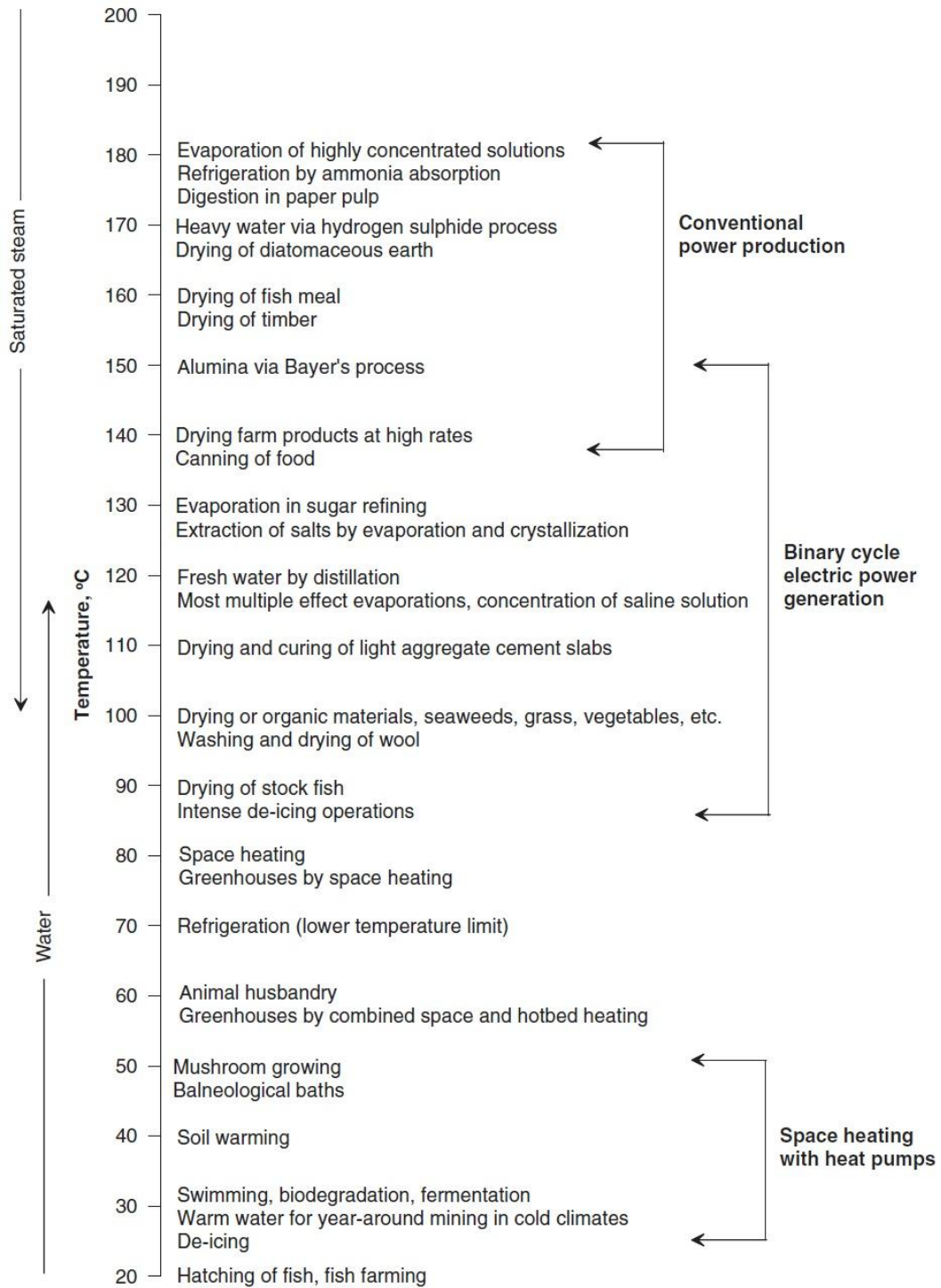


Figure 2.5 The Lindal diagram that shows the usage of geothermal energy

2.4 Usage Of Geothermal Energy In The World

A lot of geological zones are formed on the plate boundaries with subduction zones and mid-ocean ridges around the world (Figure 2.6).

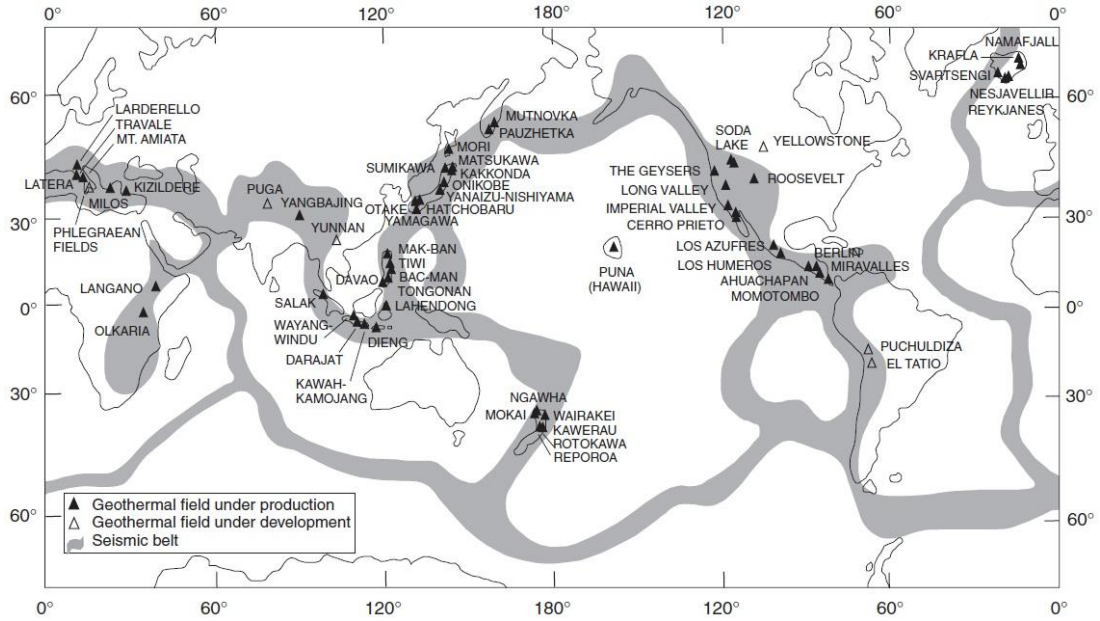


Figure 2.6 Plate boundaries and geothermal activity around the world(anonymus)

Andes-Volcanic Belt; includes Venezuela, Colombia, Ecuador, Peru, Bolivia, Chile and Argentina in the western coast of South America (Sekizinci Beş Yıllık Kalkınma Planı Madencilik Özel İhtisas Komisyonu Raporu, 2001).

Alpine-Himalayan Belt; formed as a result of collision of Indian plate and Eurasian plate and it is one of the world's largest geothermal fields. It is 150 km. to 3000 m. wide. This belt icludes Turkey and Italy, Yugoslavia, Greece, Iran, Pakistan, India, Tibet, China, Myanmar and Thailand (Sekizinci Beş Yıllık Kalkınma Planı Madencilik Özel İhtisas Komisyonu Raporu, 2001).

The East African Rift System; includes Zambia, Malawi, Uganda and Djibouti and also there is active volcanism in Kenya, Ethiopia and Tanzania (Sekizinci Beş Yıllık Kalkınma Planı Madencilik Özel İhtisas Komisyonu Raporu, 2001).

Caribbean Islands; Significant geothermal potential is in the area where active volcanism exists (Sekizinci Beş Yıllık Kalkınma Planı Madencilik Özel İhtisas Komisyonu Raporu, 2001).

Central America Volcanic Belt; is an active geothermal system which includes Guetemela, El Salvador, Nicaragua, Costa Rica and Panama (Sekizinci Beş Yıllık Kalkınma Planı Madencilik Özel İhtisas Komisyonu Raporu, 2001).

Except for these belts; America, Canada, Japan, Eastern China, Philippines, Indonesia, New Zealand, Iceland, Mexico, Northern and Eastern Europe and Commonwealth of Independent States also have efficient geothermal fields(Sekizinci Beş Yıllık Kalkınma Planı Madencilik Özel İhtisas Komisyonu Raporu, 2001).

Geothermal energy is used for lots of purposes (Sekizinci Beş Yıllık Kalkınma Planı Madencilik Özel İhtisas Komisyonu Raporu, 2001);

- generating electrical energy in U.S.A., Philippines, Mexico, Italy, New Zealand, Japan, Indonesia, El Salvador, Nicaragua, Iceland, Kenya, China, Turkey, Russia, France, Portugal, Thailand, Guatemala, Costa Rica, Ethiopia, Argentina and Australia (Table 2.1)

Table 2.1 Countries using geothermal energy in electricity generation and installed power capacity (Dokuzuncu Beş Yıllık Kalkınma Planı Madencilik Özel İhtisas Komisyonu Raporu, 2009)

COUNTRIES	MWe(2005)	COUNTRIES	MWe(2005)
U.S.A.	2544	ITALY	790
GERMANY	0.2	JAPAN	535
AUSTRALIA	0.2	KENYA	127
AUSTRIA	1	MEXICO	953
CHINA	28	NICARAGUA	77
COSTA RICA	163	PAPUA NEW GUINEA	6
EL SALVADOR	151	PHILIPPINES	1931
INDONESIA	797	PORTUGAL	16
ETHIOPIA	7	RUSSIA	79
FRANCE	157	THAILAND	0.3
GUATEMALA	33	TURKEY	20
ICELAND	202	NEW ZEALAND	435

- heating buildings and city centers by fluids with temperatures above 40°C in Iceland, France, Japan, New Zealand, Turkey, Commonwealth of Independent States, Hungary, Canada, China, Mexico, Argentina and Northern European countries

- heating greenhouses by fluids with temperatures above 30 °C in Hungary, Italy, Turkey, U.S.A., Japan, Mexico, Eastern Europe, New Zealand and Iceland

- farming tropical plants and fish in Philippines, China and Iceland

- heating poultry and livestock farms in Japan, U.S.A., New Zealand, Hungary and Commonwealth of Independent States
- heating lands, roads and airport runways in Siberia
- in swimming pools, thermal treatment and other tourist facilities in Italy, Japan, U.S.A., Iceland, Turkey, China, Indonesia, New Zealand, Argentina, Eastern Europe and Commonwealth of Independent States
- drying and sterilization of food and canned food industry in Japan, U.S.A., Iceland, Philippines, New Zealand and Thailand
- lumbering and wood paving industry in New Zealand, Iceland, Japan, China and Commonwealth of Independent States
- in paper industry in New Zealand, Iceland, Japan, China and Commonwealth of Independent States
- weaving and dyeing in New Zealand, Iceland, China and Commonwealth of Independent States
- in leather drying in Japan
- distillation of beer and similar substances in Japan
- cooling plants in Italy and Mexico
- drying of concrete blocks in Mexico
- drinking water by cooling the hot fluid in Hungary, Commonwealth of Independent States, Tunisia and Algeria
- in laundries in Japan
- obtaining chemicals such as boric acid, ammonium bicarbonate, heavy water, ammonium sulfate, potassium chloride in Italy, U.S.A., Japan, Philippines and Mexico
- dry ice extraction from geothermal fluid in Turkey and U.S.A.

Table 2.2 Direct usage of geothermal energy in the world (Dokuzuncu Beş Yıllık Kalkınma Planı Madencilik Özel İhtisas Komisyonu Raporu, 2009)

Country	Capacity(MWt)	Country	Capacity(MWt)
Albania	9.6	Italy	606.6
Algeria	152.3	Japan	413.4
Argentina	149.9	Jordan	153.3
Armenia	1	Kenya	10
Australia	109.5	South Korea	16.9
Austria	352	Lithuania	21.3
Belarus	1	Macedonia	62.3
Belgium	63.9	Mexico	164.7
Brazil	360.1	Mongolia	6.8
Bulgaria	109.6	Nepal	2.1
Canada	461	Netherlands	253.5
Caribbean Islands	0.1	New Zealand	308.1
Chili	8.7	Norway	450
China	3687	Papua New Guinea	0.1
Colombia	14.4	Peru	2.4
Costa Rica	1	Philippines	3.3
Croatia	114	Poland	170.9
Czech Republic	204.5	Portugal	30.6
Denmark	821.2	Romania	145.1
Equator	5.2	Russia	308.2
Egypt	1	Serbia	88.8
Ethiopia	1	Slovak Republic	187.7
Finland	260	Slovenia	48.6
France	308	Spain	22.3
Georgia	250	Swedish	3840
Germany	504.6	Swiss	581.6
Greece	74.8	Thailand	1.7
Guatemala	2.1	Tunis	25.4
Honduras	0.7	Turkey	1177
Hungary	694.2	Ukraine	10.9
Iceland	1791	United Kingdom	10.2
India	203	U.S.A.	7817.4
Indonesia	2.3	Venezuela	0.7
Iran	30.1	Vietnam	30.7
Ireland	20	Yemen	1
Israel	82.4	General Total	27824.8

2.5 Usage Of Geothermal Energy In Turkey

High-temperature geothermal fluids containing fields formed by tectonic activities are located in graben basins. For this reason the high-temperature geothermal areas are located on the western of Turkey. In addition, low and medium temperature geothermal fields caused by volcanism and faulting are along the line of Central and Eastern Anatolia and North Anatolian Fault (Sekizinci Beş Yıllık Kalkınma Planı Madencilik Özel İhtisas Komisyonu Raporu, 2001) (Figure 2.7).

Turkey is one of the richest countries in the world in terms of geothermal energy potential. There are about 1000 hot and mineral water springs totally in Turkey (Figure 2.8, 2.9). The 635 MWt of the geothermal energy capacity is used for heating buildings and thermal plants and 192 MWt of it is used for heating greenhouses. Also, 402 MWt is used for spa tourism. Turkey's total direct usage capacity is 1229 MWt (Dokuzuncu Beş Yıllık Kalkınma Planı Madencilik Özel İhtisas Komisyonu Raporu, 2009).

In Turkey, geothermal energy generally is used for electricity production, heating buildings and greenhouses, thermal treatment, spa tourism and dry ice extraction from CO₂ in the hot fluid.

The first geothermal power plant in Turkey was founded in 1984 in Denizli-Kızıldere area. Presently, the working plant's capacity is 20 MWe and capacity is estimated to rise 80 MWe in 2013. In addition, installed capacity in Germencik, Salavatlı, Tuzla and the other areas is expected to be 550 Mwe at the end of 2013. Geothermal power plants in Aydın-Salavatlı with 171°C temperature and 7.9 Mwe capacity, Kızıldere with 140 °C temperature and 5.5 Mwe capacity, Çanakkale-Tuzla with 173 °C temperature and 7.5 Mwe capacity and Kütahya-Simav 162 °C temperature and 10 Mwe capacity are going to be established soon (Dokuzuncu Beş Yıllık Kalkınma Planı Madencilik Özel İhtisas Komisyonu Raporu, 2009) (Table 2.3).



Figure 2.7 Map of geothermal resources and volcanic areas (MTA)

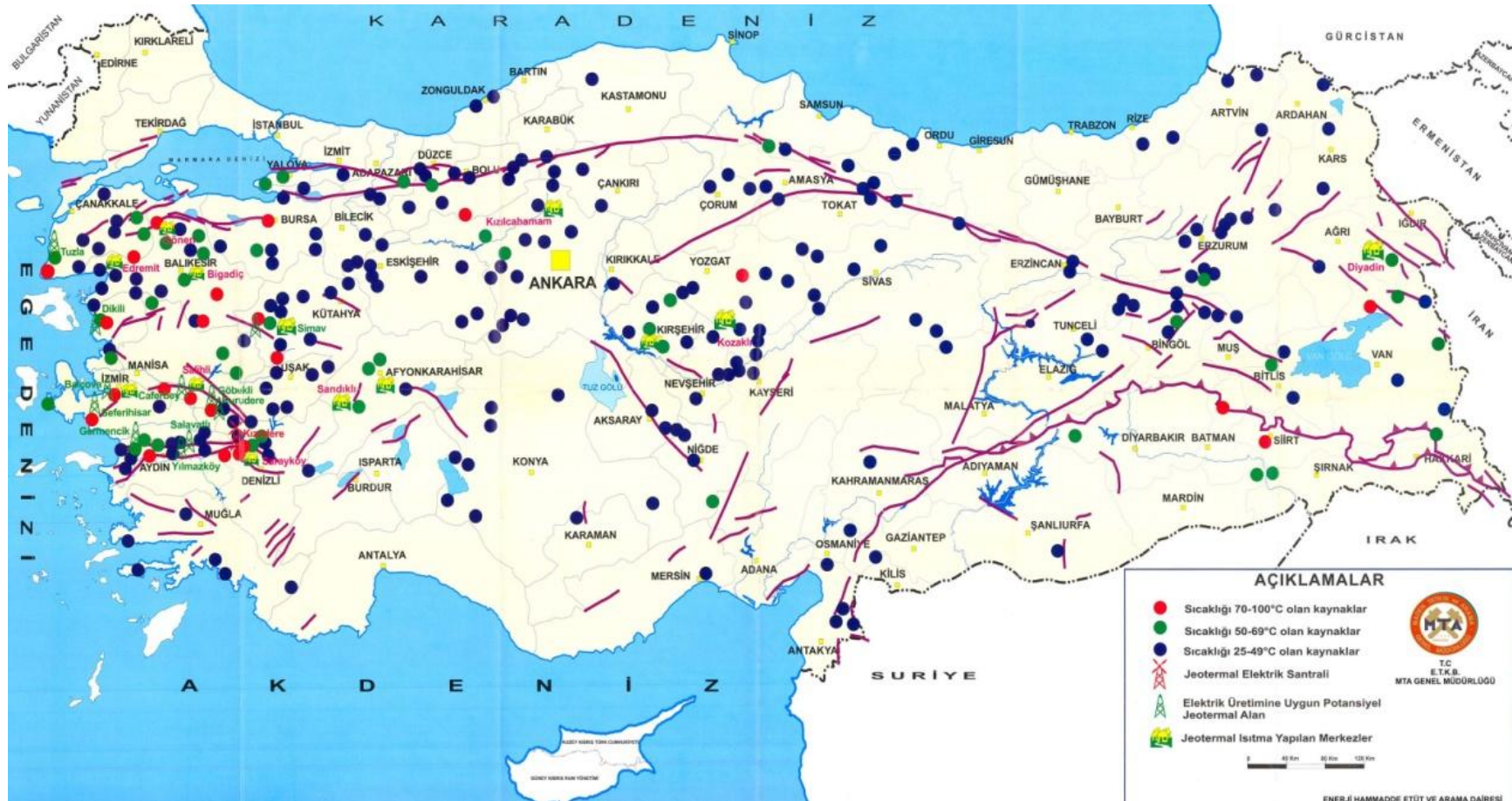


Figure 2.8 Distribution of geothermal resources (MTA)

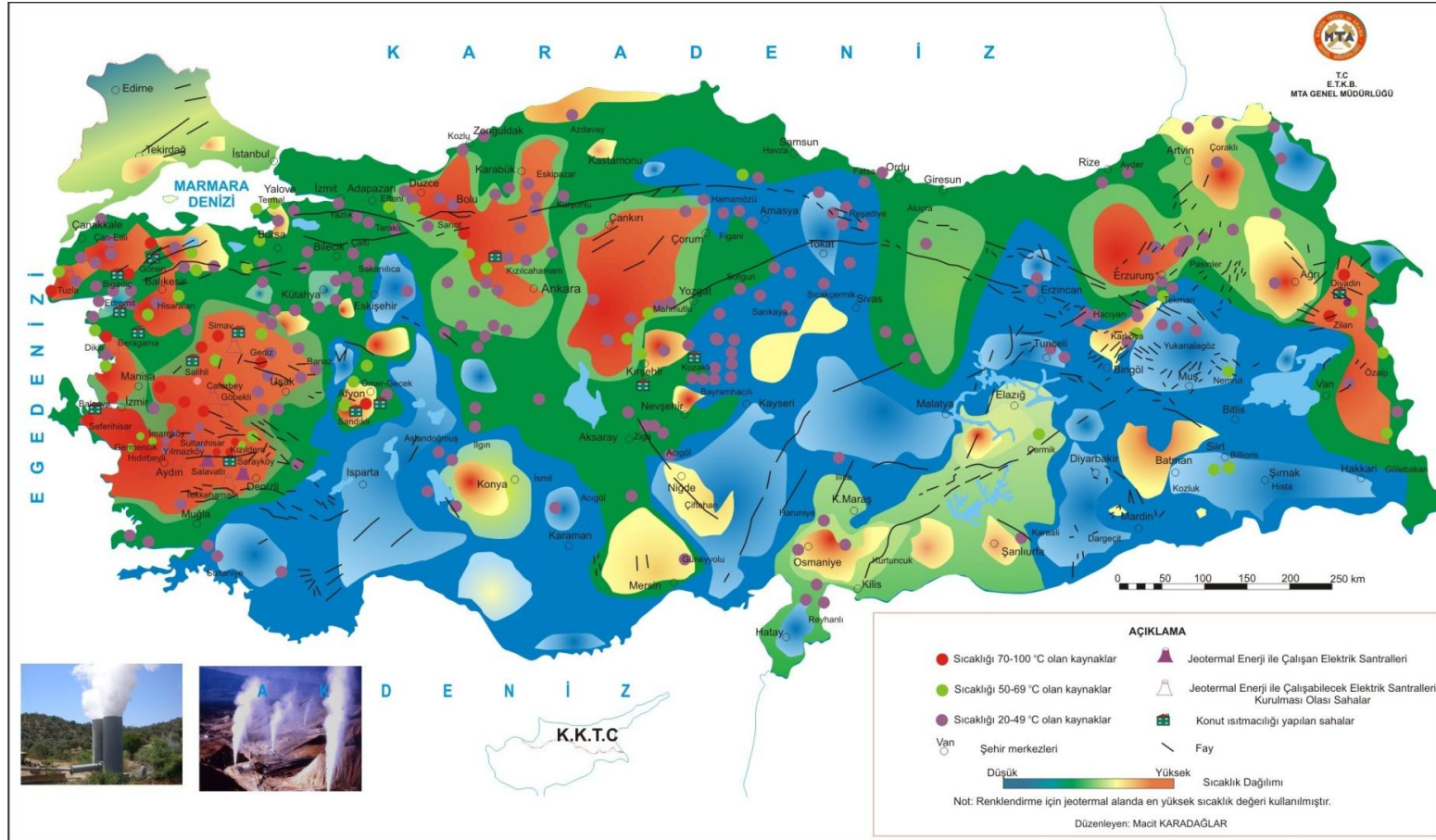


Figure 2.9 Application of geothermal resources map (MTA)

Table 2.3 Geothermal electricity generation projections (Dokuzuncu Beş Yıllık Kalkınma Planı Madencilik Özel İhtisas Komisyonu Raporu, 2009)

Field Name	Temperature	2010 Predicitons	2013 Predicitons
	°C	Mwe	Mwe
Denizli-Kızıldere	200-242	75	80
Aydın-Germencik	200-232	100	130
Manisa-Alaşehir-Kavaklıdere	213	10	15
Manisa-Salihli-Göbekli	182	10	15
Çanakkale-Tuzla	174	75	80
Aydın-Salavatlı	171	60	65
Kütahya-Simav	162	30	35
İzmir-Seferihisar	153	30	35
Manisa-Salihli-Caferbey	150	10	20
Aydın-Sultanhisar	145	10	20
Aydın-Yılmazköy	142	10	20
İzmir-Balçova	136	5	5
İzmir-Dikili	130	30	30
Total		455	550

In 1987, Turkey's first geothermal heating system was installed in Balıkesir-Gönen hotel with the capacity of 32 MWt and 3400 residential equivalent.

Turkey's first geothermal well was opened in Balçova-İzmir in 1963. The system was activated with the capacity of 143.3 MWt in 1992 and still heats 16.000 houses in Balçova. The facility also heats a thermal hotel in Balçova. The area is the largest geothermal application in Turkey with the capacity of 100.000 m² greenhouse heating and Dokuz Eylül University campus heating. Also, 5.000 houses in Simav, 1.900 houses in Kırşehir, 2.500 houses in Kızılcahamam, 4.500 houses in Afyonkarahisar, 3.600 houses in Sandıklı, 1.200 houses in Kozaklı, 150/400 houses in Diyadin, 4.100 houses in Salihli, 2.000 houses in Edremit, 1.500 houses in Sarayköy, 1.500 houses in Bigadiç and 10/2.000 houses in Sarıkaya(Yozgat) are heated with the geothermal central heating system (Dokuzuncu Beş Yıllık Kalkınma Planı Madencilik Özel İhtisas Komisyonu Raporu, 2009).

Commercial production of chemicals from geothermal resources takes place in the CO₂ plant in Denizli-Kızıldere with the capacity of 120.000 tons (installed power) per year (Dokuzuncu Beş Yıllık Kalkınma Planı Madencilik Özel İhtisas Komisyonu Raporu, 2009).

Early vegetable production, fruit growing and floriculture is carried out by heating greenhouses with geothermal energy (Dokuzuncu Beş Yıllık Kalkınma Planı Madencilik Özel İhtisas Komisyonu Raporu, 2009) (Table 2.4).

Table 2.4 Situation of greenhouse usage in Turkey(January, 2011, MTA)

Area	Greenhouse Area	Approximate Power
	(decar)	(MWt)
Afyon	50	9.8
Aydın-Gümüşköy	60	11.76
Balçova-İzmir	17	3.33
Dikili-İzmir	880	117.6
Gölemezli-Denizli	110	21.56
Kırşehir	50	9.8
Kızılcahamam-Ankara	0.5	0.1
Kozaklı-Nevşehir	67	13.13
Salihli-Manisa	250	49
Sandıklı-Afyon	81.5	15.97
Sarayköy(Tosunlar+Kızıldere)	152.8	29.94
Simav-Eynal-Kütahya	310	60.76
Sorgun-Yozgat	15	2.94
Urfa	170	33.32
Yenicekent-Denizli	53.4	10.47
Total	2267.2	444.34

According to data of February, 2005, the capacity of thermal tourism consisting of 215 spas is expected to reach 400 spas in 2013. Other capacities are expected to be 3.600 decares in greenhouse heating, 50.000 residential equivalent in cooling, 500.000 ton in drying and 400 MWt in fishing and other usage areas (Dokuzuncu Beş Yıllık Kalkınma Planı Madencilik Özel İhtisas Komisyonu Raporu, 2009) (Table 2.5).

Table 2.5 The employment projection of geothermal applications (electricity+direct use) in 2013
(Dokuzuncu Beş Yıllık Kalkınma Planı Madencilik Özel İhtisas Komisyonu Raporu, 2009)

Geothermal Assessment	February(2005)	MW	Projection of 2013	MW
Electricity generation		20 Mwe (94G Wh)		550 Mwe (2475 GWh)
House heating	103.000 residential equivalent	635 MWt	500.000	4000 MWt
Thermal tourism(spa)	215 hot springs	402 MWt	Thermal equivalent of 400 units	1100 MWt
Greenhouse	635 decares	192 MWt	5000 decares	1700 MWt
Cooling			50.000 residential equivalent	300 MWt
Drying			500.000 tons/year	500 MWt
Fishing+other applications				400 MWt
Total direct use		1229 MWt		8000 MWt

CHAPTER THREE

GEOGRAPHICAL INFORMATION SYSTEMS AND REMOTE SENSING

3.1 Geographical Information Systems

To obtain any information in a specific way for a specific purpose must be monitored and the obtained information must be used with the maximum advantage. To do this a system should be used to reach accurate and useful information. A system is a method order for obtaining a result. A system analyzes the data processed that obtained from various sources for a specific purpose and analyzing the data with the support of a computer is called information systems (Tecim, 2008).

Geographical Information Systems is a system that includes spatial and non-spatial data and uses these datas processing the spatial analysis. GIS is a system that allows operations for a particular purpose, such as gathering, archiving, updating, controlling, analyzing and displaying the information about the earth. GIS allows you to analyze and take the advantage of map-based applications in the best way. GIS supports decisions such as selection, transferring, querying, analyzing, presenting and high quality outputs according to different request by using the spatial and non-spatial datas in the wide databases (Tecim, 2008).

3.1.1 The Basic Components Of GIS

GIS consists of four main components that are connected to each other and each with its own specific purposes;

- Hardware and software
- Geographical data
- Staff
- Purpose for a specified problem

The hardware for GIS is not different from the hardware used for computers today. But system needs certain features to work correctly. GIS uses computers which have a strong central operating system capable of processing map applications

that require accuracy and precision. A large hard disk is required for storing the large amount of digital data and use the data quickly when necessary. Digital databases, portable drives and portable hard drives must be used to be reached by many users at the same time. For qualified outputs; high-resolution monitors, colored plotters and colored printers should be used. In addition, a scanner and a digitizer are needed to transfer the aerial photographs and satellite imagery to the system (Tecim, 2008).

GIS software enables the operation of special objects used in mapping together with the descriptive details of these objects within the logic of computer programming. GIS software provides the possibility to query and analyze the data with the non-spatial attribute data of the object with right projection and coordinates. SQL, Progress and Oracle database management systems, MapInfo, ArcGis and GeoMedia softwares are examples of GIS softwares (Tecim, 2008).

Geographical data is the basis of GIS. Geographical data can be defined as data associated with a specific location. Each data set in the database should include an element that signifies the geographical location. This element is generally the map coordinates, postal codes or addresses. This element that identifies the geographical location is called geocode. Geo-coding is the process of associating an object with the geocode (Tecim, 2008).

The data used in GIS is classified into two parts as vector and raster data. Vector data such as point, line and polygon is stored with the attribute information according to a particular coordinate system. For example; the electric pole place(point), the length of power line(line) and the distribution of a power plant area (polygon). Raster data stores the images in the form of grid cells. In the raster data structure each cell contains the value of attribute information of the region. Raster data cell feature is evaluated with its resolution. Satellite images are examples of raster data (Tecim, 2008).

Attribute data is meaningful information that belongs to an object on the map which does not appear on the map or does not make sense stand alone. This data allows objects to be analyzed according to specific purposes. The population or the economy in the province border is an example for attribute data (Tecim, 2008).

GIS staff consists of qualified technicians who design and maintain the systems and use these systems to improve the performance of daily works.

GIS technology can be used for purposes such as; scientific research, resource management, asset management, infrastructure(gas, electricity, water), archeology, environmental impact assessment, urban planning, cartography, criminology, geographic history, marketing, logistic, mineral mapping, cultivated agricultural land determination and calculation of the total crop, military applications, air, sea and land traffic monitoring, vehicle tracking systems, meteorology, search and rescue.

3.2 Remote Sensing

Remote sensing is considered to be the most successful method of determining, mapping, planning, tracking and controlling the present state of the earth, detecting the damages and managing of natural resources. However, satellite images is the most important data sources in obtaining the up date spatial information.

Remote sensing is a method of acquiring information about an object, a land structure or physical and chemical properties of a natural phenomenon without any physical contact by the help of data collected by sensors positioned on earth, in air or in space.

Nowadays, remotely sensed data is obtained by planes, unmanned aerial vehicles and satellites equipped with cameras and sensors. Cameras and sensors create images by measuring energy which is reflected and transmitted from the surface of the earth.

3.2.1 Electromagnetic Spectrum

Electromagnetic spectrum consists of categorized energy which is recorded by the remote sensing sensors. Electromagnetic spectrum takes place between the short-wavelength including gamma and x-rays and long-wavelength including microwave and TV/radio waves (Figure 3.1).

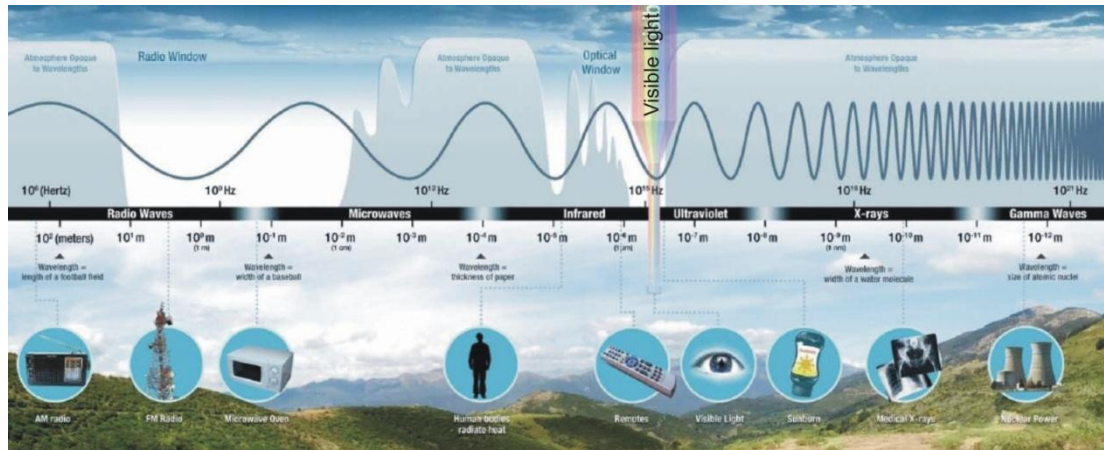


Figure 3.1 Electromagnetic spectrum (NASA)

The basic requirement of remote sensing is a target enlightened with an energy source. This source is generally the sun. The sun radiates energy at a short wavelength. This energy spreads in the form of sinusoidal electromagnetic emission. Electromagnetic emission includes an electric field that is perpendicular to direction of propagation and a magnetic field that is perpendicular to the electric field (Figure 3.2).

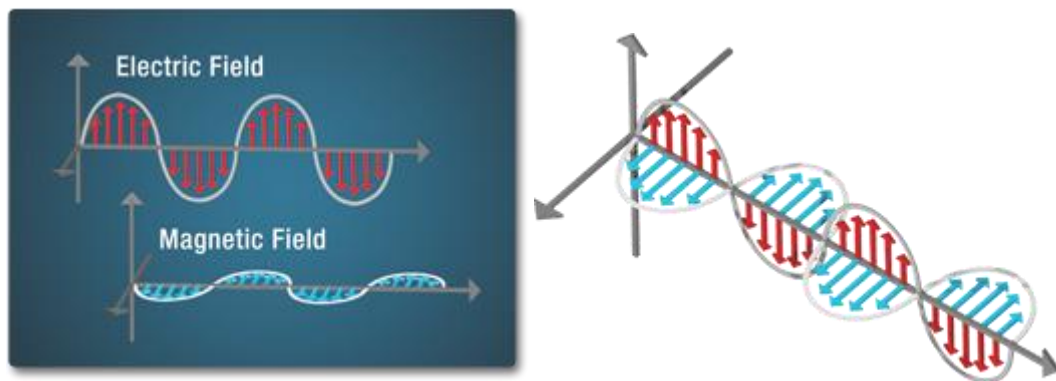


Figure 3.2 Electric and magnetic field and their motion (NASA)

Wavelength(λ) and frequency are the elements of electromagnetic emission. Wavelength is the distance between peaks of successive waves and can be expressed by nanometers(nm), micrometers(μ m), centimeters(cm) and meters(m). Frequency of the wave is the number of cycles per second and can be expressed by ‘hertz’. Objects with high energy emit energy in short wavelength and high frequency and objects with low energy emit in long wavelength and low frequency (Figure 3.3).

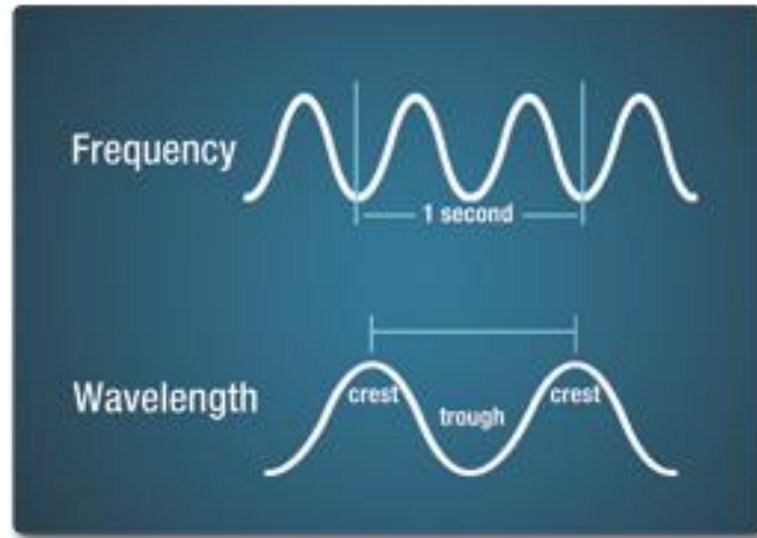


Figure 3.3 Wavelength and frequency (NASA)

3.2.2 Remote Sensing Operations

Remote sensing operations are carried out in seven steps depending on the interaction between the target and incident beam (Figure 3.4).

Energy source and lightening: generally the sun is the source of energy for lightening.

Emission and atmosphere: While the energy used for displaying objects spreads from the source to the target, it is blocked by the atmosphere. This blockage occurs for the second time while energy reaches the target. Particles and gases in the atmosphere can change the direction of energy propagation. This effect can occur as a form of scattering and absorption. Scattering changes according to the wavelength, abundance of the particles in the atmosphere and the distance the beam travels.

Obstruction of earth's surface: the energy that reaches from the source to the earth's surface is blocked according to the characteristics of the surface and emission. Energy come across three types of prevention; absorption, transmission or passing and reflection. Affect of each of prevention changes depending on the wavelength of the energy, the material on the surface and conditions. When the energy faced the absorption, absorbed energy does not return to the sensor. However,

reflection sends back all the energy or a part of it to the sensor. This reflected energy is recorded by sensors.

Sensor records the energy; sensor collects and records the energy that spreads from the source or reflects from the target.

Sending, receiving and processing; the energy that sensor recorded is sent to the station where it will be processed.

Assessment and analysis; images are evaluated according to the purposes that reached to the processing station.

Application; the information obtained is made functional to help to solve problems or use in various fields.

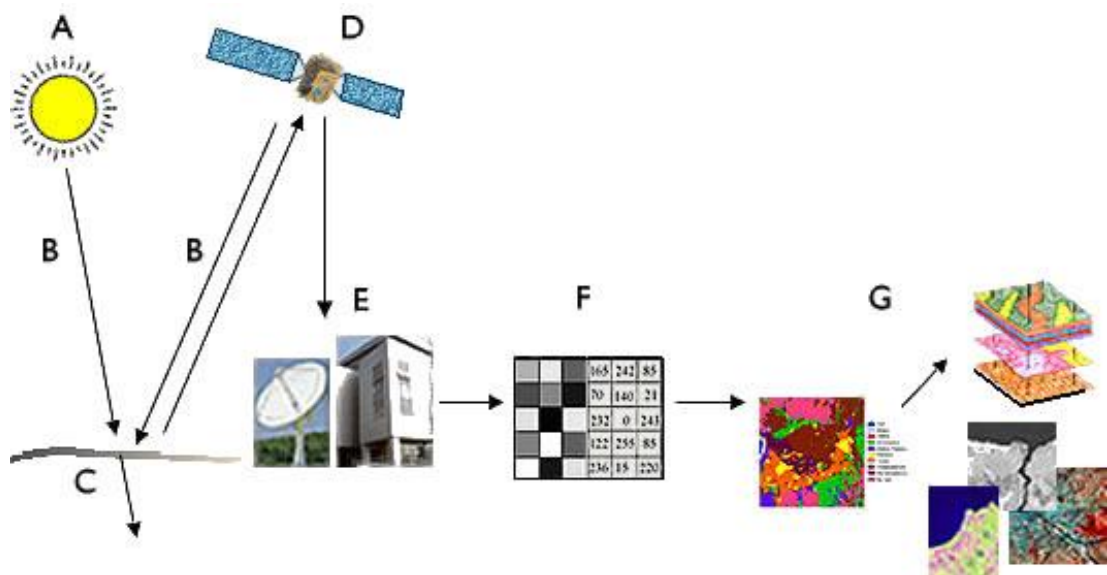


Figure 3.4 Remote sensing operations (İşlem GIS) A) Energy source and lightening B) Emission and atmosphere C) Prevention of earth's surface D) Sensor records the energy E) Assessment and analysis F,G) Application

3.2.3 Characteristics Of Remote Sensing Images

Electromagnetic energy can be determined as photographic or electronic. Photographs are obtained by recording and printing the energy within wavelengths of between 0.3-0.9 μm on film. Images are acquired by recording the energy

regardless of the energy wavelength by analogue recording and converting it to digitized images and they are displayed on the computer.

3.2.3.1 Pixel

The energy recorded is converted to numeric values as a separate pictorial structure. This numeric values are digital numbers that stored as pixels. The image consists of same sized and shaped pixel grids presented in digital format. For each pixel there is a digital number value measured by the sensor. These digital number values represent a certain brightness and displayed as an image on computer. In the transformation of digital number values to image format some loss of detail could be seen. Small sized pixels provide details to be more visible (Figure 3.5, 3.6).

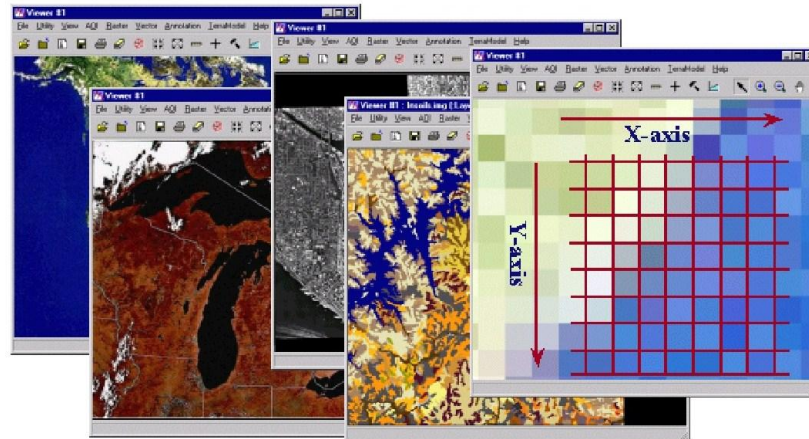


Figure 3.5 Image structure (İşlem GIS)

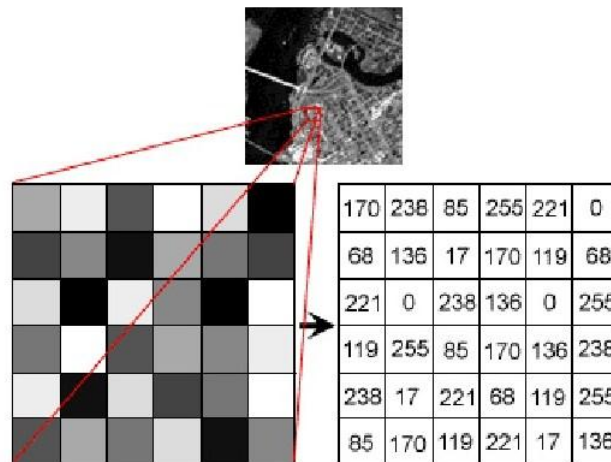


Figure 3.6 Pixel structure (İşlem GIS)

3.2.3.2 Swath

The area in the earth's surface that the satellites sees and sense while flying on their orbit is called swath. Swath is composed of a matrix of pixels representing the energy recorded by the sensor. Swath can change according to the orbit heights (Figure 3.7).

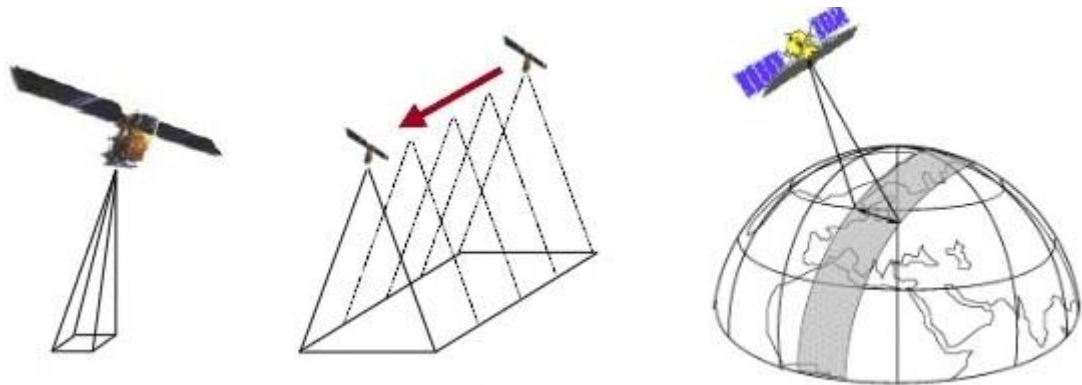


Figure 3.7 Swath (İşlem GIS)

3.2.3.3 Bands

Bands consists of a combination of pixels. Bands also referred to as channels. Images composed as a combination of one or more bands. Each band represented by a primary color (Figure 3.8).

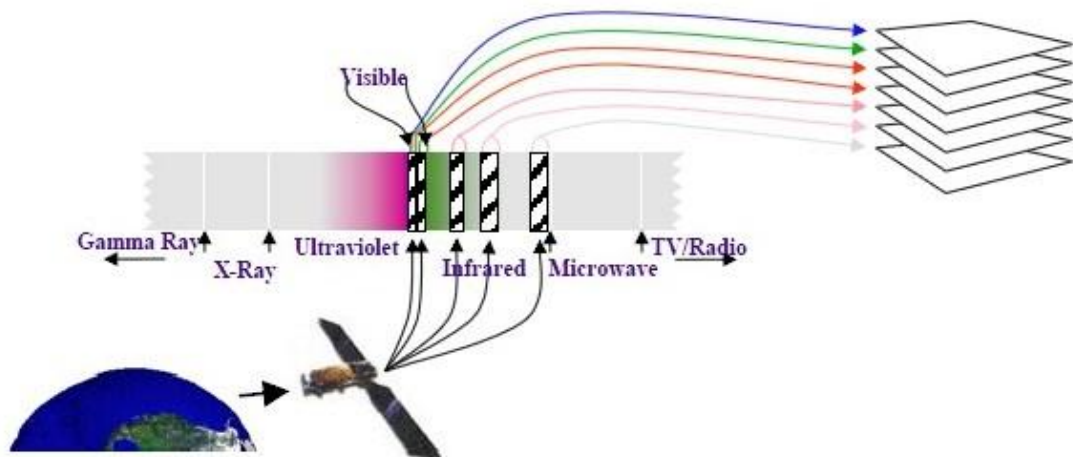


Figure 3.8 Bands (İşlem GIS)

3.2.3.4 Resolution

Resolution represents the amount of pixels on the computer screen or the pixels of an area on the earth. Resolution expresses the quality of the image is divided into four different types;

Spatial resolution; the ability to distinguish adjacent objects. Low spatial resolution shows good sensitivity. For example; 10 m. spatial resolution provides more detail than 20 m. spatial resolution (Figure 3.9).

Spectral resolution; is the record by the sensor between specific wavelengths of electromagnetic spectrum. If recorded energy's wavelength range is wide, spectral resolution would be low and if wavelength range is narrow, spectral resolution would be high. For example; Landsat satellite's spectral resolution is seven because Landsat scans the same area in seven different bands and seven different wavelength range (Figure 3.10).

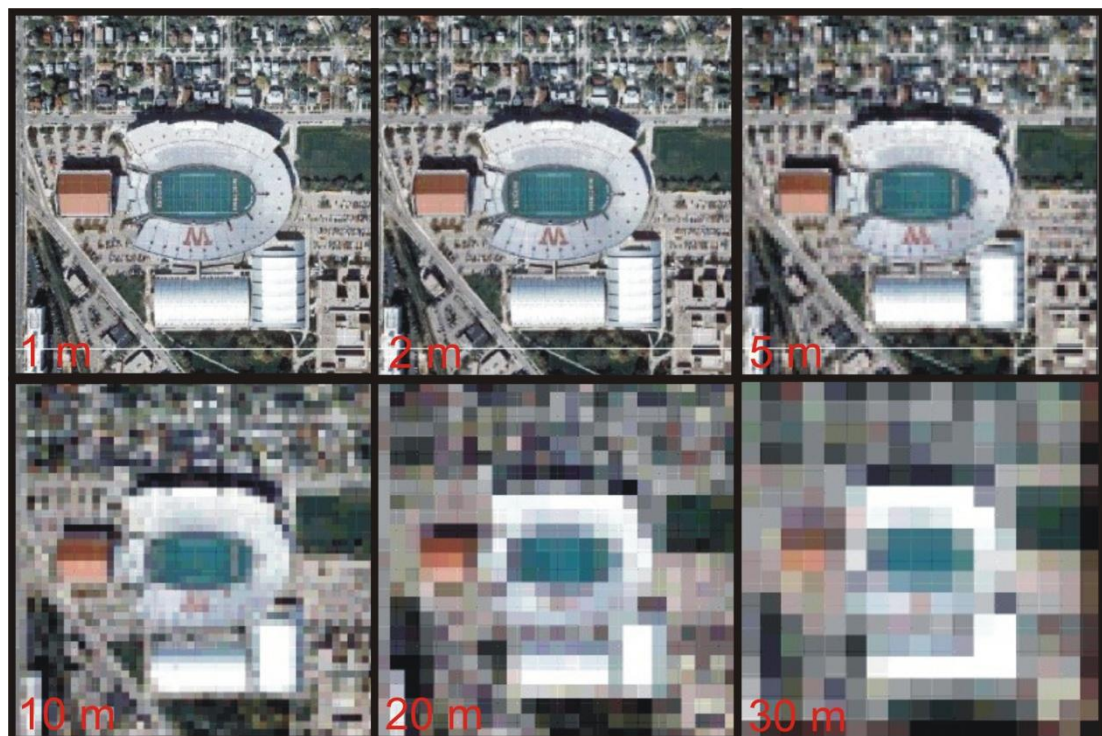


Figure 3.9 Spatial resolution (anonymus)

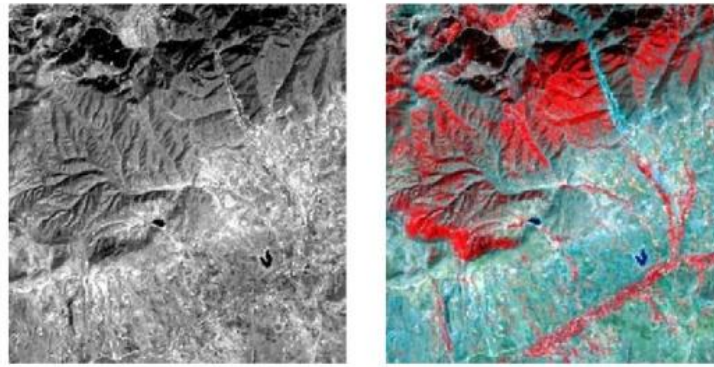


Figure 3.10 Image of one band and image of three bands (İşlem GIS)

Radiometric resolution; indicates the sensitivity of the sensor to the difference of brightness. Image value is expressed by the digital numbers. These numbers are arranged according to a binary number system. Many sensors have data in form of 8 bit ($2^8=256$). This data corresponds to a value between 0 and 256 for each pixel. Value of 0 represents the colour black and value of 256 represents the colour white. Therefore, the image is usually displayed in grayscale. The more existence of shades of colour means the more qualified image (Figure 3.11).

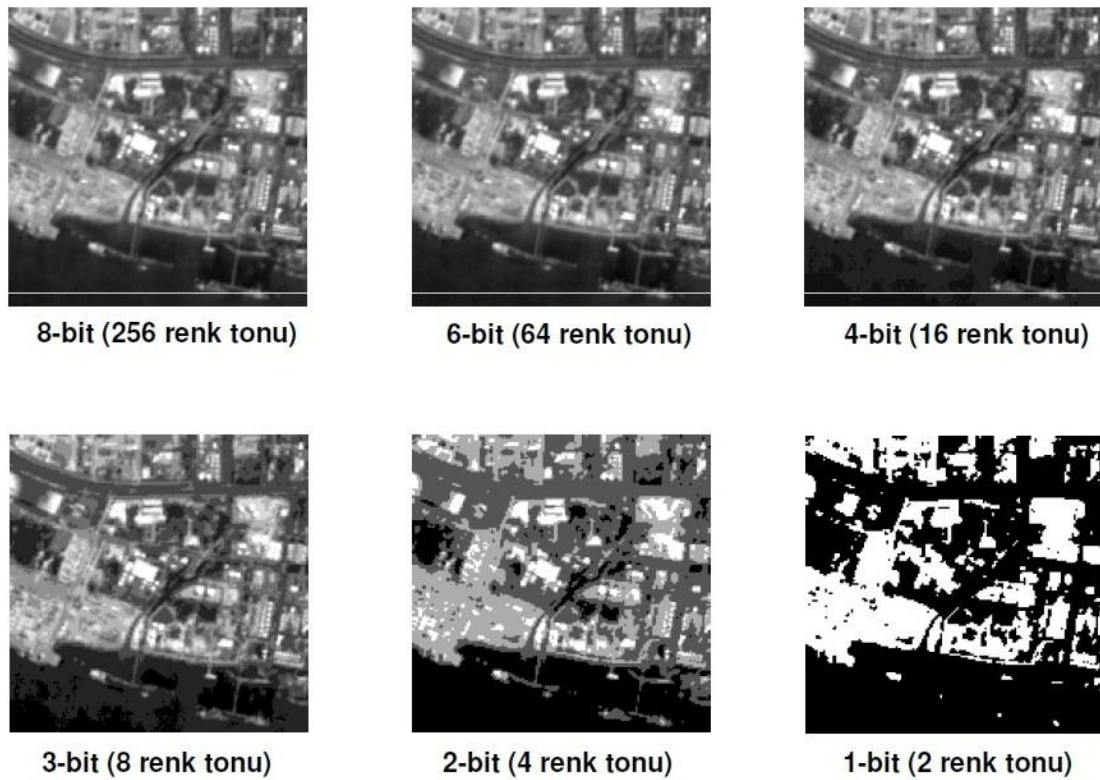


Figure 3.11 Radiometric resolution (İşlem GIS)

Temporal resolution: is the resolution of re-scanning the same area. Temporal resolution refers to the time that takes until a satellite scans a particular region again. Temporal resolution varies according to the altitude and the orbit of each satellite. For example; re-scan time of Landsat is 16 days and 26 days for Spot.

3.2.4 Types Of Images

Remotely sensed images are stored in photographic and digital platforms. Accordingly, remote sensing images can be divided into two groups as aerial photographs and satellite images.

Aerial photographs are obtained with various cameras, films and filters. Photographs are provided with cameras that can save images in wavelength between 0.3-0.9 μm and these cameras are installed into bottom of aircrafts, spacecrafts and helicopters. The scale and quality of the photographs varies by the height of plane, the type of the photograph and the camera used. Depending on the purpose, black and white, coloured or infrared films are used.

Satellite images can record data collected from two or more spectral region. As a result, multi-band satellite images can be obtained. Satellite images can be divided into two groups as single-band images and multispectral images.

Single-band satellite images can be defined as panchromatic images. Panchromatic images show only a certain part of the electromagnetic spectrum. They are usually displayed in grayscale.

Sensors detect two or more regions of the electromagnetic spectrum while recording multispectral images. In these images each band represents a range of a specific wavelength of the electromagnetic spectrum. For example; one of the sensors records the red band and the other sensor records the near red band. These bands are combined to create a coloured image. Today, satellites can record images three to seven bands at a time (Figure 3.12).

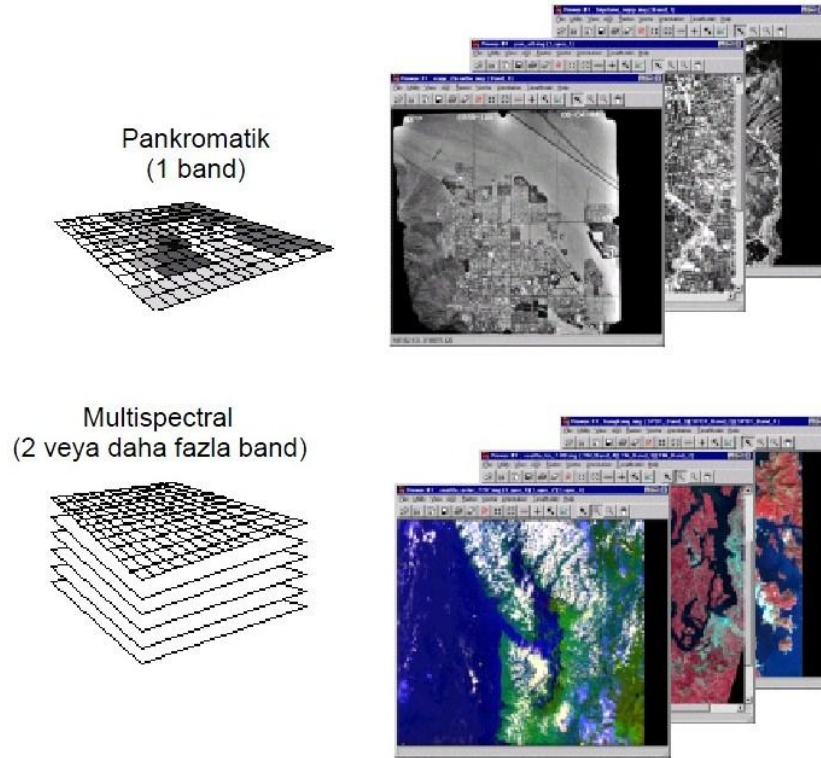


Figure 3.12 Panchromatic and multispectral images (İşlem GIS)

3.2.5 Remote Sensing Systems

Satellite systems can be categorized as passive and active sensors in terms of detecting fundamentals.

Passive sensors measure the energy which comes from the sun and is reflected from the earth. These sensors do not have their own energy source. Those type of sensors work only in daylight (Figure 3.13).

Active sensors provide the required energy from their own energy source independently from the sun. Active sensors are called Syntetic Aperture Radar (SAR). SAR radiates a radar signal at micro wavelength and measures the signal reflected from the earth. These type of satellites can create images in the dark, foggy and cloudy areas (Figure 3.14).

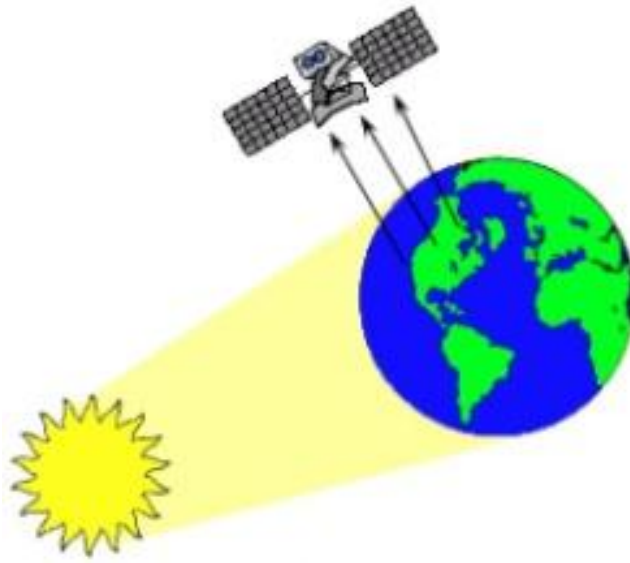


Figure 3.13 Working principle of passive sensors (İşlem GIS)

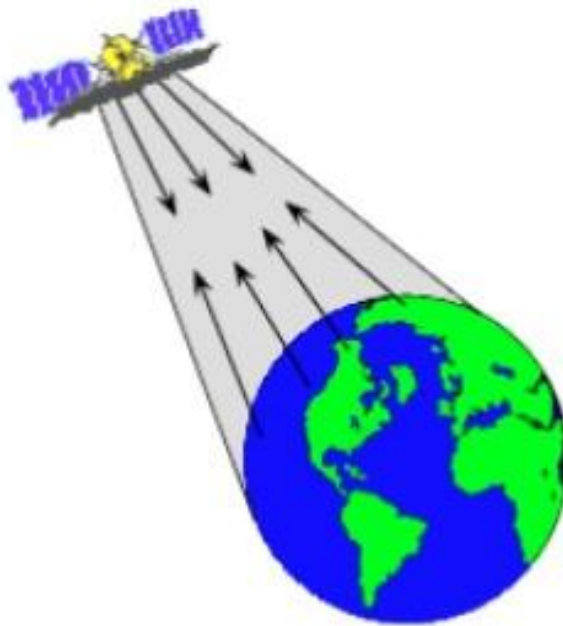


Figure 3.14 Working principle of active sensors (İşlem GIS)

3.2.6 Satellites

Satellites can be categorized as meteorological satellites, the satellites observing earth's surface, radars, satellites for marine research and satellites for planets. There are various satellites in the world used for different purposes (Figure 3.15, 3.16, 3.17). The characteristics of satellites that are widely used in geology will be discussed in this section.

Sensör/Uydu Sensor/Satellite	Operatör / Ülke Operator/ Country	Başlangıç ve Sonlama Tarihi (launch & end date)	Sensör Tipi (Sensor type)	Çözünürlük (Resolution)			Şerit Geniğiği Swath(km)	Görüntüleme Sıklığı (gün) Revisit (days)		
				Spektral çözünürlük (µm) (S=Stereo) veya Polarimetri Spectral Resolution (µm) or Polarimetry	Yersel (m) Spatial (m)	Radyometrik Radiometric (bit)				
ALI/ EO-1	NASA/USA	2000	PAN	0.48-0.69	10	16	37	16 (7-9)		
			Multi	0.433-0.453,0.45-0.515,0.525-0.605,0.63-0.69 0.775-0.805,0.845-0.89,1.2-1.3,1.55-1.75,2.08-2.35	30	16	37			
ALOS	JAXA / Japan	2006	PALSAR PRISM AVNIR-2	L-Band 1270 MHz, 23.6 cm. (see/Bkz: PALSAR-ALOS) Pan:0.52-0.77 (Triplet) 0.42-0.50,0.52-0.60,0.61-0.69,0.76-0.89	10-100 2.5 10	3/5 8 8	20-350 70(nadir) 35(back) 70(nadir)	46 (2)		
ALSAT-1	DMC- Algeria	2002	Multi	0.52-0.62(Green), 0.63-0.69(red),0.76-0.9(NIR)	32	10	640	4		
ASTER/TERRA	METI & NASA / Japan -USA	1999	VNIR	0.52-0.60,0.63-0.69,0.76-0.86 (S)	15	8	60	48 (16)		
			SWIR	1.60-1.70,2.145-2.185,2.185-2.225,2.235-2.285, 2.295-2.365,2.360-2.430	30	8				
TIR				8.125-8.475,8.475-8.825,8.925-9.275,10.25-10.95 10.95-11.65	90	12				
BEIJING-1	BLMIT-DMC/China	2005	PAN Multi	0.5-0.8 0.52-0.62, 0.63-0.69, 0.76-0.9	4 32	8 10	24 640	14(7) 5 (7)		
BİLSAT	TUBITAK SPACE- DMC / Türkiye	2003-2006	PAN Multi	0.45-0.90 0.45-0.52,0.52-0.60,0.63-0.69,NIR:0.76-0.90	12.6 27.6	8 8	25 55	116(5) 52 (4)		
CARTOSAT-1 (IRS-P5)	ISRO / India	2005	PAN	0.5-0.85 (S)	2.5	10	27.5 (S)/55 (M)	126 (5)		
CARTOSAT-2	ISRO /India	2007	Mono Paint-Brush Multi-View	0.45-0.85	0.8	10	(9.6/28/50)x9.6 9.6x38, 28x29, 50x19 (9.6/15/28)x9.6	4-5		
CBERS-1/2	INPE -CAST / Brasil- China	1999/2003	PAN	0.51-0.73 (S)	20	8	113	26 (3)		
			Multi	0.45-0.53, 0.52-0.59,0.63-0.69, NIR:0.77-0.89	20	8	113	26 (3)		
CBERS-2B		2007	IRMSS	0.50-1.10(P), 1.55-1.75, 2.08-2.35(S), 10.40-12.50(T)	80/160(T)	-	120	26		
			WFI-Multi	0.63-0.69, NIR: 0.77-0.89	260	-	890	5		
			HRC	0.50-0.80 (Additional for Cybers-2B)	2.7	8	27	130		
COSMOSKY-MED-1, 2 &3	Agenzia Spaziale / Italiana	2007/2008/2009	SpotLight1	X-Band	λ: 0.031m FRQ:9.6 GHz	Gaz/Classified Single: HH / HV Dual:HH+VV / HH+HV / VV+VH Single:HH / HV/ VH / VV Single:HV / HV / VH / VV Single:HV / HV / VH / VV	-	-	-	
			SpotLight2				1	3	10	
			PingPong				15	8	30	
			StripMap				3-15	3	40	
			WideRegion				30	8	100	
HugeRegion	100	8	200							
DEIMOS-1	Deimos/Spain	2009	MS	0.52-0.60, 0.63-0.69, 0.77-0.90	22	8	600	1		
DUBAISAT-1	EAST/UAE	2009	PAN	0.42 -0.89 (S CT)	2.5	8	20	5(3)		
			MS	0.42-0.51, 0.51-0.58, 0.60-0.72, 0.76-0.89 (S-CT)	5	8	20	5(3)		
ENVISAT	ESA /EU	2002	ASAR-Image	C-band	λ: 0.056m FRQ:5.33 GHz	Single: HH/VV Alternate: HH+HV/VV+VH/HH+VV Single:HH / VV	30	1.5-3.5	56-100	
			ASAR-Alt.Pol.				30		56-100	
			ASAR-WS				150		405	
MERIS	15 bands (0.39-1.040)	300/1200	8	1150	35 (3)					
EROS A1	ImageSat /Israel	2000	PAN	0.5-0.9 (S)	1.9/0.9	10	14/7	1.8-4		
EROS B1	ImageSat / Israel	2006	PAN	0.5-0.9 (S)	0.7	10	7	1.8-4		
ERS-1/2	ESA /EU	91-00/95	SAR Image Mode	C-Band	λ: Frqz:5.3GHz	Single:VV	30	-	100	3-35

Figure 3.15 Technical specifications of earth observing satellites (Nik System)

Sensör/Uydu Sensor/Satellite	Operatör / Ülke Operator/ Country	Başlangıç ve Sonlama Tarihi (launch & end date)	Sensör Tipi (Sensor type)	Çözünürlük (Resolution)			Şerit Geniliği Swath(km)	Görüntüleme Sıklığı (gün) Revisit (days)
				Spektral çözünürlük (µm) (S=Stereo) veya Polarimetri Spectral Resolution (µm) or Polarimetry	Yersel (m) Spatial (m)	Radyometrik Radiometric (bit)		
FORMOSAT	NSPO / Tayvan	2004	PAN	0.45-0.90	2	8	24	1
			Multi	0.45-0.52, 0.52-0.60, 0.63-0.69, 0.76-0.90	8	8	24	1
GEOEYE-1	GeoEye / USA	2008	PAN	0.45-0.80	0.41	11	15.2	<3
			Multi	0.45-0.51, 0.51-0.58, 0.655-0.69, 0.78-0.92	1.65	11	15.2	<3
HYPERION/ EO-1	NASA / USA	2000	HYPERION	220 spektral band (0.4-2.5µm arası - hyperspektral)	30	16	7.7	16 (7-9)
IKONOS-2	GeoEye /USA (Space Imaging)	1999	PAN	0.526-0.929 (S)	0.82	11	11.3	3.5-5
			Multi	0.445-0.516,0.506-0.595,0.632-0.698,0.757-0.853 (S)	3.2	11	11.3	3.5-5
IRS 1C/D	ISRO / India	1995/97	PAN	0.5-0.75 (S)	5.8	6	70.5	
			LISS-III	VNIR:0.52-0.59,0.62-0.68,0.77-0.86,SWIR:1.55-1.70	23	7	141	24/25
			WIFS	0.62-0.68,0.77-0.86	188	7	812	
IRS-P6 (ResourceSat-1)	ISRO / India	2003	LISS-III	0.52-0.59,0.62-0.68,0.77-0.86 SWIR:1.55-1.70	23.5	7-10 SWIR	140	24
			LISS-IV	MX:0.52-0.59,0.62-0.68,0.77-0.86 / Mono:0.62-068	5.8	7	24/70 (M)	5
			AWIFS	0.52-0.59,0.62-0.68,0.77-0.86 SWIR:1.55-1.70	56-70	10	2 x 370	5
JERS 1	JAXA / Japan	1992- 1999	OPS	VNIR:0.52-0.60,0.63-0.69,0.76-0.86 (S)	18	6	75	44
			OPS	SWIR:1.60-1.71,2.01-2.12,2.13-2.25,2.27-2.40	18	6	75	44
KOMPSAT-1	KARI /G.Korea	1999	EOC	PAN:0.51-0.73	6.6	8	17	28
			OSMI(ocean)	MS:0.412-0.443,0.490-0.555,0.765-0.865	1000	-	800	28
KOMPSAT-2	KARI /G.Korea	2006	PAN	0.50-0.90	1	10	15	28 (3)
			MSC	0.45-0.52, 0.52-0.60, 0.63-0.69, 0.76-0.90	4	10	15	28 (3)
LANDSAT-1/2/3	NASA-EOSAT/USA	1972/75/78 1978/82/83	MSS	VNIR:0.5-0.6,0.6-0.7,0.7-0.8,0.8-0.11	80	8	180	18
LANDSAT-4/5	Space Imaging- NASA/USA	1982/84, 1987/-	TM	VNIR:0.45-0.52,0.52-0.60,0.63-0.69,0.76-0.90	30	8	183	16
			TM	SWIR:1.55-1.75,2.08-2.35	30	8	183	16
			TM	TIR:10.42-12.5	120	8	183	16
LANDSAT-7	NASA /USA	1999-2003 (sic- off)	PAN	0.52-0.9	15	8	185	16
			ETM	VNIR ve SWIR Landsat 5 ile aynı (same as Landsat-5)	30	8	185	16
			ETM	TIR:10.42-12.5 (Low-High gain)	60	8	185	16
MODIS/TERRA	METI-NASA /JP-USA	1999	MODIS	2 spektral band	250	8	2330	1-2
			MODIS	7 spektral band	500	8	2330	1-2
MONITOR-E	GKNPT & RSA /RU	2005-2007	PAN	0.54-0.84	8	8	96	-
NIGERIASAT-1	NIGERIA	2003	Multi	0.52-0.62,0.63-0.69,0.76-0.90(NIR)	20	8	160	-
ORBVIEW-3	GeoEye (ORBIMAGE) / USA	2003-2007	PAN	0.45-0.90	1	11	8	8
			Multi	0.45-0.52,0.52-0.60,0.62-0.695,0.76-0.9(S)	4	11	8	8
ORBVIEW-2 (SeaStar)	GEOEYE(ORBIMAGE) NASA	1997	SeaWifs	0.402-0.422,0.433-0.453,0.480-0.500,0.500-0.520	4500 GAC	10	1500 GAC	1
			SeaWifs	0.545-0.565,0.660-0.680,0.745-0.785,0.845-0.885	1130 LAC	10	2800 LAC	1
PALSAR/ALOS	JAXA - METI/ Japan	2006	Fine ScanSAR (1) ScanSAR (2)	L-Band λ:0.236 m Frq:1.27 GHz, Single: HH/VV Dual:HH +HV / VV+VH Full Polarimetry:HH+HV+VH+VV Single: HH/VV Single: HH/VV	6.25	5	40-70	46 (2)
					12.5	5	40-70	
					25	3/5	20-65	
					50	5	250-350	
					25	5	250-350	
PLEIADES-1 &2	CNES/France	2010/2012	PAN	0.480-0.830 (S)	0.5 (0.7)	12	20	26 (1)
			MS	0.43-0.55, 0.49-0.61, 0.60-0.72, 0.75-0.95 (S)	2	12	20	26 (1)
PROBA	ESA	2001	HRC	PAN	8	-	8.2	-
			CHRIS	0.415-1.050 with 5-12nm spectral res. 19 bands	18	-	14	-

Figure 3.16 Technical specifications of earth observing satellites (Nik System)

Sensör / Uydu Sensor/Satellite	Operatör / Ülke Operator/ Country	Başlangıç ve Sonlama Tarihi (launch & end date)	Sensör Tipi (Sensor type)	Çözünürlük (Resolution)			Yersel (m) Spatial (m)	Radyometrik Radiometric (bit)	Şerit Geniğiği Swath(km)	Görüntüleme Sıklığı (gün) Revisit (days)
				Spektral çözünürlük (µm) (S=Stereo) veya Polarimetri Spectral Resolution (µm) or Polarimetry						
RADARSAT -1	CSA / Kanada	1995	SAR	C Band	A:0.057m, Frq:5.3 GHz	HH Pol.16 beam mode, (S)	8-100	-	50-500	24 (3-35)
RADARSAT - 2	CSA-MDA/ Kanada	2007	SAR	C Band	A:0.055m, Frq:5.405GHz	HH,VV,HV,VH (S) Single, Dual ve Quad Pol. (S)	3-100	-	20-500	24 (3-35)
RAPIDEYE- 1/2/3/4/5	RapidEye / DE.	2008	Multi		0.44-0.51, 0.52-0.59, 0.63-0.685, 0.69-0.73, 0.76-0.85		6.5	12	77	5.5 (1)
RASAT	TUBITAK-SPACE /TR	2010	PAN MS		0.42-0.73 0.42-0.55, 0.55-0.56, 0.58-0.73		7.5 15	8 8	30 30	4
RAZAKSAT-1	ATSB & TPM /Malasia	2009	PAN MS		0.51-0.73 0.45-0.52, 0.52-0.60, 0.63-0.69, 0.76-0.89		2.5 5	8 (10) 8 (10)	20 20	14
RESOURCE-DK1	Ts-SKB/Rus	2006	PAN Multi		0.58-0.8 0.5-0.6, 0.6-0.7, 0.7-0.8		1 2-3	- -	28 28	- -
RISAT-1	ISRO	2009	SAR	C Band	A:0.056m, Frq:5.35 GHz	Single, Dual & Quad Pol.,	3-50	-	30-240	12
SAC-C	CONAE / Argentina	2000	MMRS HRTC HSTC	S VNIR PAN-VNIR PAN-VNIR			175 35 250	8 8 8	360 90 1000	9 (7) 16 2
SAOCOM-1	CONAE / Argentina	2010	SAR	L Band	A:0.235m Frqz:1.275GHz		7-100	-	50-400	16
SPIN 2 ve Mekikler	RUSSIA	88/95 98/05 Periyodik	MK-4 KVR-1000/DK1 TK-350	Visible:0.515-0.565,0.635-0.690,0.810-0.900 Pan 0.49-0.59 Topoğrafik Kamera: 0.49 -0.59 (S)			15,8,15 2-1 10	Film	150 40 200	8 - -
SPOT -1/2/3	CNES & Astrium /France	1986/90/93 - / - / 96	HRV-PAN HRV	0.51-0.73 (S) VNIR:0.50-0.59,0.61-0.68,0.79-0.89 (S)			10 20	8 8	60 60	26(1-4)
SPOT-4	CNES & Astrium /FR	1998	HRV-PAN HRVIR Vegetation	0.61-0.68 (S) VNIR:0.50-0.59,0.61-0.68,0.79-0.89, SWIR: 1.58-1.75 0.43-0.47,0.61-0.68,0.78-0.89,1.58-1.75			10 20 1000	8 8 4/8	60 60 2200	26(1-4) 26(1-4) 1
SPOT-5	CNES & Astrium /FR	2002	HRS-PAN HRG-PAN HRG HRG Vegetation	0.49-0.69 (S) 0.49-0.69 Super mode (S) VNIR:0.49-0.61,0.61-0.68,0.78-0.89(S) SWIR:1.58-1.75 0.43-0.47,0.61-0.68,0.78-0.89,1.58-1.75			10 2.5 - 5 10 20 1000	8 8 8 8 4/8 bit	120 60 60 60 2250	26(1-4) 26(1-4) 26(1-4) 26(1-4) 1
QUICKBIRD	Digital Globe /USA	2001	PAN Multi	0.445-0.900 (S) VNIR:0.45-0.52,0.52-0.60,0.63-0.69,0.76-0.89 (S)			0.61-0.73 2.5-2.9	11 11	16.5 16.5	3.5
TANDEM-X	DLR&EADS-Astrium/ Germany	2010	SAR	TerraSAR-X ile aynı özelliklerde ve aynı yörüngede Tandem konfigürasyonunda olacaktır to TerraSAR-X in tandem orbit configuration			Properties are similar			
TERRASAR-X	DLR&EADS-Astrium/ Germany	2007	Spotlight StripMap ScanSAR	X-Band	A:0.031m Frqz:9.65GHz	Dual (HH+VV),Single (VV/HH) Single:VV/HH: Dual :HH+VV/ HH+HV / VV+HV Single:VV / HH	1 3 5 16	- - - -	5 x10 15 30 100	15
THEOS	GISTA/Thailand	2008	PAN MS		0.45 - 0.90 0.45-0.52, 0.53-0.60, 0.62-0.69, 0.77-0.90		2 15	8 8	22 90	26 (14-5)
TOPSAT	BNSC-UK MoD/ UK	2005	PAN MS		0.50-0.70 0.40-0.50, 0.50-0.60,0.60-0.70		2.8 5.6	- -	17 17	4 (2-2.5)
UK-DMC1	DMCII / UK	2003	MS		0.52-0.62, 0.63-0.69,0.76-0.90		30-40	8	640	14
UK-DMC2	DMCII / UK	2009	MS		0.52-0.60, 0.63-0.69, 0.77-0.90		22	8	660	-
WORLDVIEW-1	Digital Globe / USA	2007	PAN		0.40-0.90 (S)		0.5	11	17.6	5
WORLDVIEW-2	Digital Globe / USA	2009	PAN MS		0.45-0.80 (S) 0.40-0.45, 0.45-0.51, 0.51-0.58, 0.585-0.625, 0.63-0.69, 0.705- 0.745, 0.77-0.895, 0.860-1.04 (S)		0.46 1.84	11 11	16.4 16.4	7 (1.1)

Figure 3.17 Technical specifications of earth observing satellites (Nik System)

3.2.6.1 Landsat

NASA (National Aeronautical and Space Administration) launched Landsat 1-2 and 3 satellites in space to observe the surface of the earth in 1972. Then, Landsat 4-5 and 7 took the place of Landsat 1-2 and 3. Landsat 4 and 5 contain MSS (Multispectral Scanner) and TM (Thematic Mapper) sensors and Landsat 7 contains ETM (Enhanced Thematic Mapper) sensor. This satellite is used for geological purposes such as identification of main rock types (igneous, metamorphic, sedimentary), mapping the volcanic activity, determination of dom-caldera structures, large regional structures, linear and circular structures, hydrothermal alteration zones and geothermal studies (Table 3.1, 3.2).

Table 3.1 Technical specification of Landsat sensors

Sensors	LANDSAT 4-5 MSS	LANDSAT 4-5 TM	LANDSAT 7
Spatial Resolution	PAN: 30 m. MS: 79 m.	28.5 m.	PAN: 15 m. MS: 30-60 m.
Spectral Resolution	0.50-1.10	0.45-12.50	0.45-12.50
Radiometric Resolution	6 bit	8 bit	8 bit
Temporal Resolution	16 Days		
Swath(Scan Width)	185x170 km.		185 km.
Orbital Height	900 km.	705 km.	
LANDSAT 4-5 MSS			
Bands	Wavelength(μm)		Usage Areas
Band 1: Green	0.50-0.60		Determining healthy plants and water basins
Band 2: Red	0.60-0.70		Separation plants, determining soil and geological boundaries
Band 3: Near IR	0.70-0.80		Product yield prediction, soil/crop and land/water classification
Band 4: Near IR	0.80-1.10		Monitoring plants and penetrate mist

Table 3.2 Technical specification of Landsat sensors

Bands	Wavelength(μm)	Usage Areas
LANDSAT 4-5 TM		
Band 1: Blue	0.45-0.52	Discrimination soil/vegetation, mapping bathmetry/coast, determining cultural/residential properties
Band 2: Green	0.52-0.60	Mapping green plants and determining cultural/residential properties
Band 3: Red	0.63-0.69	Seperate plant species, soil/crop and land/water classification
Band 4: Near IR	0.76-0.90	The amount of live and healthy plants, land/crop and land/water classification
Band 5: Middle IR	1.55-1.75	Seperation moisture, snowand ice in vegetation and soil and cloudy areas
Band 6: Thermal IR	10.40-12.50	Seperation plant and unhealthy products, insecticidal treatments, heat density and thermal pollution
Band 7: Middle IR	2.08-2.35	Distinguish the boundaries of geological rock and soil types, determining moisture in soil and plants
LANDSAT 7		
Band 1: Blue	0.45-0.515	They used in the same areas that Landsat 4-5 MSS and TM are used
Band 2: Green	0.525-0.605	
Band 3: Red	0.63-0.69	
Band 4: Near IR	0.75-0.90	
Band 5: Middle IR	1.55-1.75	
Band 6: Thermal IR	10.40-12.50	
Band 7: Middle IR	2.08-2.35	
PAN	0.52-0.90	

3.2.6.2 Terra Aster

Aster sensor was mounted on Terra satellite of NASA by the USA in cooperation with Japan in 1999. There are five different modules on Terra satellite as; ASTER, MODIS, CERES, MOPITT and MISR. Aster has 8 bit radiometric resolution and scans the same area in 16 days. Aster images are used for geological purposes such as; description of rock types, detailed mapping of volcanic activity, determination of linear and circular structures, mapping of hydrothermal alteration zones and mineralogical zones, determination of geothermal fields and acquisition three

dimensional stereoscopic images. The most important of these areas is the mapping of minerals and alterations because of Aster can create images in 14 bands (Table 3.3).

Table 3.3 Technical specification of Aster sensor

Band	Label	Wavelength	Resolution	Nadir or
		(μm)	(m)	Backward
B1	VNIR_Band1	0.520–0.600	15	Nadir
B2	VNIR_Band2	0.630–0.690	15	Nadir
B3	VNIR_Band3N	0.760–0.860	15	Nadir
B4	VNIR_Band3B	0.760–0.860	15	Backward
B5	SWIR_Band4	1.600–1.700	30	Nadir
B6	SWIR_Band5	2.145–2.185	30	Nadir
B7	SWIR_Band6	2.185–2.225	30	Nadir
B8	SWIR_Band7	2.235–2.285	30	Nadir
B9	SWIR_Band8	2.295–2.365	30	Nadir
B10	SWIR_Band9	2.360–2.430	30	Nadir
B11	TIR_Band10	8.125–8.475	90	Nadir
B12	TIR_Band11	8.475–8.825	90	Nadir
B13	TIR_Band12	8.925–9.275	90	Nadir
B14	TIR_Band13	10.250–10.950	90	Nadir
B15	TIR_Band14	10.950–11.650	90	Nadir

3.2.6.3 Spot

French satellite Spot-1 was launched in 1986 and Spot-4 in 1998. The most important feature of the Spot sensors is detecting three-dimensional images and thus it can create digital elevation models (DEM) of the area (Table 3.4).

3.2.6.4 Ikonos

It was launched in 1999 by the United States. It is largely used for military purposes (Table 3.5).

Table 3.4 Technical specification of Spot sensors

Sensors	SPOT PAN	SPOT XS	SPOT 4
Spatial Resolution	10 m.	20 m.	10 and 20 m.
Spectral Resolution	0.51-0.73	0.50-0.89	0.50-1.75
Radiometric Resolution	8 bit		
Temporal Resolution	26 days		5 days
Swath(Scan Width)	60 km.		
Orbital Height	832 km.		
Bands	Wavelength(μm)	Usage Areas	
SPOT PAN			
PAN	0.51-0.73	plant and timber management, route and location analysis, flood and erosion analysis / management, groundwater and watershed analysis	
SPOT XS			
Band 1: Green	0.50-0.59	Determining healthy plants	
Band 2: Red	0.61-0.68	Seperation planr species, qualification soil and geological boundaries	
Band 3: Near IR	0.79-0.89	The amount of live and healthy plants, soil/crop and land/water classification	
SPOT 4			
Band 1: Green	0.50-0.59	Used more carefully in the areas where PAN and XS modes have used	
Band 2: Red	0.61-0.68		
Band 3: Near IR	0.79-0.89		
Band 4: Near IR	1.58-1.75		
PAN	0.61-0.68		

Table 3.5 Technical specification of Spot sensors

Spatial Resolution	Pancromatic: 1m, Multispectral: 4m	
Spectral Resolution	0.45-0.90	
Radiometric Resolution		
Temporal Resolution	2.9 Days	
Swath(Scan Width)	13 km.	
Orbital Height	681 km.	
Bands	Wavelength(μm)	Usage Areas
Band 1: Blue	0.45-0.52	The usage areas are the same as Landsat and Spot satellites'.
Band 2: Green	0.52-0.60	
Band 3: Red	0.63-0.69	
Band 4: Near IR	0.76-0.90	
PAN	0.45-0.90	

3.2.7 Image Processing

The developments in technology enabled most of the remotely sensed data to be recorded in digital format and caused it to be dependent on some aspects of enhancement analysis and digital procedures. In order to carry out these processes in a better way; operations like formatting, correcting and developing the data are done completely by computers. Computers that contain hardware and software enabling the remotely sensed images to be processed are called 'Image Processing Systems'.

Image processing operations are carried out in four stages;

- Image restoration
- Image enhancement
- Image classification
- Image transformation

3.2.7.1 Image Restoration

Image restoration process can be classified as two types;

- Radiometric restoration
- Geometric restoration

3.2.7.1.1 Radiometric Restoration. Radiometric restoration is the process of elimination and exreaction of atmospheric noise and unwanted objects detected irregularly by the sensor. This operation corrects the errors caused by sensors which lose their sensivity in time, differences in illumination, geometry of sensor sight, atmospheric conditions (water vapor, volcanic gases, CO₂, clouds or haze) or interferences that sensors create.

Radiometric restorations are carried out in various methods;

- *Sensor Calibration*
- *Radiance Calibration*; synchronizing the spectral brightness values of the digital numbers(DN) with the brightness values of the image.
- *Band Striping*; correcting the error which occurs as a result of scanning the same area with sensors at different heights (Figure 3.18).

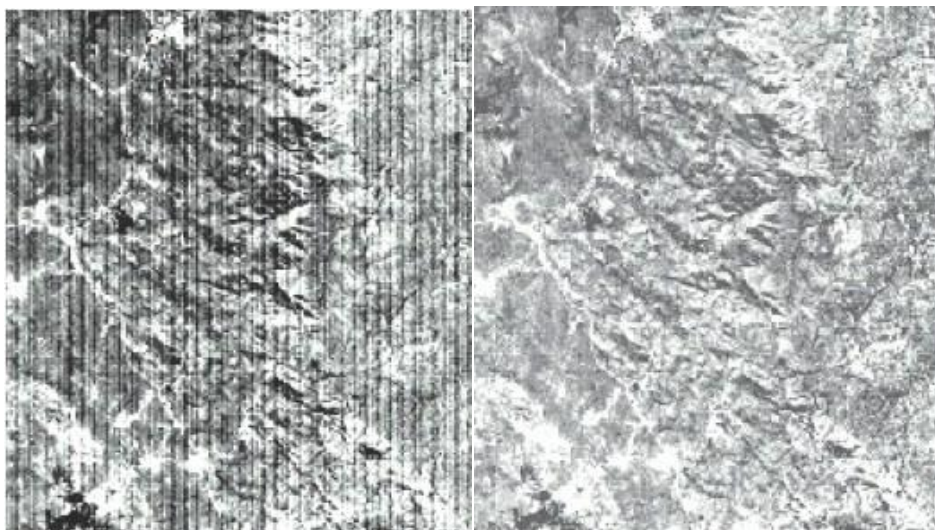


Figure 3.18 Band striping error image and image after correction (IDRISI Manual)

- Mosaicing; a multi-image of a particular area created by comparing the images recorded at different days and hours.
- Atmospheric Correction; rectification of the effect of the atmosphere on the remotely sensed image.
- Dark Object Subtraction Model; removal of dark areas of the image.
- Cos(t) Model; reducing the effects of absorption of the energy by the atmospheric gases.
- Full Correction Model; correction of the scattering depending on the thickness of the atmosphere.
- Apparent Reflectance Model; converting the DN values to the approximate reflectance values.
- An Alternative Haze Removal Strategy (Figure 3.19)



Figure 3.19 Landsat TM Band 1 images before and after haze removal (IDRISI Manual)

- Band Ratioing; dividing the image of a band by another image of a band.
- Image Partitioning; correcting the illumination errors resulting from the slope and aspect of the area.
- Illumination Modelling
- Noise Elimination
- Scan Line Drop Out; correcting the data loss caused by the interruption of the signal reaching the sensor.

3.2.7.1.1 Geometric Restoration. Geometric restoration is the process of eliminating the geometric distortion in the raw image and placing the image into a defined coordinate system by using ground control points. This operation corrects the errors caused by the global structure of the earth, the point of view of the satellite, unequal movements of the sensors according to each other and the movement of the loop of the satellite.

The images without coordinate system are corrected by the process called resampling. Three different methods are used for resampling;

- *Nearest Neighbour Method*; the pixels taken from the original image are adapted to the nearest pixel in the digitally rectified image.
- *Bilinear Interpolation Method*; the weighted average of four pixels taken from the original image is calculated and adapted to the new pixel locations.
- *Cubic Convolution Method*; as in the Bilinear Method, this time sixteen pixels are adapted to the new pixel locations.

3.2.7.2 Image Enhancement

Image enhancement is the operation done in order to increase the visual quality of the raw remotely sensed image.

Image enhancement techniques are divided into four groups;

- *Contrast Stretch*; creation of a histogram, which is a graphic indicates the brightness values of the image and clarifying the details by increasing the contrast of the image (Figure 3.20).
- *Composite Generation*; combining the different bands for the visual analysis (Figure 3.21).
- *Digital Filtering*; is an operation for sharpening, clarifying or removing the image features. Low-Pass Filter is used for reducing and High-Pass Filter for clarifying the details in the images. Also, clarifying the linear details such as roads and faults Directional/Edge Detection Filter is used.

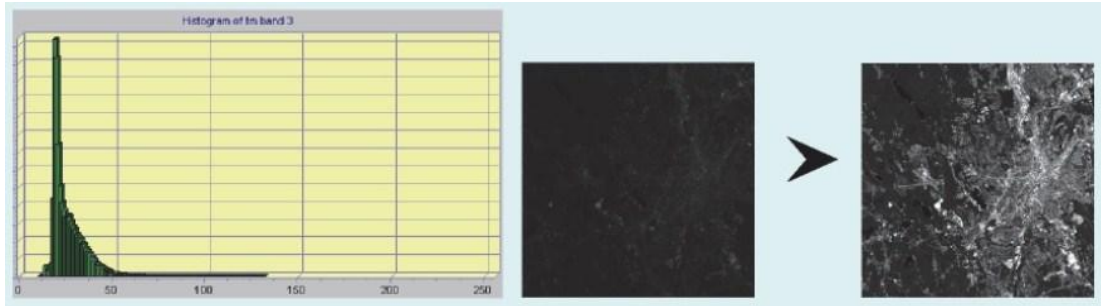


Figure 3.20 TM Band 3 (visible red) and its histogram and after contrast stretching values between 12 and 60 (IDRISI Manual)

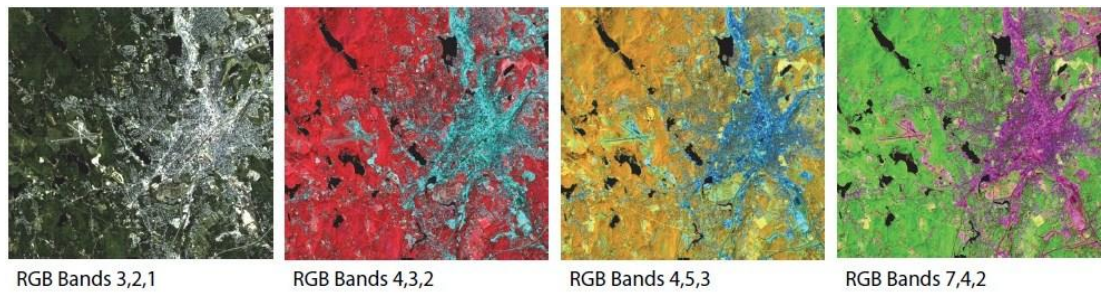


Figure 3.21 Several composites made with different band combinations from the same set of TM images (IDRISI Manual)

- *Pansharpening*; combining the high-resolution panchromatic image with the low-resolution multispectral image to display more details (Figure 3.22).



Figure 3.22 Panchromatic merge using Quickbird imagery-multispectral at 2.4 m, panchromatic at 0.6 m. Raw image is on the left and image on right is after the merge (IDRISI Manual)

3.2.7.3 Image Classification

Image classification is a process of creating thematic maps of an image data set. Classification is carried out by the method of Spectral Pattern Recognition. This method categorizes the image into a limited number of discrete classes by comparing the undefined signatures with the defined signatures automatically.

Classification of an image is carried out by two methods;

- Unsupervised Classification; is a method that computers execute automatically (Figure 3.23).

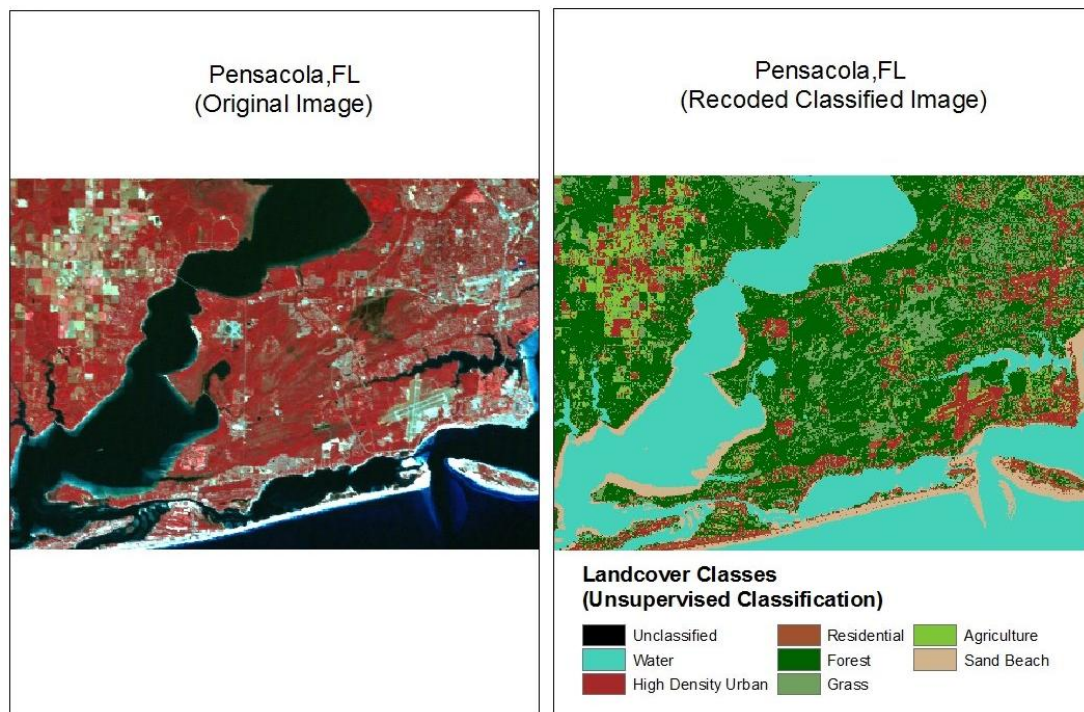


Figure 3.23 Unsupervised classification image of Pensacola, FL (anonymus)

- Supervised Classification; is a method that computer users carry out according to the determined number of classes (Figure 3.24). Supervised classification can be performed by Minimum Distance Method, Maximum Likelihood Method, Parallelepiped Method or Linear Discrimination Method.

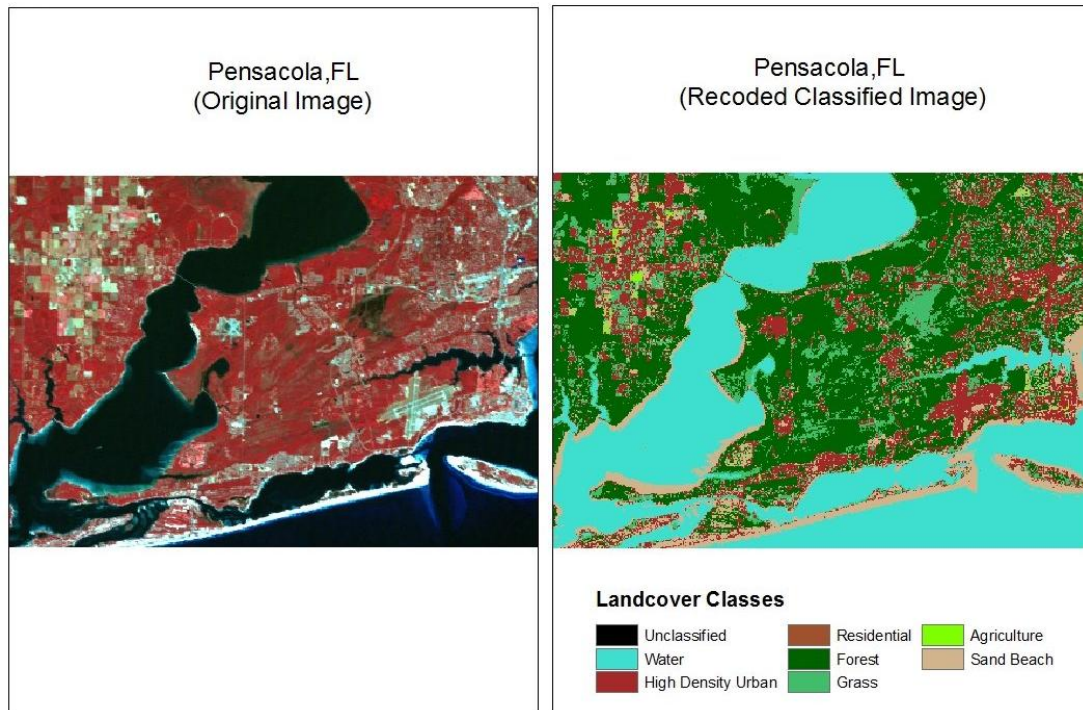


Figure 3.24 Supervised classification image of Pensacola,FL (anonymus)

3.2.7.4 Image Transformation

Image transformation is a process of obtaining a new image from a multispectral image or from two or more images of the same area recorded at different dates. The process is carried out by the help of the arithmetic operations.

Arithmetics of images can be processed as;

- *Image Subtraction*; determining the changes between two images recorded at different dates.
- *Image Rationing*; determining the characteristics of the vegetation.

Also, Principal Component Analysis is a method for converting images easier and more efficiently. The analysis provides more information about the image by reducing the amounts of bands in the multispectral data sets or using the relationship between the bands. For example; the first 3 bands in the 7-band Thematic Mapper (TM) data set contains 90% of the information. By combining these 3 bands PCA creates a single image and this helps for determining anomaly areas of the image.

3.2.8 Usage Areas Of Remote Sensing

Remote sensing satellites are designed for specific purposes. As a result of this, remote sensing is used in many fields ranging from military purposes to daily life. It is used in areas such as; mapping (creating digital terrain models, monitoring the deformation of surface and production of topographic maps), hydrology (management of water resources, analyzing the water quality, examination of the pollution in sea, lake and river, mapping the flood, determination of sea level temperature and amount of ice and its movement and monitoring ship waste), agriculture (separation of plant type, monitoring plant growth, determination of crop yield and determination the type of soil and its humidity), geology (researching and mapping of geological structures, identification of faults, lineaments and fractures, geothermal, earthquake and volcanic research, exploration of minerals, earth resources and oil and determination of rock types) and forestry (mapping forest species, monitoring the tree diseases and desertification, planning of timber production and monitoring forest fire).

3.2.9 Remote Sensing In Turkey

The applications of remote sensing technology is increasing rapidly in Turkey. Over the past twenty years, General Command of Mapping has been using the remote sensing data for the creation of topographic maps. Also, projects are carried out by universities to establish ground stations.

Turkey's first earth observation and remote sensing satellite Bilsat-1 was launched in 2003 by Tubitak Uzay. It rotates in a circular sun-synchronous orbit at 686 km. height and it weighs 129 kg. It will be in service for 15 years and during the first five years of this period the satellite can be controlled. It is able to achieve multispectral images in four bands and its spatial resolution is 27.6 m. It also has a black-white camera with 12.6 m. spatial resolution (Figure 3.25, 3.26) (Table 3.6). Then, mission loads, called Çoban and Gezgin were launched. Çoban can record images with resolution of 640x480 from 120 m. of sampling distance. Gezgin captures images in JPEG2000 format with the size of 2048x2048 pixels from four different cameras (Figure 3.27).



Figure 3.25 BilSAT satellite (TUBITAK UZAY)

Table 3.6 Technical specification of BilSAT (TUBITAK UZAY)

BAND	RESOLUTION (μM)
1	0.45-0.52(Blue)
2	0.52-0.60(Green)
3	0.63-0.69(Red)
4	0.76-0.90(Near IR)

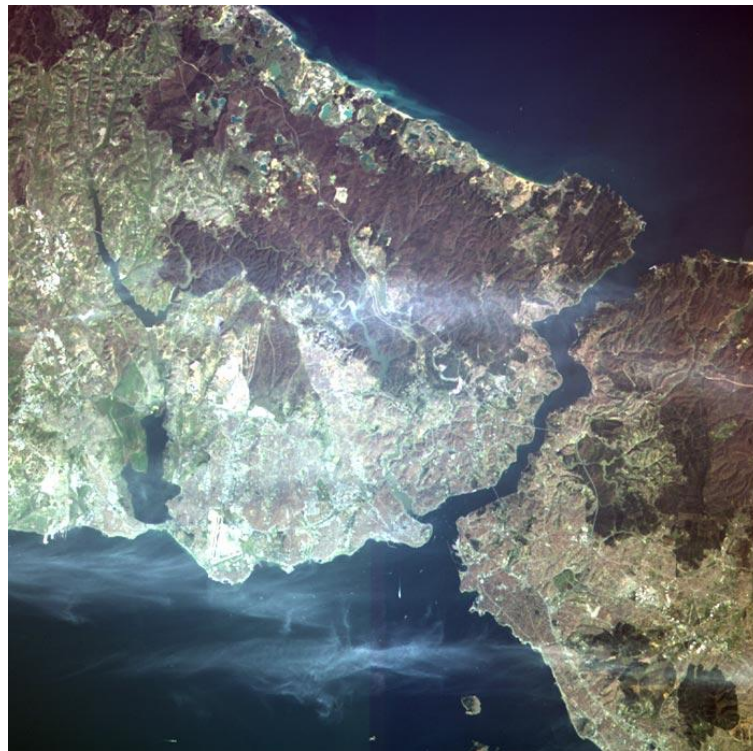


Figure 3.26 İstanbul, Turkey image recorded by BilSAT (TUBITAK UZAY)

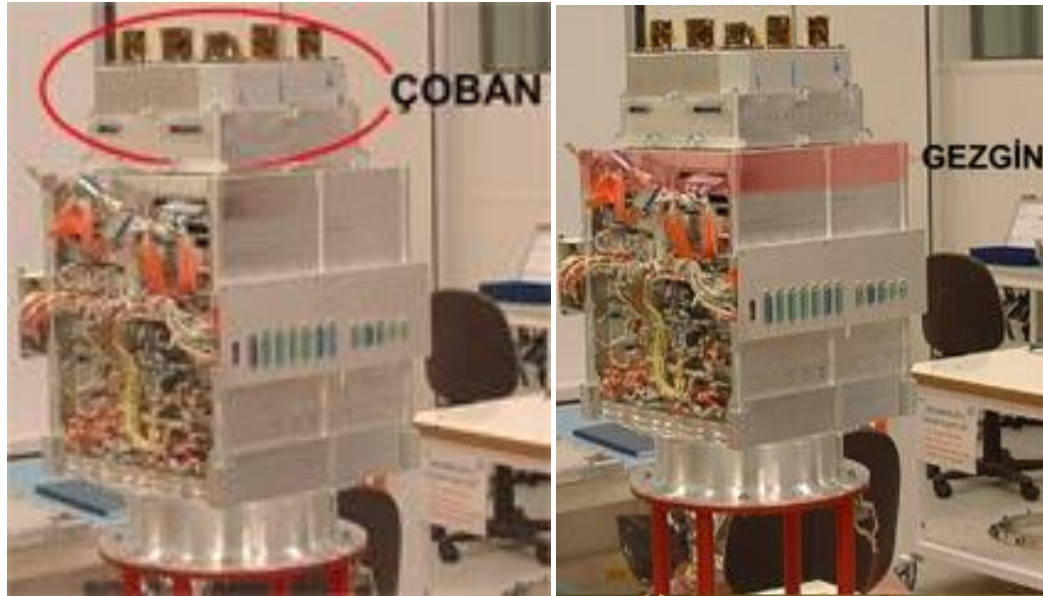


Figure 3.27 Çoban and Gezgin (TUBITAK UZAY)

Bilsat project aims to;

- have the necessary technical knowledge, production facilities (clean rooms, laboratories etc.) and trained manpower to gain the talent of designing and manufacturing satellites
- have the ability to manage every stage of a satellite project
- have an earth observation satellite and experience with the satellite image processing
- have a basis for developing more complex systems
- have subsystems for developing other satellite systems
- be a center in satellite design in Turkey.

Rasat, which is being constructed, will be the first observation satellite designed and manufactured in Turkey. The recorded data by Rasat will be used in monitoring disasters, environment and urban planning (Figure 3.28) (Table 3.7).

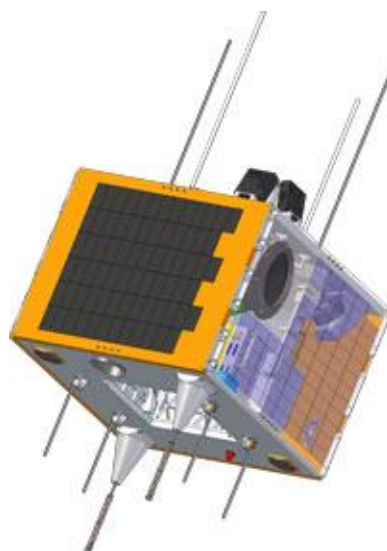


Figure 3.28 Rasat (TUBITAK UZAY)

Table 3.7 Technical specification of Rasat

Weight	93 kg
Orbit	at 689 km circular, sun-synchronized
Control of Management	3 controlled axis
Orbital Period	98.8 seconds
Local Time of Transition from the Equator	10:30
Spatial Resolution	Panchromatic: 7.5 m
	Multispectral: 15 m
Service Life	3 years
Spectral Resolution (μm)	0.42 – 0.73 (Panchromatic)
	1. Band: 0.42 – 0.55 (Blue)
	2. Band: 0.55 – 0.58 (Green)
	3. Band: 0.58 – 0.73 (Red)
Radiometric Resolution	8 bit
Temporal Resolution	4 days
Swath	30 km
Payloads	Optical payload: consists of Pushbroom viewer capable of stereoscopic vision.
	BiLGE: Spacewire datapath using flight computer.
	GEZGiN-2: Next generation image processing board that capable of encrypt and compress by JPEG2000 algorithms with high speed.
	X-Band Transmitter Module: Communication system with 100Mb/s transmission line and 7W output.

In addition, Göktürk-2 project became valid for creation of facilities, equipment and staff in designing, manufacturing, intergration, testing and developing satellite software and obtaining the necessary satellite needs by national resources in partnership with Ministry of National Defense, Tubitak and TAI in 2007. Göktürk-2 was launched from Jiuquan Satellite Launch Base in China on December 18, 2012 (Figure 3.29) (Table 3.8).

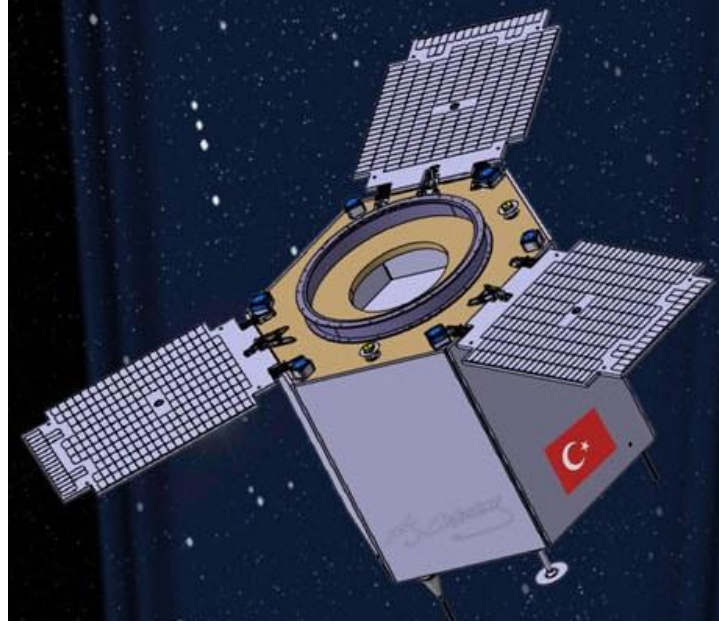


Figure 3.29 Göktürk-2 (TUBITAK UZAY)

Table 3.8 Technical specification of Göktürk-2

Orbit	Sun-synchronized
Orbital Altitude	700 km
Tour Time Around the World	98 seconds
Daily Exposure Time with the Ground	40 seconds(day and night)
Weight	409 kg
Image Storage Capacity	15 Gbit
Resolution	2.5 m

CHAPTER FOUR APPLICATIONS

4.1 Georeferencing

The process of georeferencing is done by matching the points on scanned maps or on satellite images mutually. Determining the location of these points is the most important step of the process. In order to avoid major disruptions georeferencing should be carried out meticulously and patiently.

A geological map of the study area is needed to define the geological units, identify the fault lines and make interpretation correctly.

First; the geological map and the active fault map of the area were converted to JPEG format from pdf format. ArcGis 10 software was used for digitizing process. Georeferencing Tool of ArcMap interface was used to coordinate the raster data.

After digitizing, geological units and fault lines were drawn and an attribute table was created by the help of the software called MapInfo Professional 11 (Figure 4.1, 4.2).

ID	GeologicalFormation	FormationAge	FormationTyp
7	Undifferentiated volcanic rocks (generally andesitic)	Lower-middle miocene	Volcanic
1	Undifferentiated quarternary	Quarternary	Sedimentary
2	Undifferentiated continental clastic rocks	Pliosen	Sedimentary
11	Carbonate and clastic rocks	Lower-middle triassic	Sedimentary
12	Carbonate rocks, clastic rokcs inplaces	Carboniferous	Sedimentary
3	Continental carbonate rocks	Middle-upper miocene	Sedimentary
6	Pyroclastic rocks	Lower-middle miocene	Volcanic
8	Clastic and carbonate rocks (flysch)	Upper senonian	Sedimentary
9	Neritic limestone	Lower jurassic	Sedimentary
5	Lacustrine limestone, marl, shale etc.	Lower-middle miocene	Sedimentary
4	Continental clastic rokcs	Lower-middle miocene	Sedimentary
10	Neritic limestone	Middle triassic-jurassic	Sedimentary

ID	Fault_Class	Fault_Name
0	Quaternary Fault	
0	Quaternary Fault	
0	Quaternary Fault	
0	Holocene Fault	Gulbahçe Fault Zone
0	Holocene Fault	Gulbahçe Fault Zone
0	Holocene Fault	Gulbahçe Fault Zone
0	Holocene Fault	Gulbahçe Fault Zone
0	Holocene Fault	Gulbahçe Fault Zone
0	Holocene Fault	Gulbahçe Fault Zone
0	Holocene Fault	Gulbahçe Fault Zone
0	Holocene Fault	Gulbahçe Fault Zone
0	Holocene Fault	Gulbahçe Fault Zone
0	Holocene Fault	Gulbahçe Fault Zone
0	Holocene Fault	Gulbahçe Fault Zone
0	Holocene Fault	Gulbahçe Fault Zone

Figure 4.1 The attribute tables of formations and faults created with MapInfo

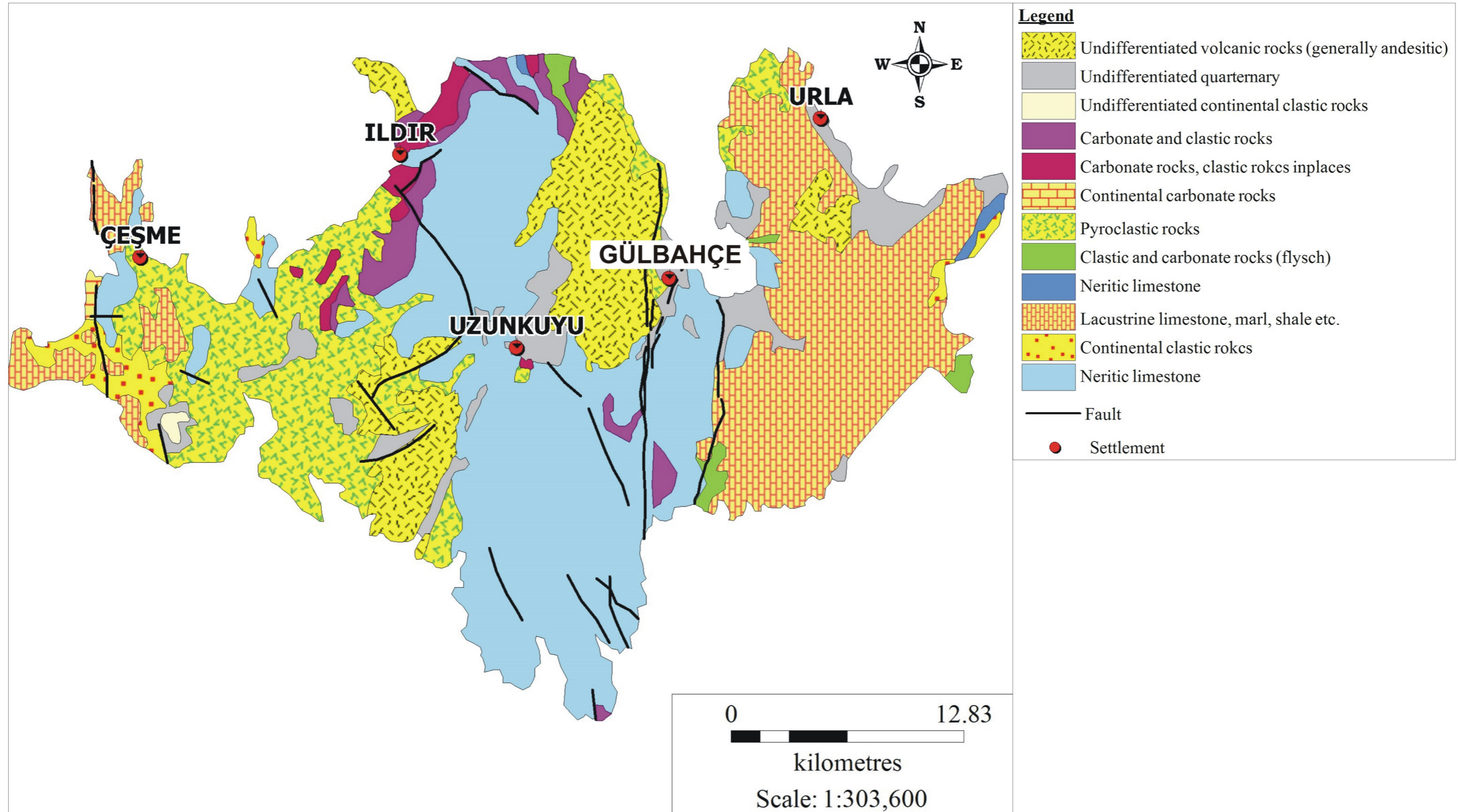


Figure 4.2 The geological map and active fault map of the study area after georeferencing process

4.2 Remote Sensing Applications

The markers detected by remote sensing techniques for geothermal resources explorations can be counted as thermal anomalies, cluster of minerals formed in specific regions as a result of hydrothermal alteration and the measurable effects of the heat on the vegetation. Also, remote sensing techniques are used for determining folds and faults by geomorphology operations (Çapar, 2009). Remote sensing applications are carried out with the Idrisi Selva software.

4.2.1 Filtering

The lineaments in the study area are determined by interpreting and filtering the panchromatic images. High-pass filters and directional/edge detection filters are used for this process. By using the filtering technique, details of the image with high frequency or low frequency and the edges can be enhanced in the desired regions of the image.

The output value of high-pass filtering is the sum of the products of each pixel value and its corresponding kernel value. Kernels are set by default as follows:

3X3		
-1/9	-1/9	-1/9
-1/9	+8/9	-1/9
-1/9	-1/9	-1/9

5X5				
-1/25	-1/25	-1/25	-1/25	-1/25
-1/25	-1/25	-1/25	-1/25	-1/25
-1/25	-1/25	24/25	-1/25	-1/25
-1/25	-1/25	-1/25	-1/25	-1/25
-1/25	-1/25	-1/25	-1/25	-1/25

7X7						
-1/49	-1/49	-1/49	-1/49	-1/49	-1/49	-1/49
-1/49	-1/49	-1/49	-1/49	-1/49	-1/49	-1/49
-1/49	-1/49	-1/49	-1/49	-1/49	-1/49	-1/49
-1/49	-1/49	-1/49	48/49	-1/49	-1/49	-1/49
-1/49	-1/49	-1/49	-1/49	-1/49	-1/49	-1/49
-1/49	-1/49	-1/49	-1/49	-1/49	-1/49	-1/49
-1/49	-1/49	-1/49	-1/49	-1/49	-1/49	-1/49

The 8th band of Landsat 7 was filtered using 3x3 kernel. For a better view, the contrast of display was set to be min -80 and max 60. By examining the new image

possible fault lines were aimed to determine. Then, to provide the accuracy of the predictions, the vector file of the fault lines was opened over the filtered image. It was observed that the actual fault line overlaps the possible fault line on the filtered image. The fault lines in the entire study area were analyzed and a portion of lines can not be identified by the filtered image.

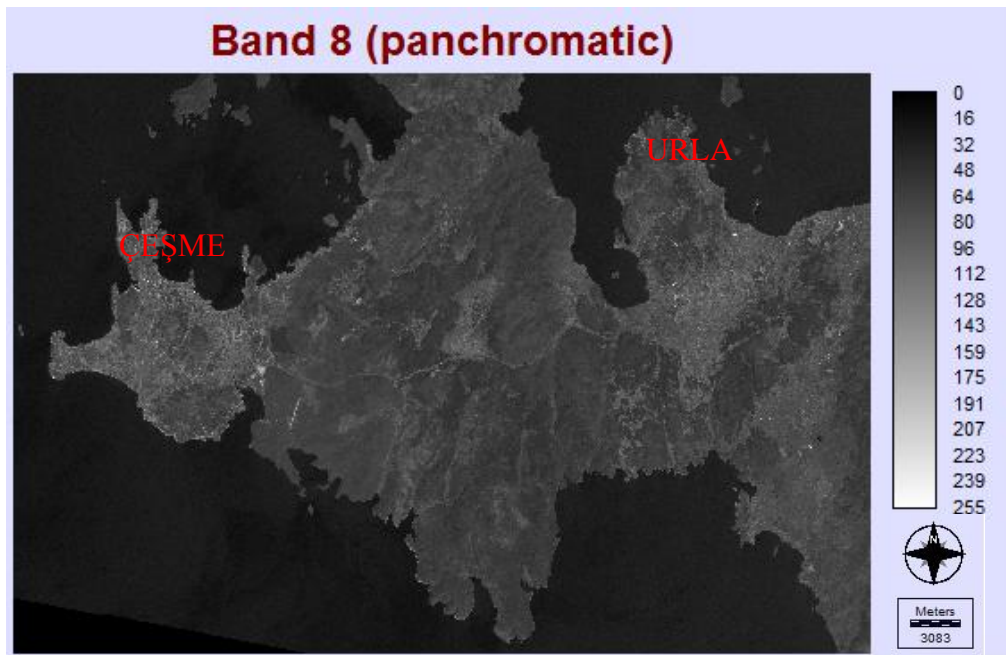


Figure 4.3 Band 8 of Landsat 7

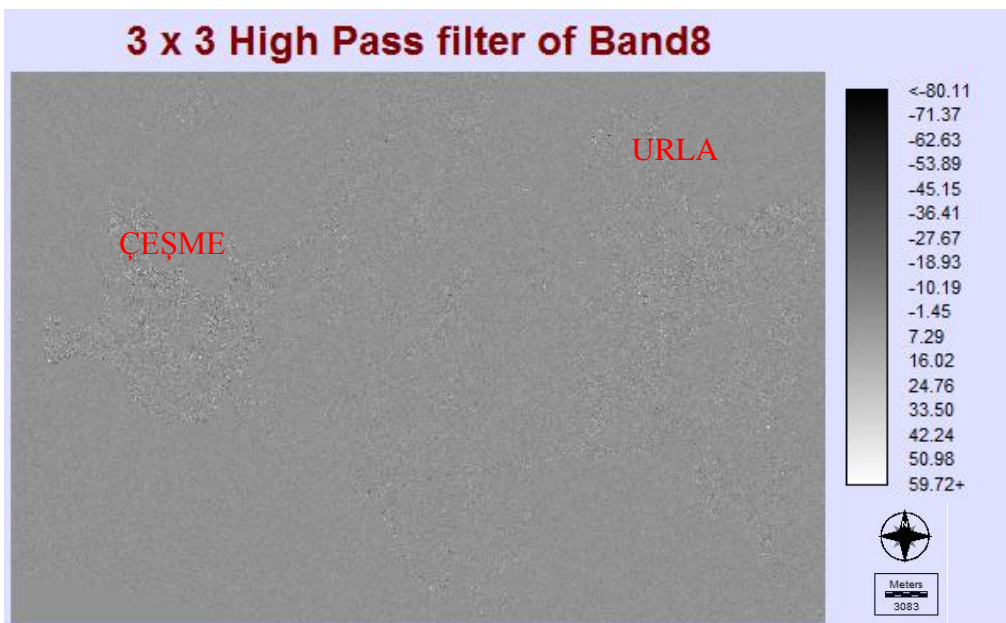


Figure 4.4 Band 8 after filtering with 3x3 kernel of high-pass filter

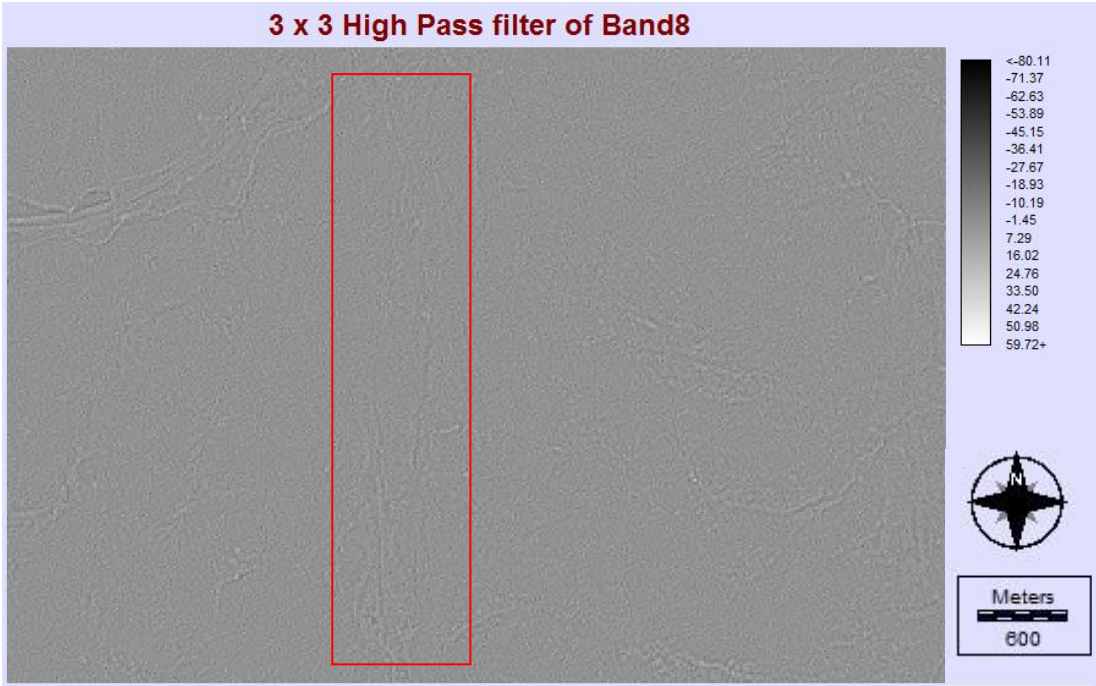


Figure 4.5 A closer look to possible fault zone

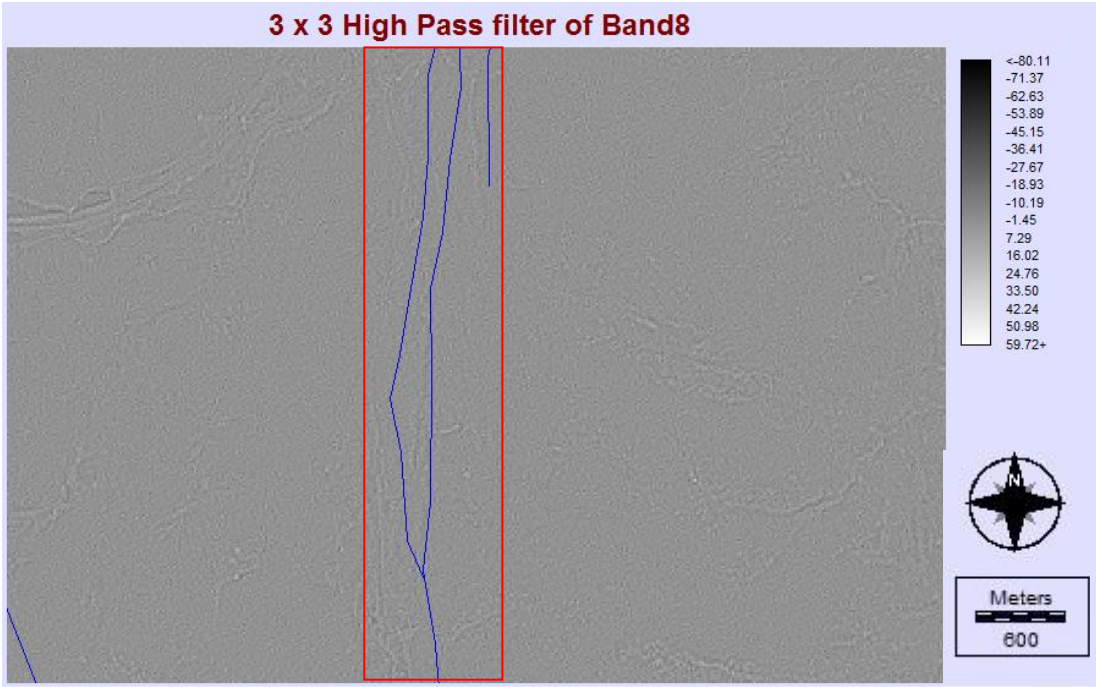


Figure 4.6 Actual fault overlapping the possible fault line

Edge detection filters allow to detect the objects more easily than the surroundings by enhancing the edges. The edges in the image are defined as sharp changes that an

eye can detect due to the differences of the brightness values between two pixels. For this process we can use Laplacian edge detection filters.

A more easily interpreted image can be obtained by subtracting or adding the Laplacian filtered edges from the original image. In addition, this process sharpens the image by increasing the contrast of the discontinuities in the image (Çapar, 2009). The output value is the sum of the products of each pixel value and its corresponding kernel value.

Kernels of Laplacian method are set by default as follows:

3X3		
-1	-1	-1
-1	8	-1
-1	-1	-1

5X5				
0	-1	-1	-1	0
-1	-1	-1	-1	-1
-1	-1	20	-1	-1
-1	-1	-1	-1	-1
0	-1	-1	-1	0

7X7						
0	0	-1	-1	-1	0	0
0	-1	-3	-3	-3	-1	0
-1	-3	0	7	0	-3	-1
-1	-3	7	24	7	-3	-1
-1	-3	0	7	0	-3	-1
0	-1	-3	-3	-3	-1	0
0	0	-1	-1	-1	0	0

Band 8 was filtered by 7x7 kernel of Laplacian filter. The new image was analyzed considering the potential fault lines and the edges of the of study area. The existence of the fault lines were confirmed by comparing the potential fault lines and the actual faults.



Figure 4.7 Band 8 after filtering with 7x7 kernel of Laplacian filter

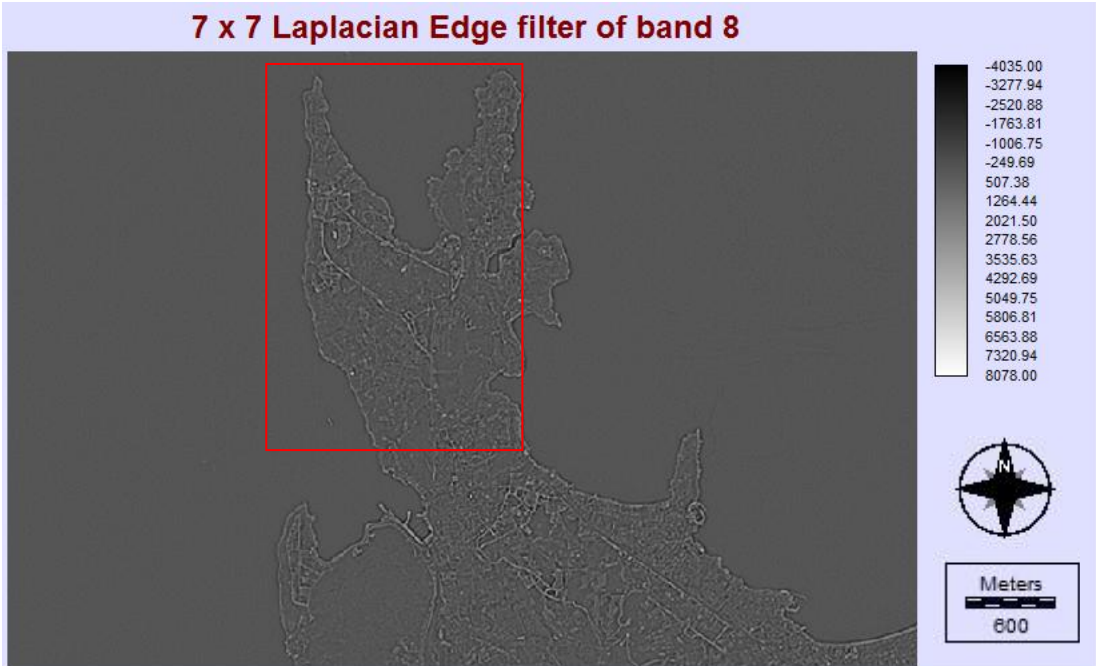


Figure 4.8 A closer look to possible fault zone and the edge of the area



Figure 4.9 Actual fault overlapping the possible fault line

Directional filters are used to highlight the differences in a particular direction. Filter does not respond to the pixels that do not have different values from the surrounding pixels because of the sum of the coefficients in the filter is zero (Çapar, 2009).

The filters for directional filtering process are shown below with their directions.

Northwest			North			Northeast		
1	1	1	1	1	1	1	1	1
1	-2	-1	1	-2	1	-1	-2	1
1	-1	-1	-1	-1	-1	-1	-1	1
Southwest			South			Southeast		
1	-1	-1	-1	-1	-1	-1	-1	1
1	-2	-1	1	-2	1	-1	-2	1
1	1	1	1	1	1	1	1	1

West		
1	1	-1
1	-2	-1
1	1	-1

East		
-1	1	1
-1	-2	1
-1	1	1

To use the directional filters, the directions of the faults must be considered. The directions of the faults in the study area are generally northeast- southwest and northwest-southeast. According to this, northwest, northeast, southwest and southeast filters were selected for the directional filtering.

The images after the filtering process were compared with the real fault lines and it confirmed the existence of the faults and their directions. Especially, the data about the Gülbahçe Fault Zone which runs in NE-SW direction can be determined better with the northeast and southwest directional filters.

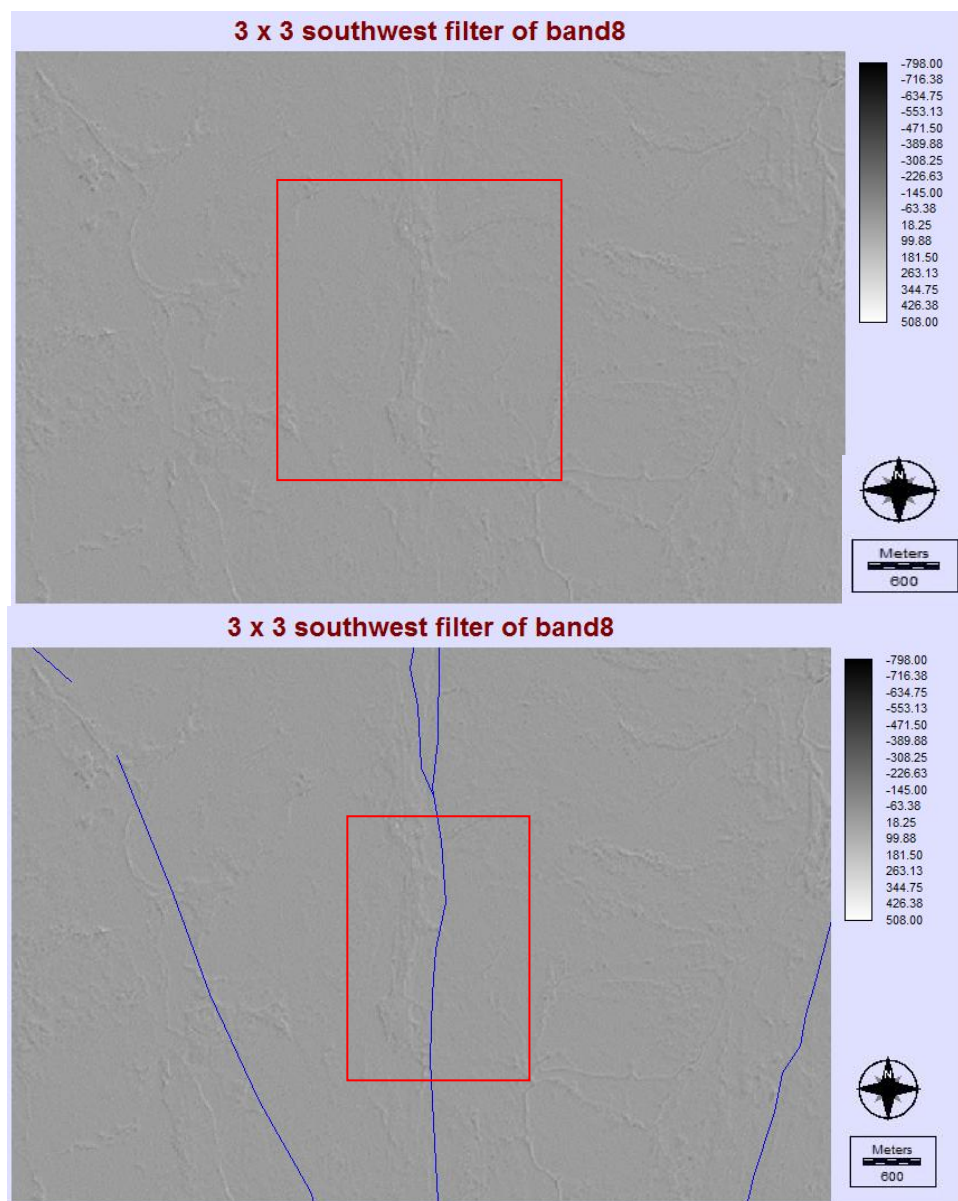


Figure 4.10 Southwest directional filter and overlapping fault

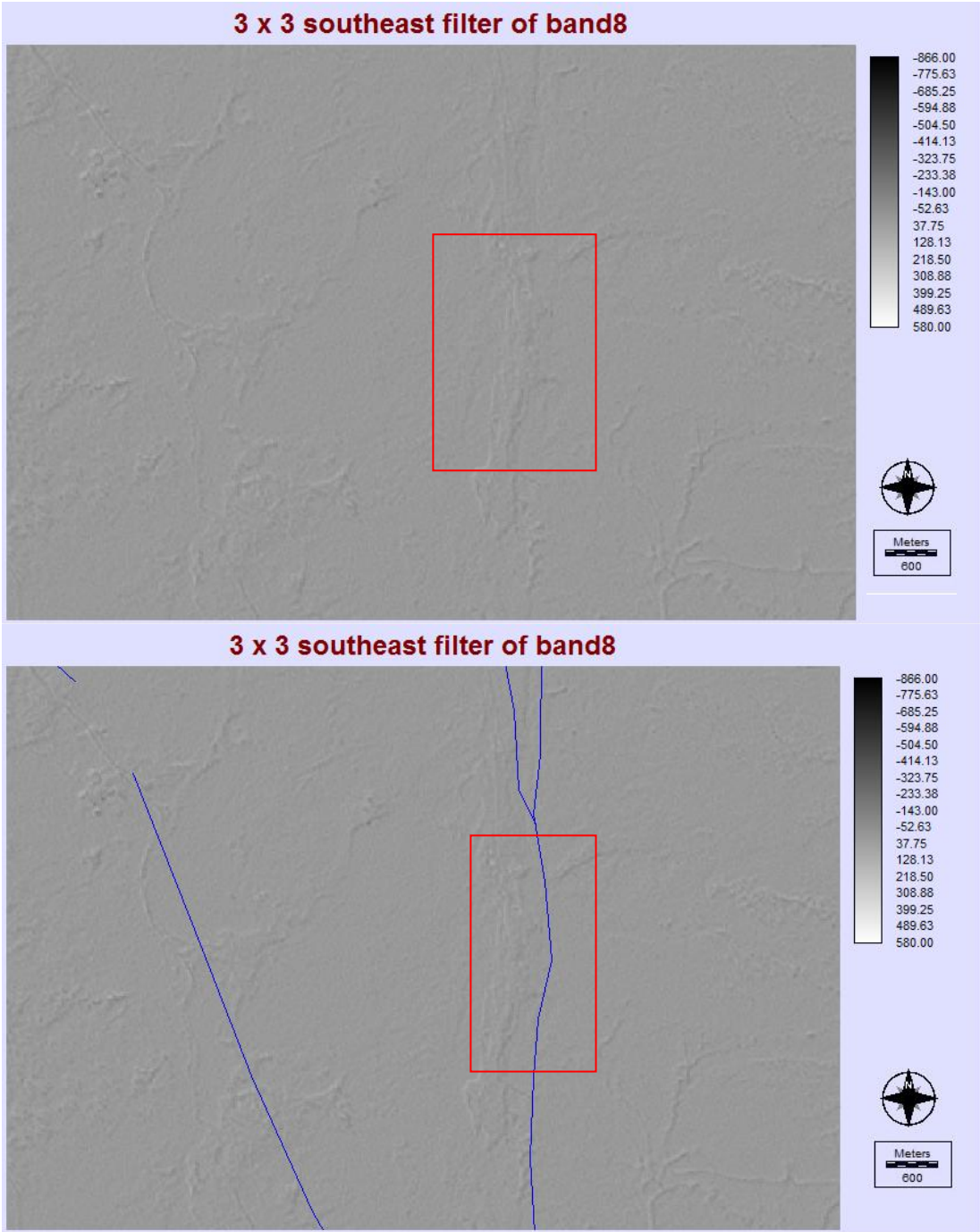


Figure 4.11 Southeast directional filter and overlapping fault

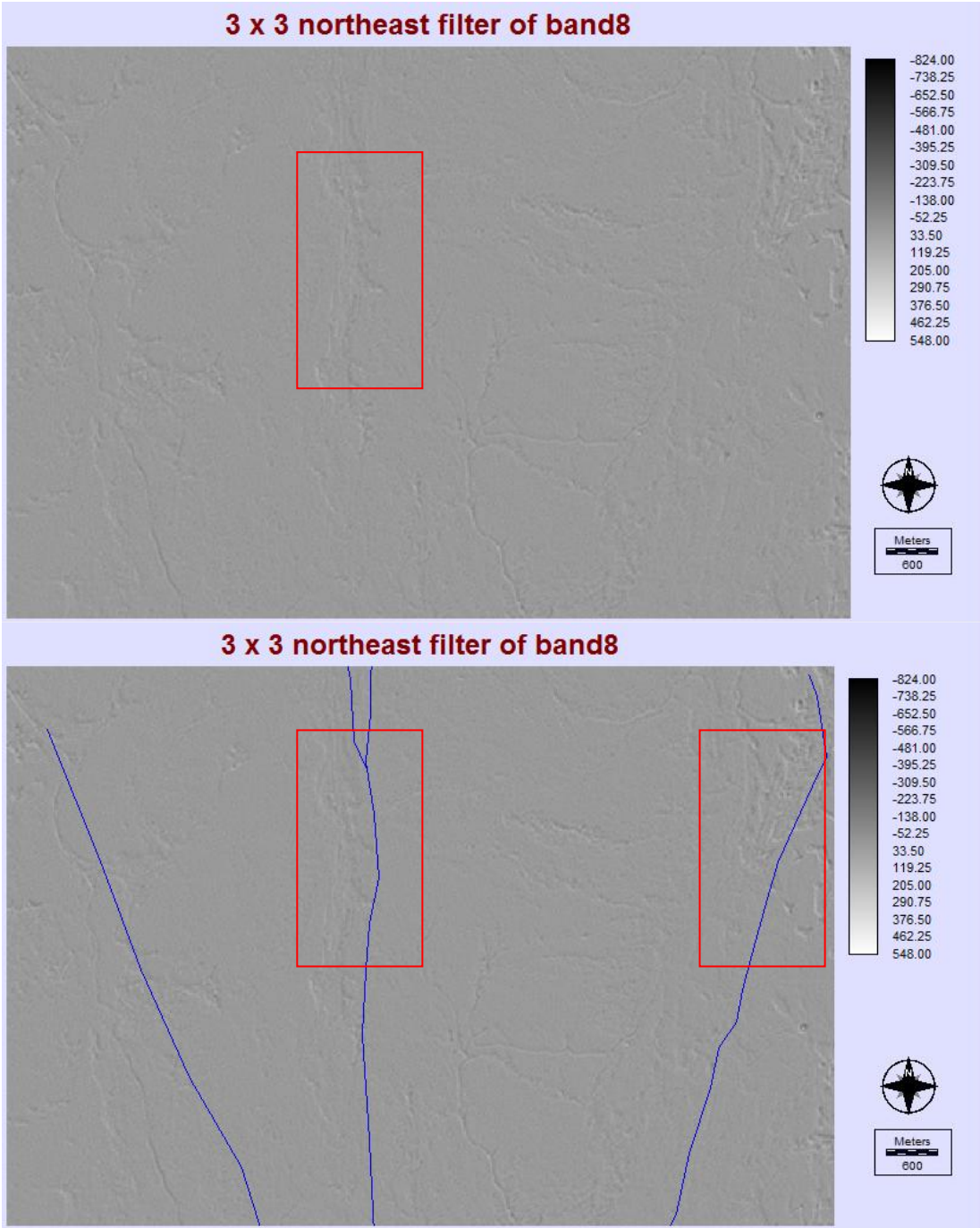


Figure 4.12 Northeast directional filter and overlapping fault

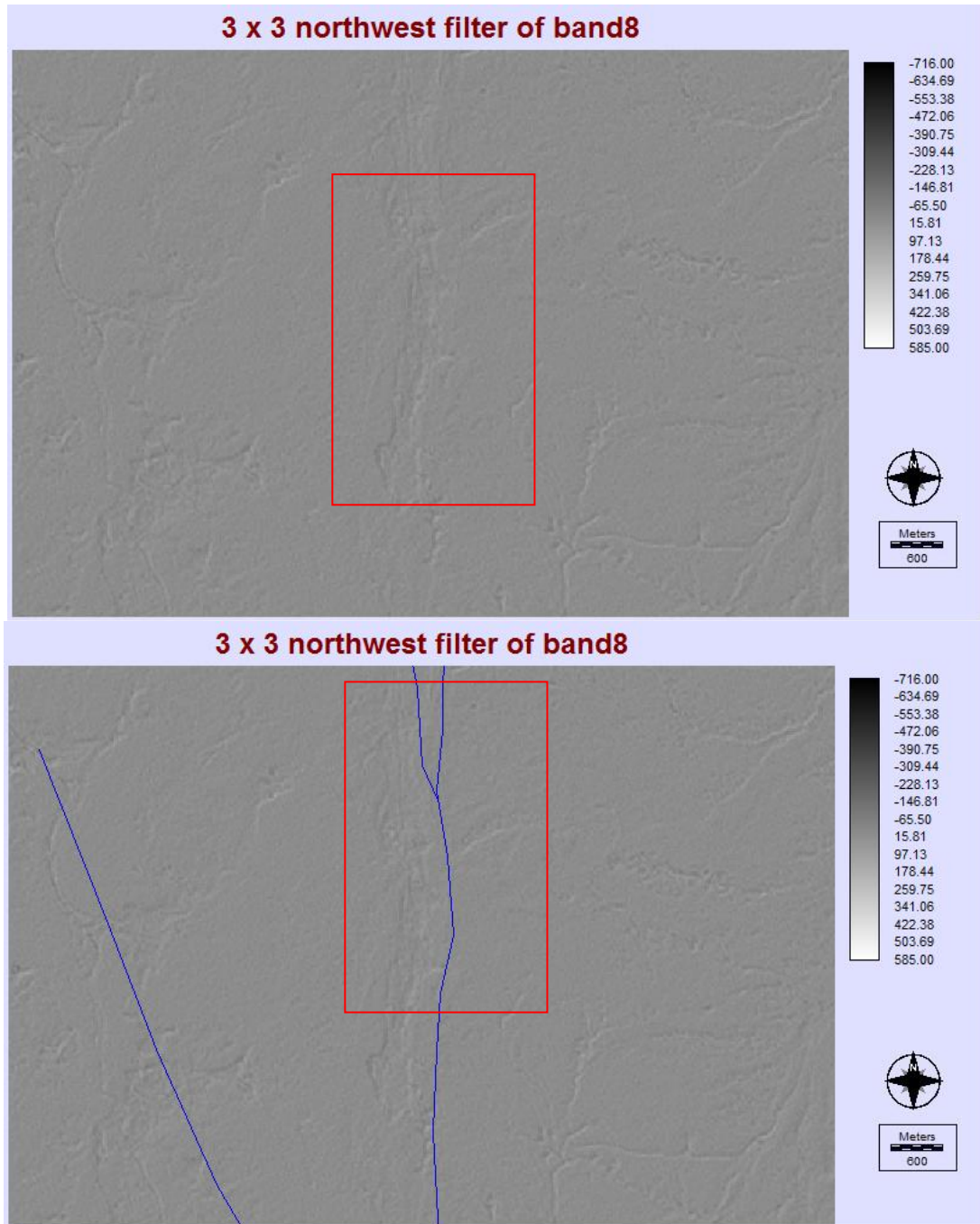


Figure 4.13 Northwest directional filter and overlapping fault

4.2.2 Digital Elevation Model

Lineaments and formation boundaries can be determined by examining the changes of colours and colour tones and especially the fault traces. Drainage patterns

play an important role in determining the faults. In other words, drainage patterns give plenty of information about faults.

Faults are very common in areas where drainage patterns are shaped like an angular fracture and rectangular cage. Drainage patterns can be achieved from digital elevation models (DEM) automatically.

In this study, GDEMv2 of ASTER satellite that has spatial resolution from 10 to 25 m. was used. A shaded relief image was created with 315° sun azimuth clockwise from north. Possible fracture lines and drainage lines were obtained from the shaded image with greyscale. Estimated fault lines confirmed by overlapping the actual faults on the shaded image.

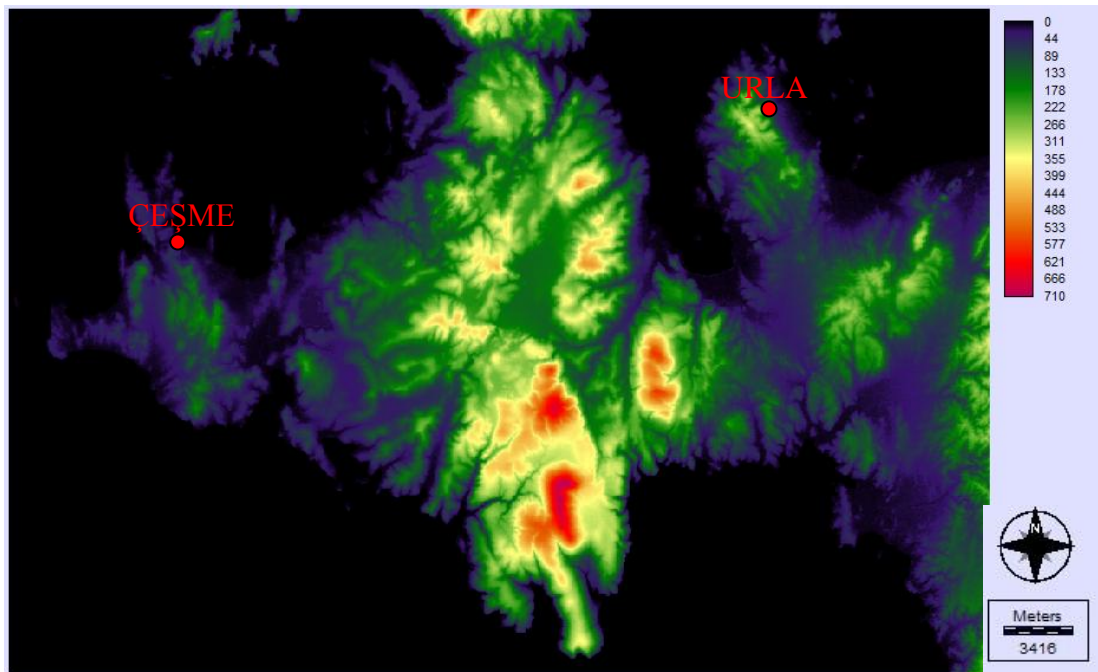


Figure 4.14 Digital Elevation Model (DEM) of the study area

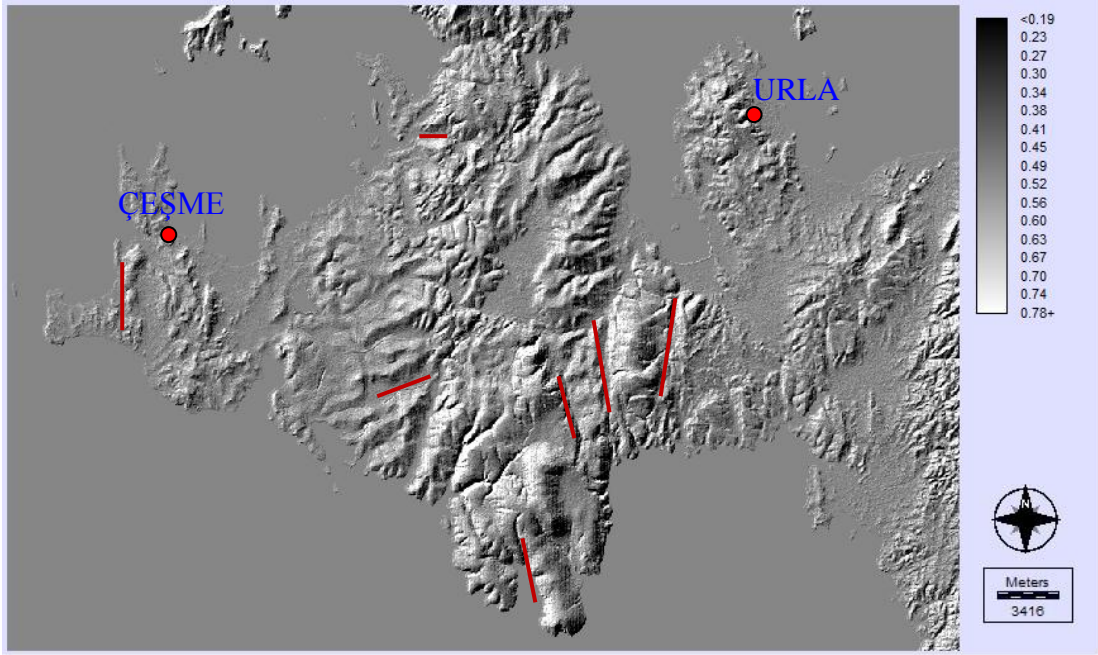


Figure 4.15 Possible fault lines

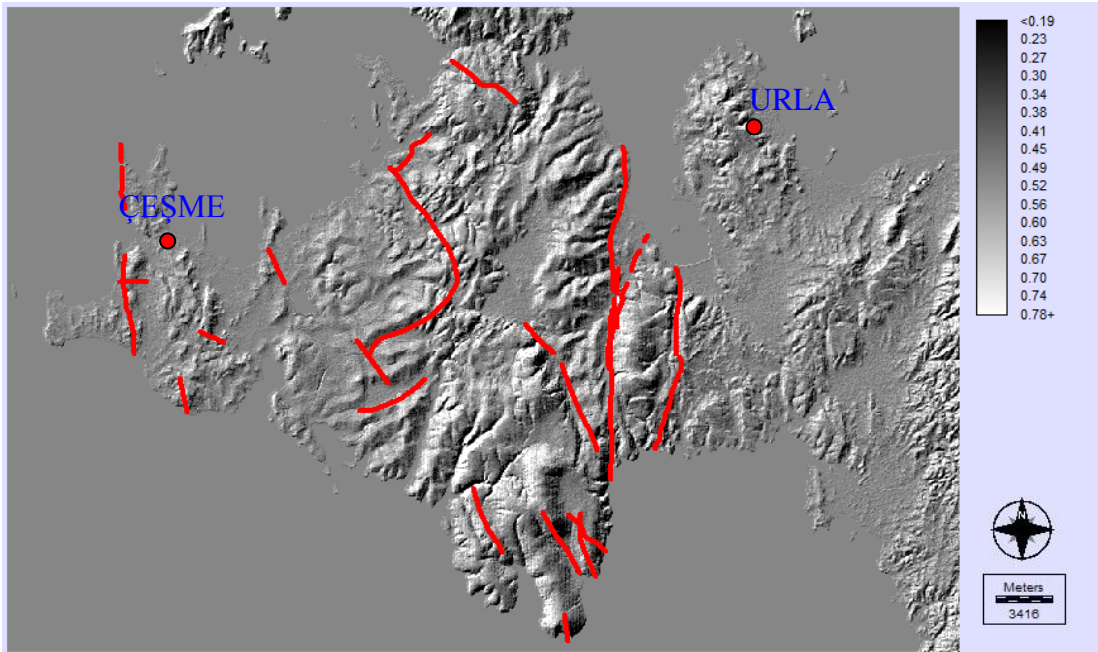


Figure 4.16 Actual fault zones

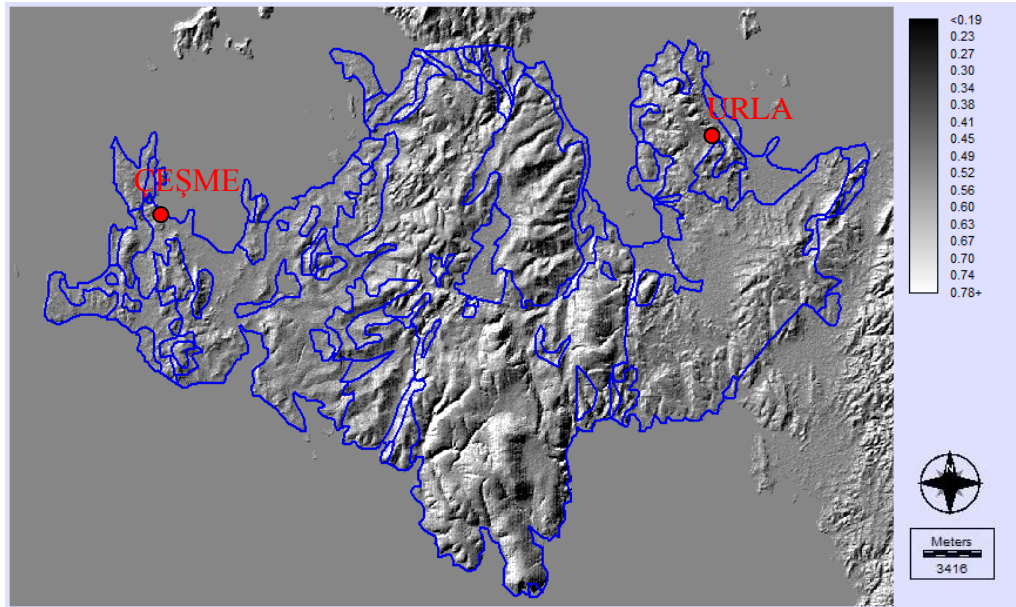


Figure 4.17 Formation boundaries

Seismic data was used to determine the regions that tectonic activity concentrates in and to control the possible faults on the panchromatic images. The epicenter map of earthquakes recorded between 01.01.1950 – 23.03.2013 is presented in Figure 4.18. The epicenters of earthquakes concentrate in the area of faults lines. This concentration supports the forecast of the possible fault lines.

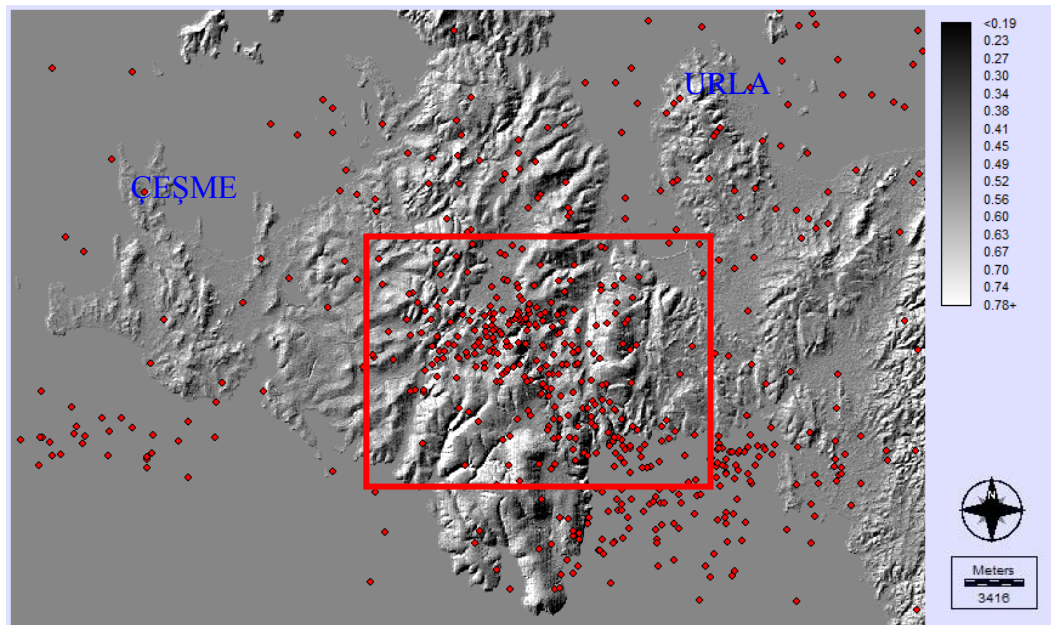


Figure 4.18 Earthquake epicenters recorded between 01.01.1950 – 23.03.2013 and the square box shows the concentration of the earthquakes

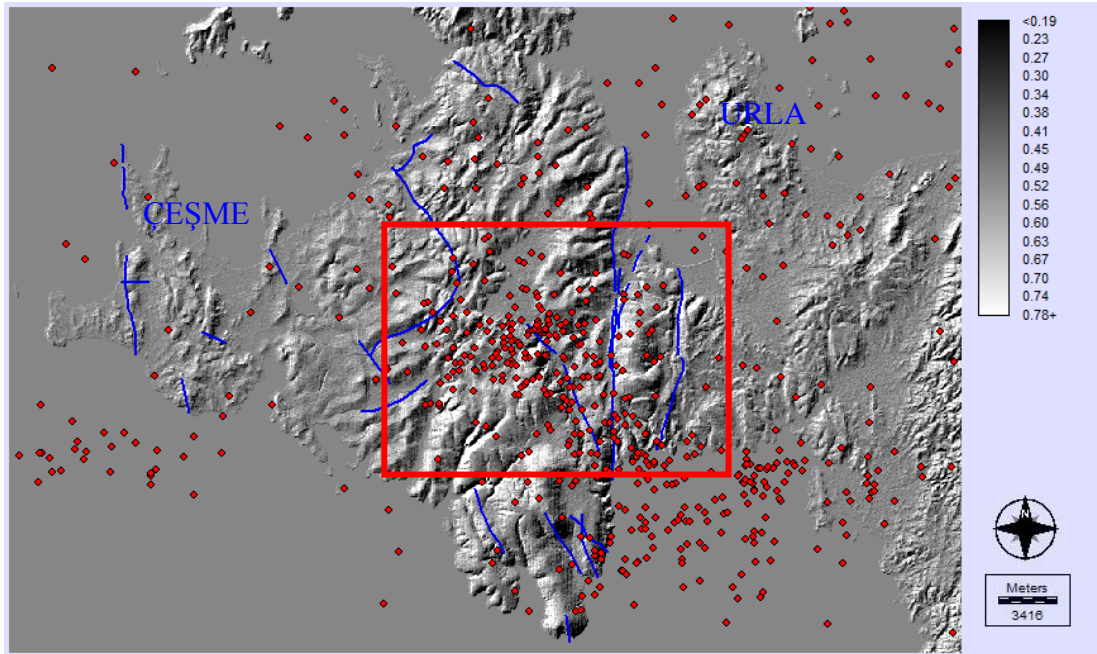


Figure 4.19 Earthquake epicenters and actual fault lines

4.2.3 Classification

Classification is the process of developing interpreted maps from remotely sensed images. Traditionally, classification was achieved by visual interpretation of features and the manual delineation of their boundaries.

In this study; supervised classification method was used. This process was performed by four different modules offered by the software IDRISI. Thus, the most appropriate module was chosen and the most accurate information was obtained. These modules are listed as; Minimum Distance Classification, Maximum Likelihood Classification, Parallepiped Classification and Linear Discriminant Analysis (Fisher).

Five different pixel classes were determined for the process; water mass, urban area, vegetation, free field and agricultural area. The images created according to these classes were examined and the most appropriate methods were determined as Max. Likelihood and Fisher. Those images are the guides to the analysis to be made. For example; images can be used to ignore the roads or settlements while searching for the possible fault lines.

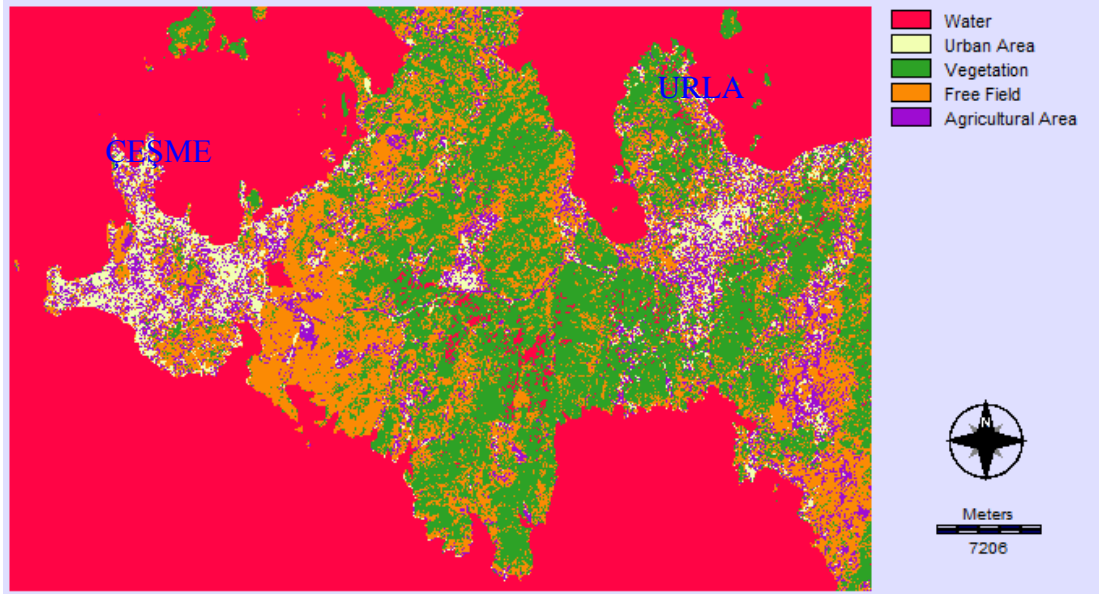


Figure 4.20 Minimum distance classification of Çeşme and Urla

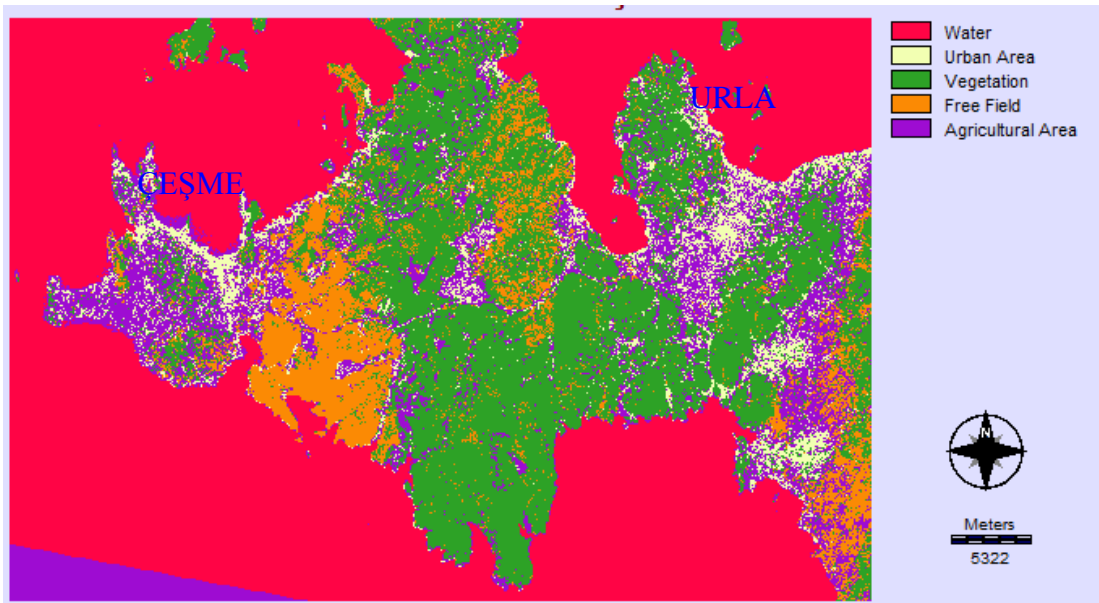


Figure 4.21 Maximum likelihood classification of Çeşme and Urla

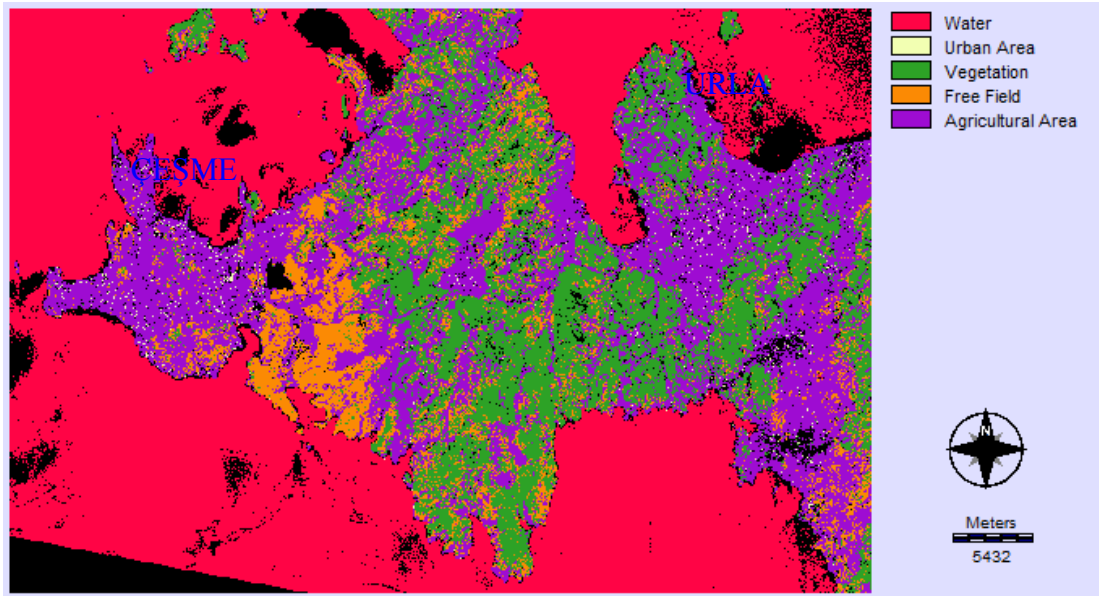


Figure 4.22 Parallelepiped classification of Çeşme and Urla

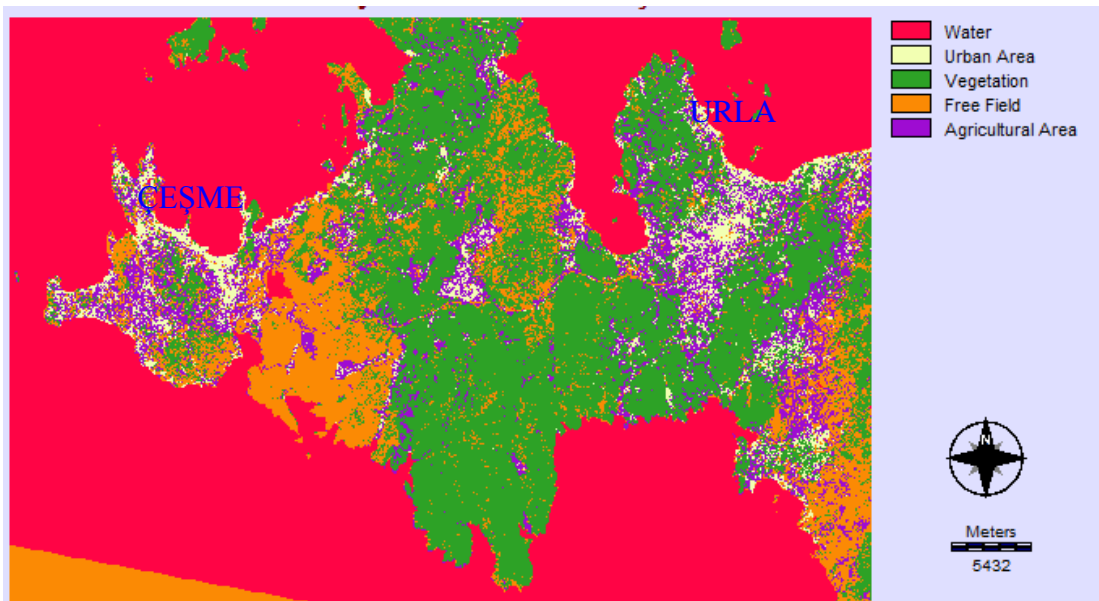


Figure 4.23 Linear discriminant analysis (Fisher) classification of Çeşme and Urla

4.2.4 Principal Components Analysis

PCA produces a new set of images, known as components, that are uncorrelated with one another and are ordered according to the amount of variance they explain from the original band set.

PCA has a number of practical applications. If an image has seven spectral channels but only the first four principal components have a useful amount of information in them, the useful part of the image can be stored or transmitted more easily by storing or transmitting only the first four principal components.

It is common to present remotely sensed images in colour, by displaying three of the available spectral channels as red, green and blue. If an instrument has more than three channels, we have to decide which three channels to display.

An alternative method, which gathers as much information as possible into the three colours, is to display the first three principal components as red, green and blue.

The PCA images enable the geological units or other different types of ground covers in the study area to be noticed easily.

Six components were created as a result of PCA analysis with bands 1, 2, 3, 4, 5 and 7 and different RGB images were obtained by combining different band combinations.

To determine the formation boundaries, band combinations that are generally used in geological research were created.

RGB band combinations, respectively, are as follows; (2-3-1), (1-2-3), (3-2-1), (3-7-4), (4-3-7), (2-3-4), (7-4-2), (4-3-2), (7-1-4) and (7-3-4).

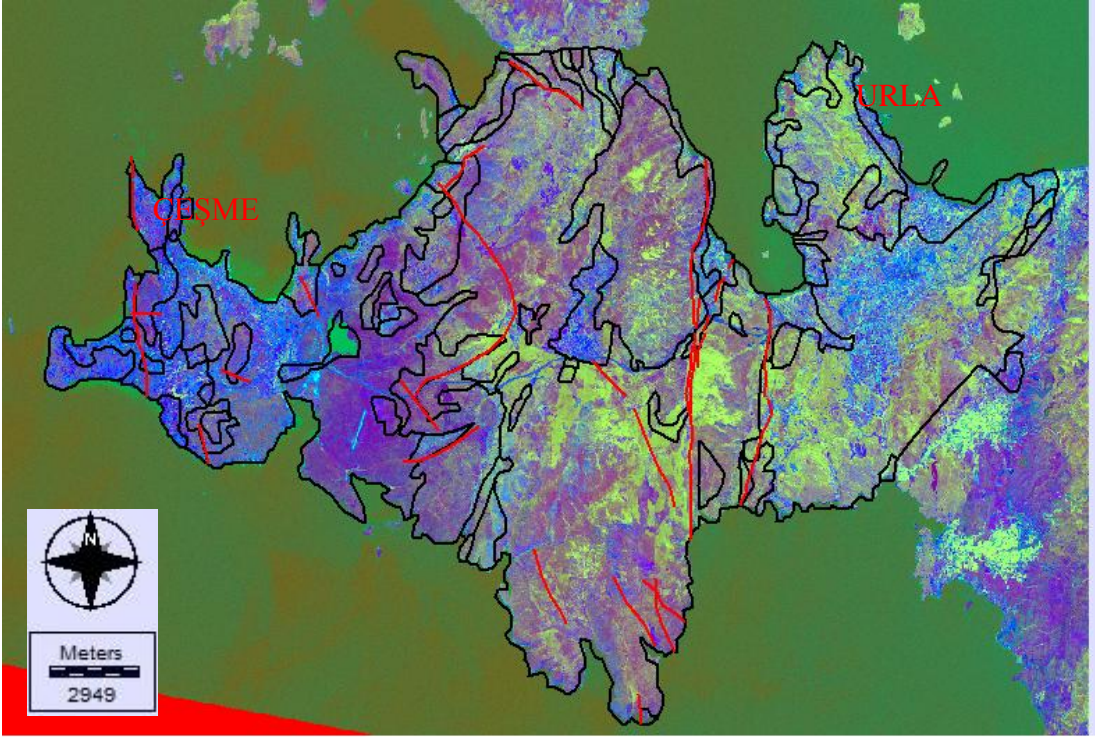


Figure 4.24 The image created with the combinaton 2-3-1 (RGB) after PCA analysis

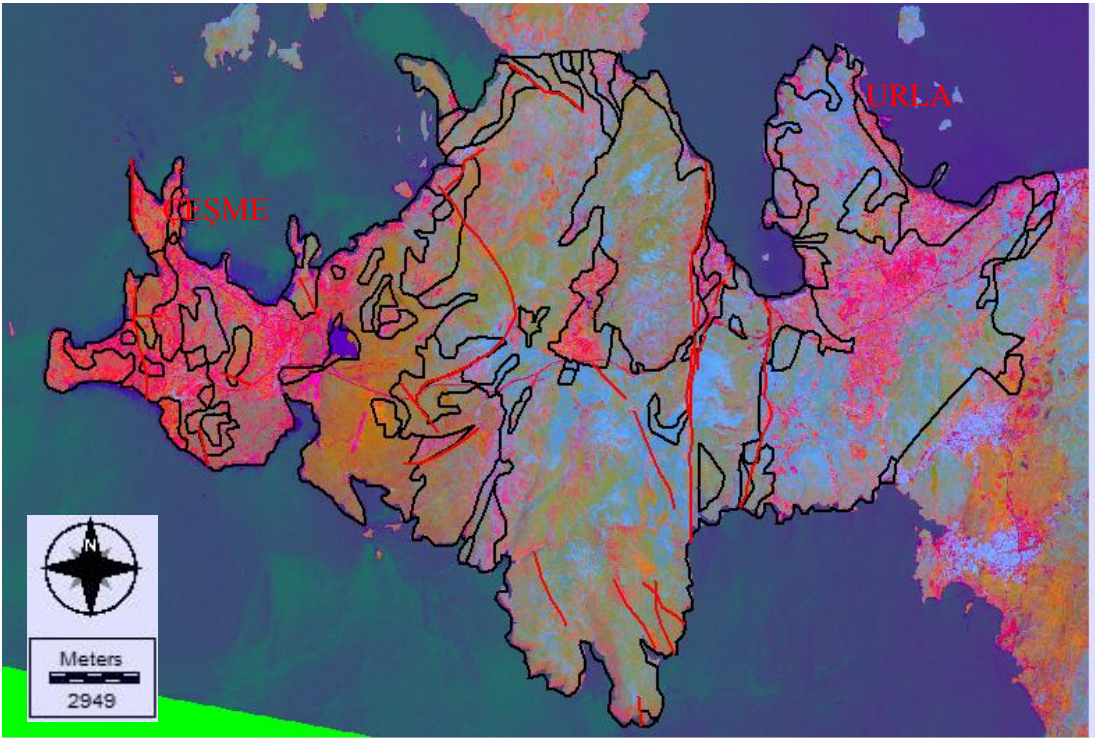


Figure 4.25 The image created with the combinaton 1-2-3 (RGB) after PCA analysis

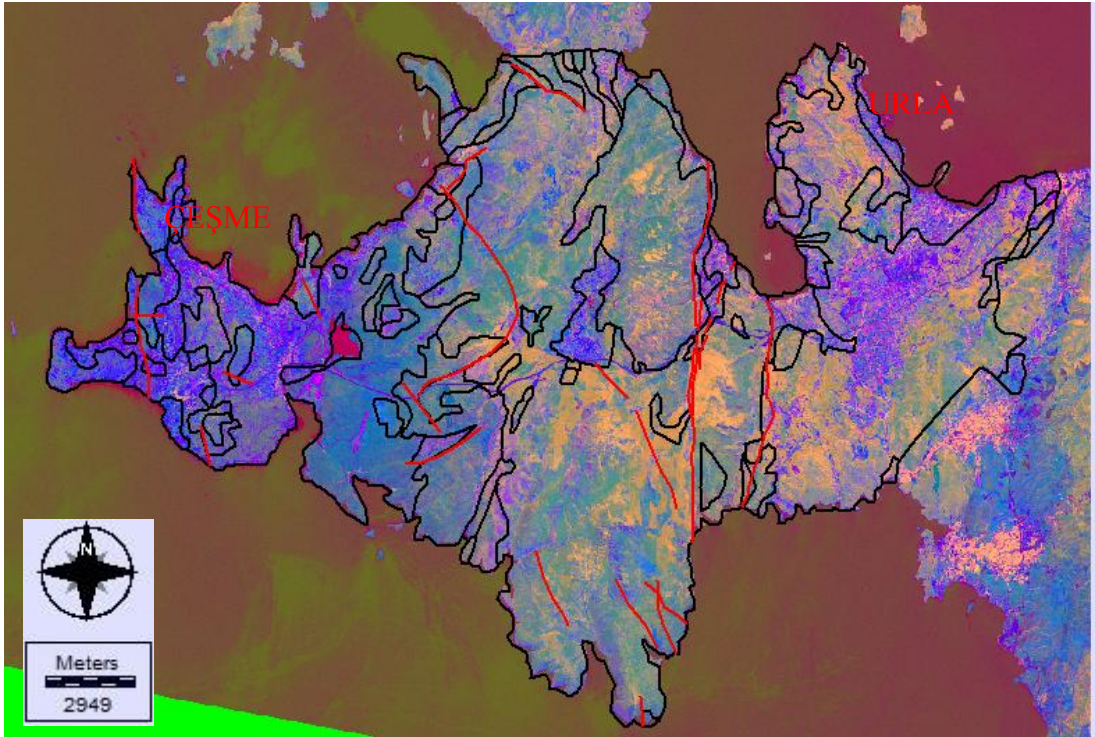


Figure 4.26 The image created with the combinaton 3-2-1 (RGB) after PCA analysis

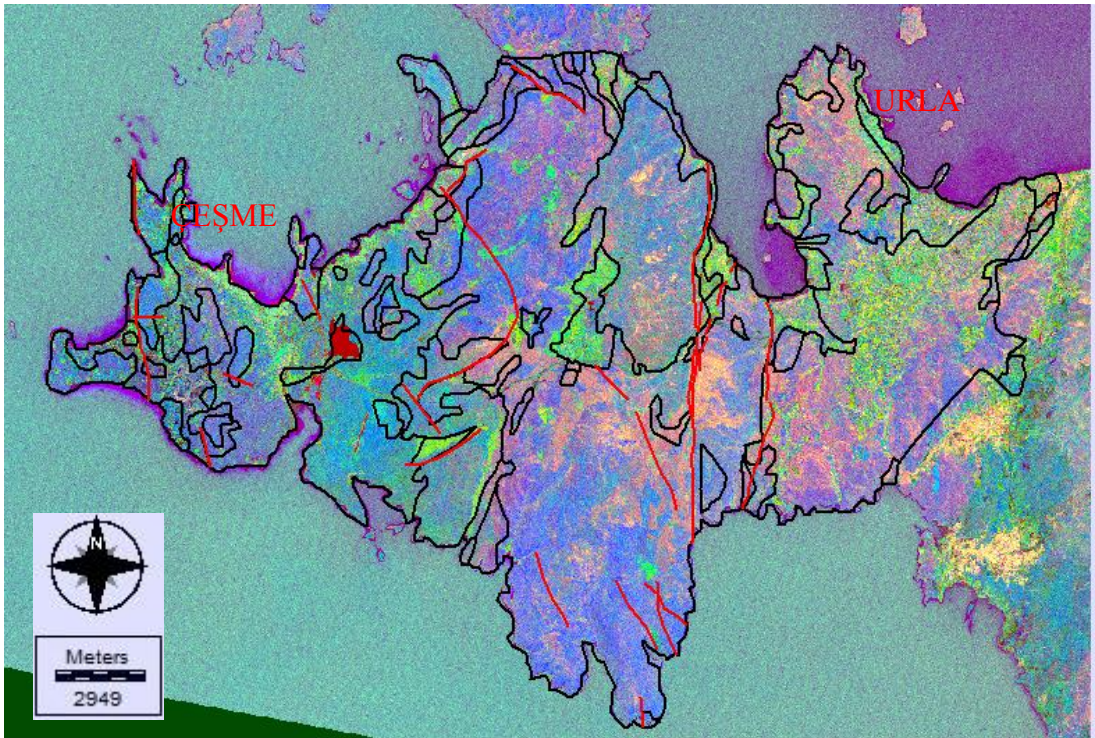


Figure 4.27 The image created with the combinaton 3-7-4 (RGB) after PCA analysis

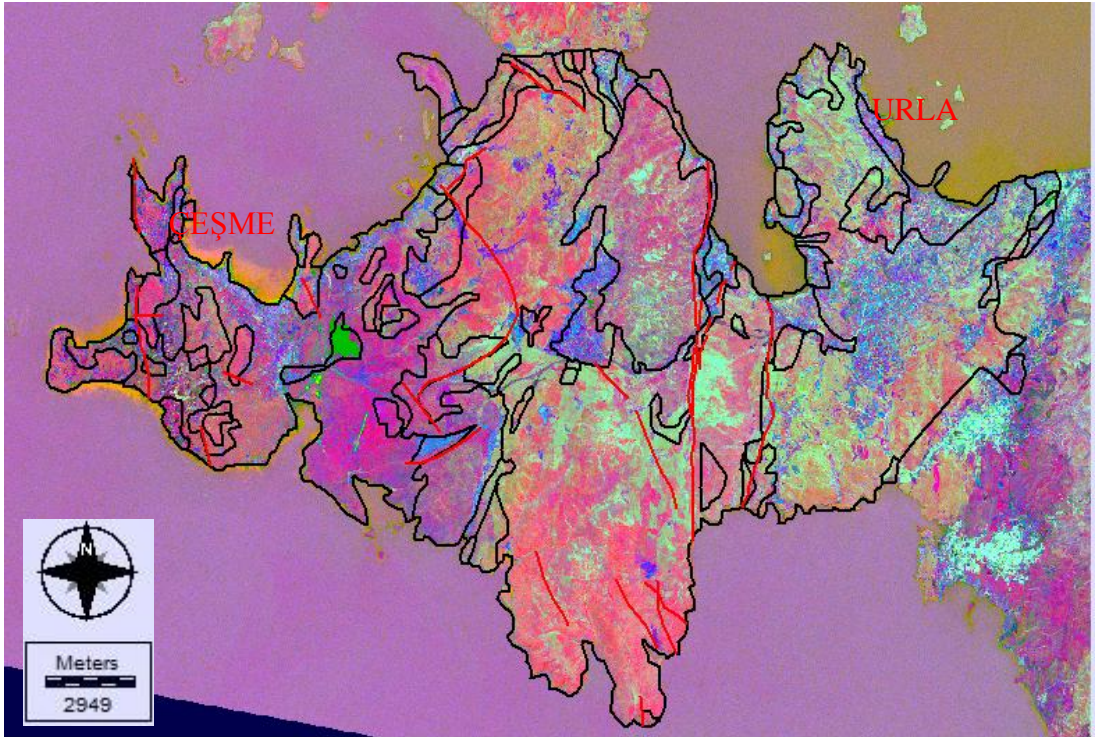


Figure 4.28 The image created with the combinaton 4-3-7 (RGB) after PCA analysis

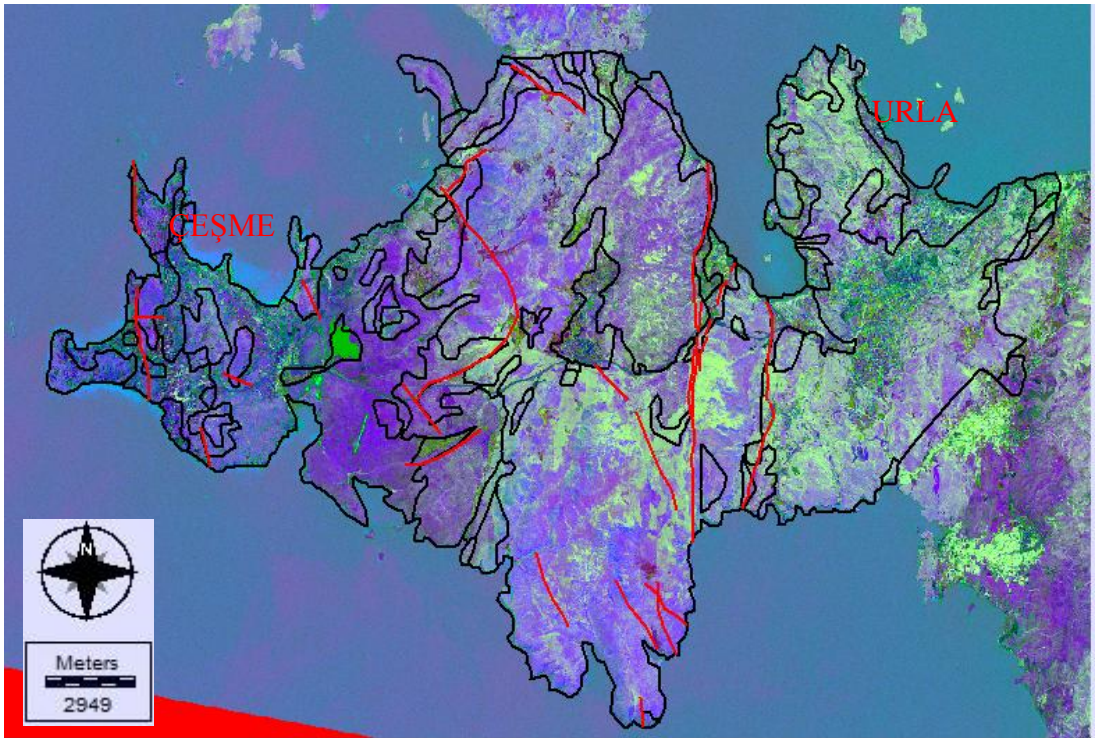


Figure 4.29 The image created with the combinaton 2-3-4 (RGB) after PCA analysis

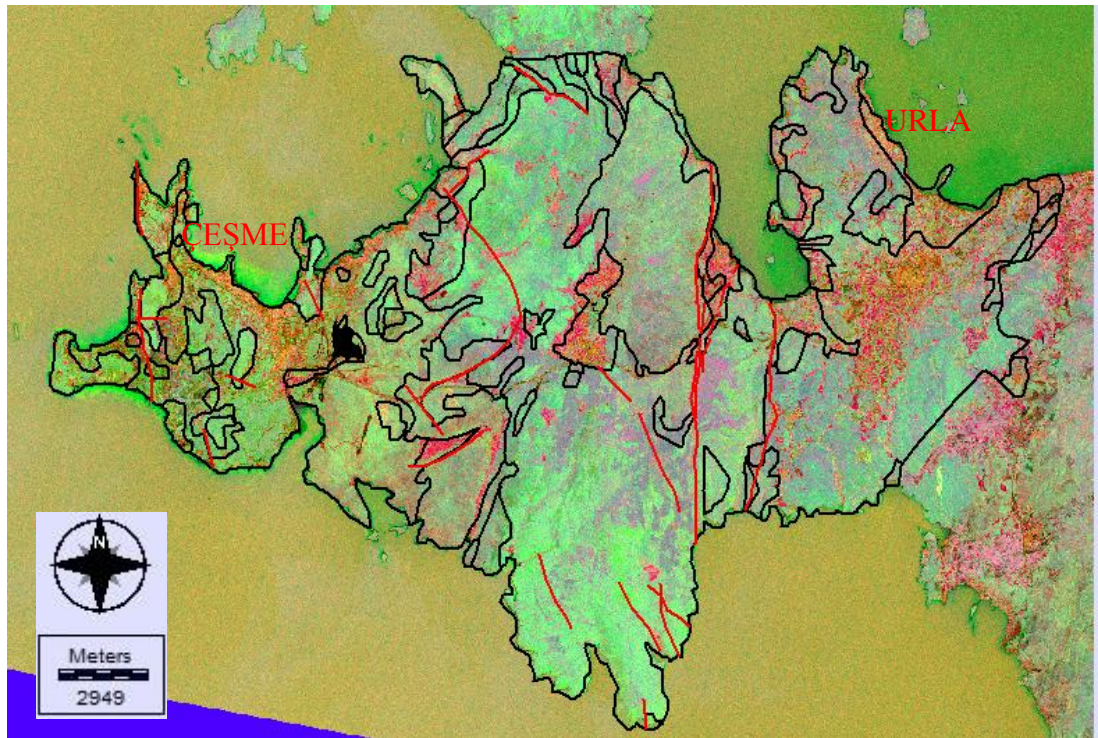


Figure 4.30 The image created with the combination 7-4-2 (RGB) after PCA analysis

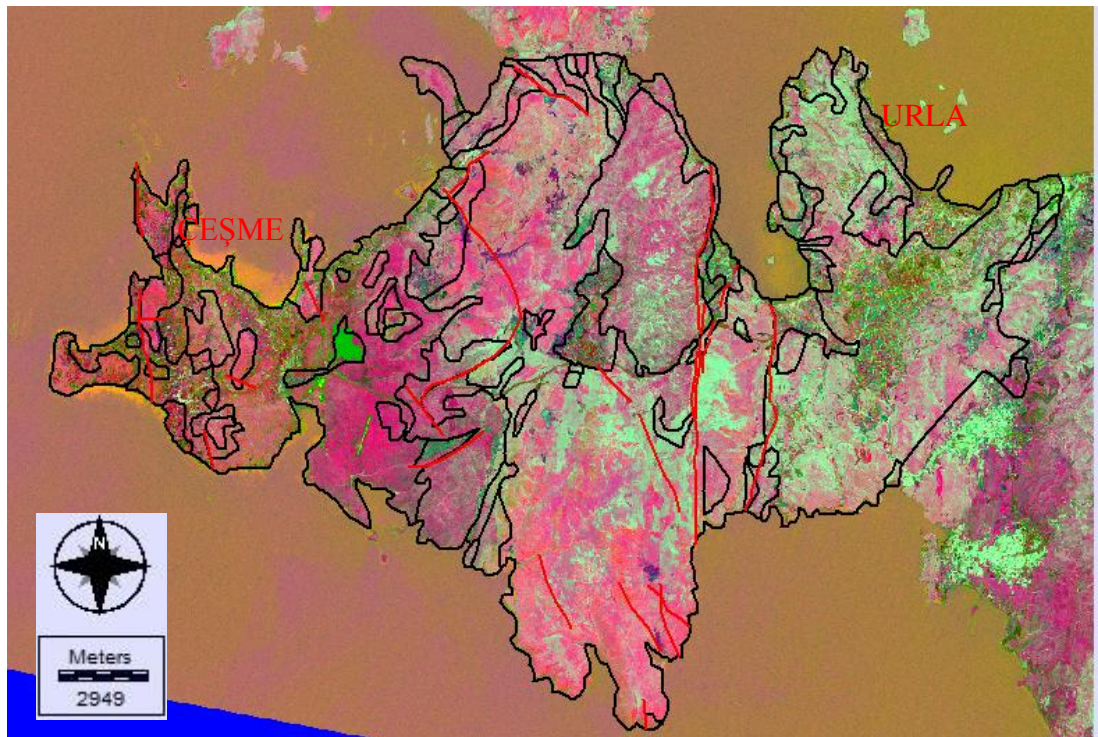


Figure 4.31 The image created with the combination 4-3-2 (RGB) after PCA analysis

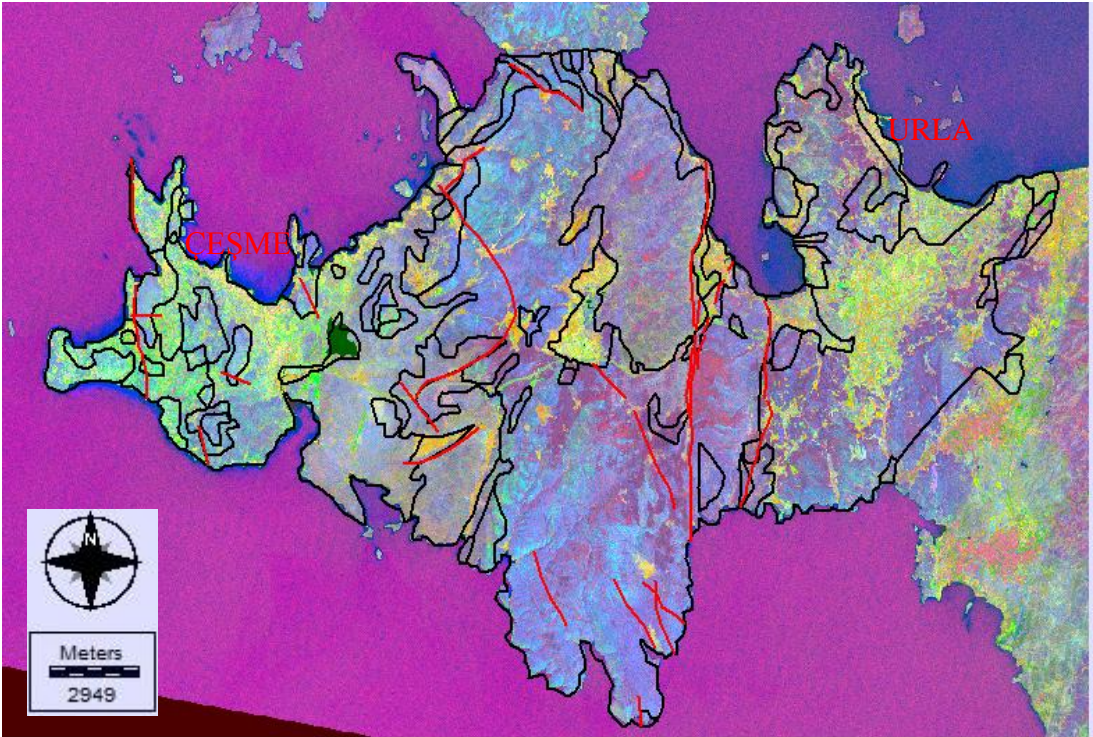


Figure 4.32 The image created with the combinaton 7-1-4 (RGB) after PCA analysis

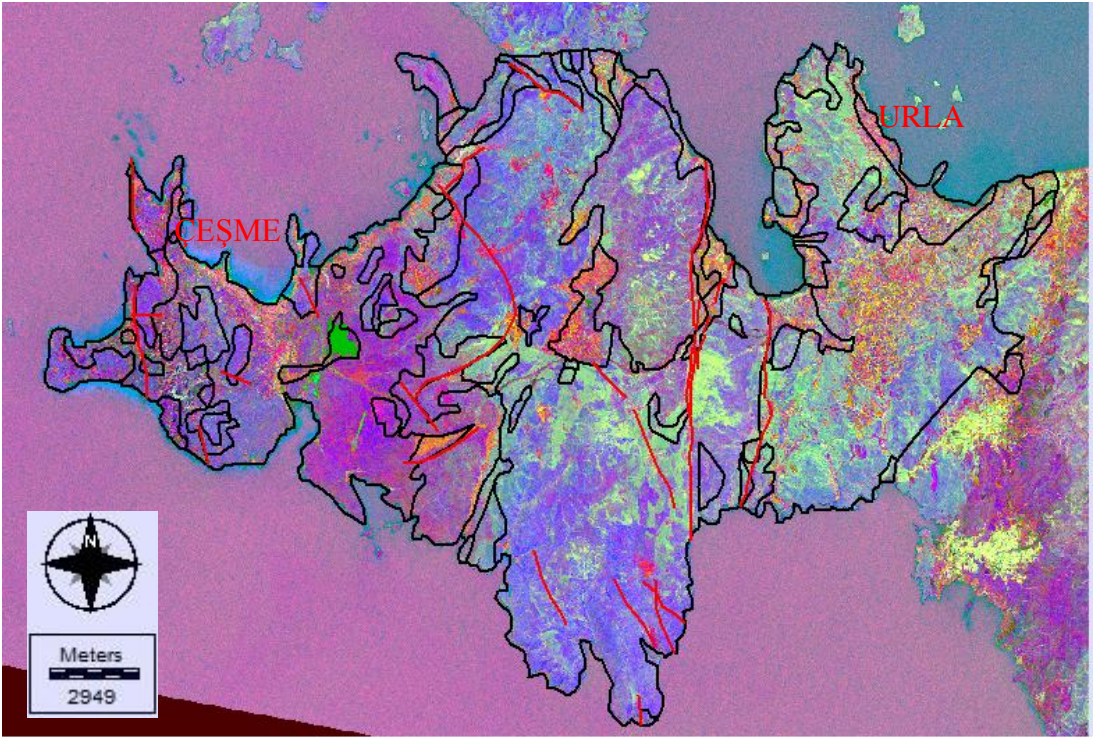


Figure 4.33 The image created with the combinaton 7-3-4 (RGB) after PCA analysis

4.2.5 Band Ratioing

Ratioing is expressed as the mathematical division of a spectral band by another band. Spectral differences between the materials are highlighted with the band ratioing. With this process, it is possible to interpret about the propagation of different types of rocks by dividing the high-reflectance value of objects on earth by the band with the low-reflectance value.

Materials, especially ironoxide/hydroxide and hydrothermal alteration minerals such as clay minerals show high reflectance values in the specific spectral ranges whereas they show absorption characteristics in some spectral ranges. Spectral properties of the materials can be made more specific than their surroundings by using the band ratioing method.

RGB composite images can be created with the help of band ratios.

Specific bands of Landsat image, help to determine the boundaries of lithological units by displaying as RGB composite.

False colour composite RGB images were created and examined to find the altered areas by using 5/7, 5/4, 4/3, 2/3, 4/5 and 3/1 band ratios. Light coloured and white areas indicate the clay minerals, ironoxides, thermal water effects along the faults or fracture lines and high deformation regions.

Table 4.1 Band ratios that used for RGB combinations

Red	Green	Blue
5/7	5/4	3/1
5/7	3/1	4/3
5/7	2/3	4/5

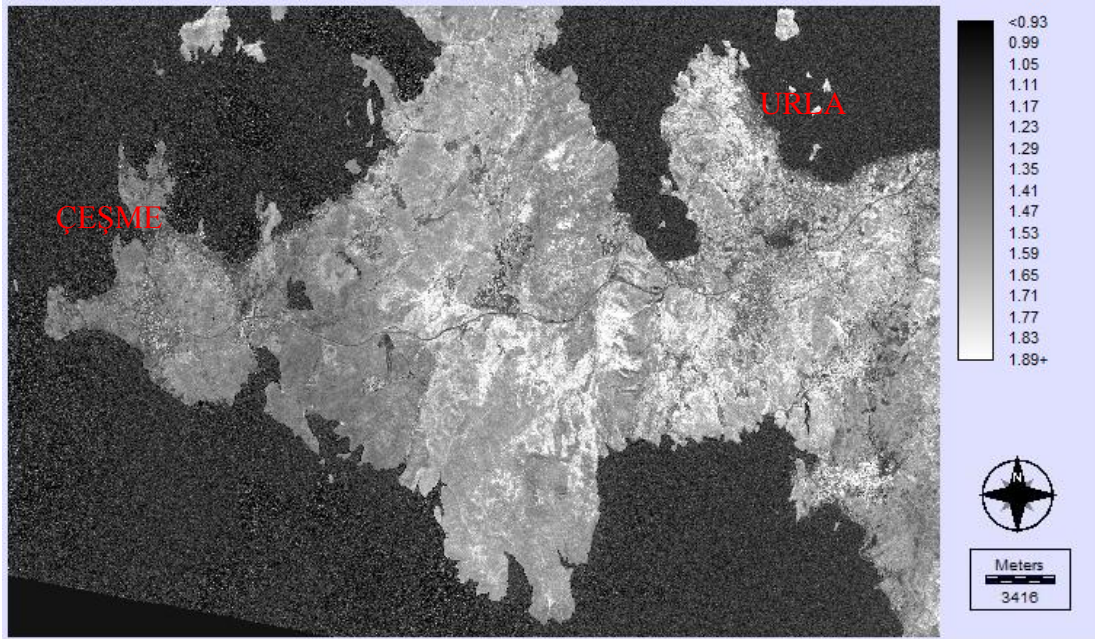


Figure 4.34 Ratio image obtained using band ratio 5/7

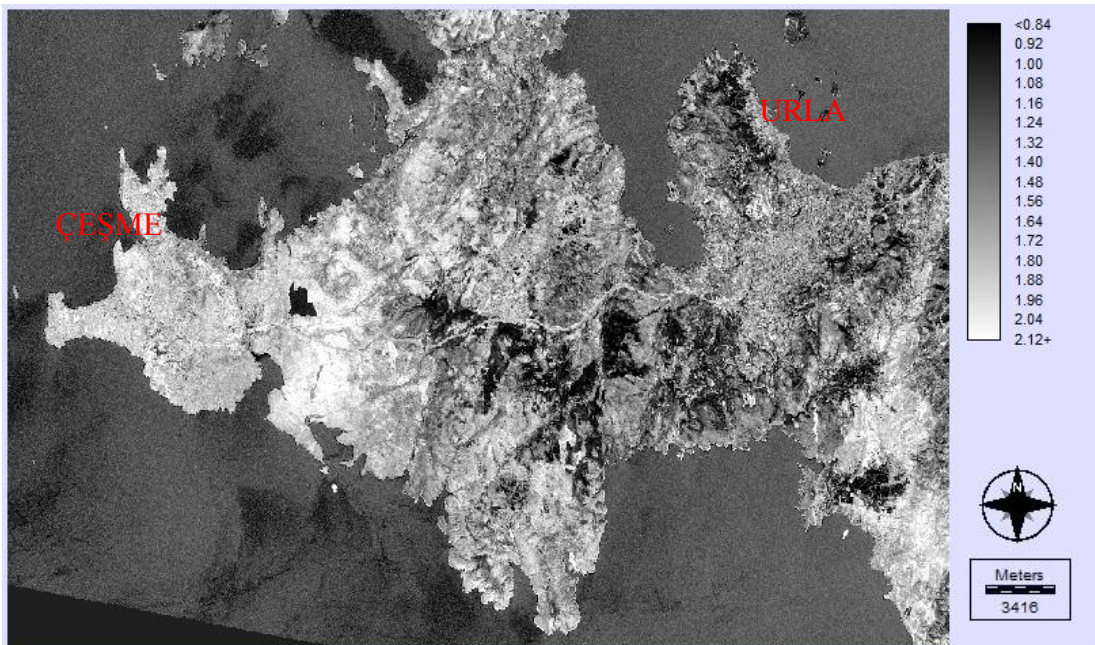


Figure 4.35 Ratio image obtained using band ratio 5/4

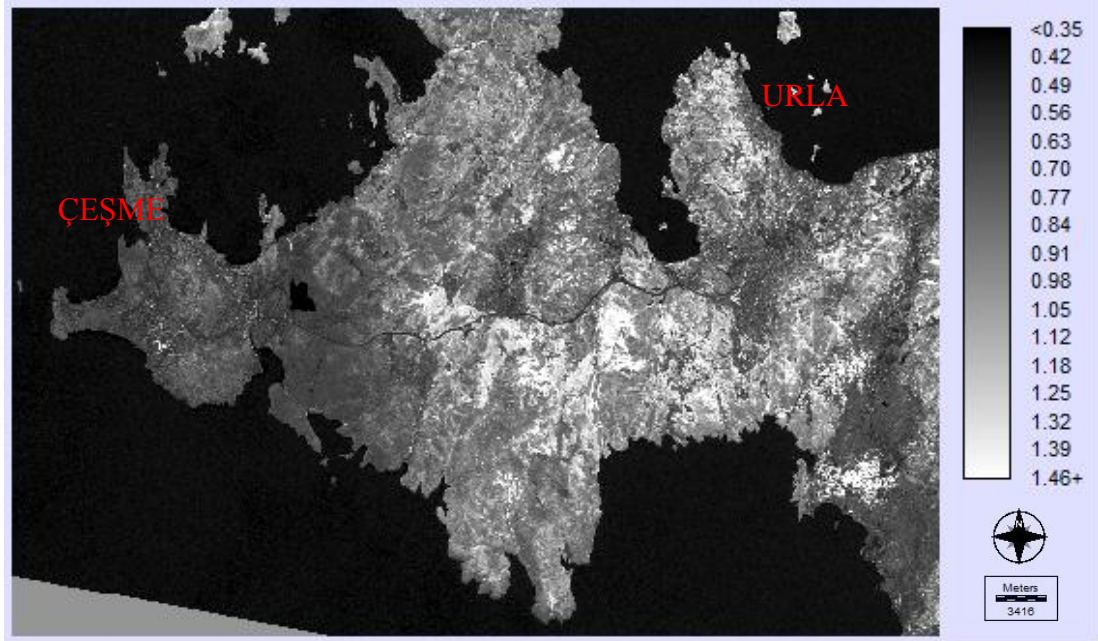


Figure 4.36 Ratio image obtained using band ratio 4/3

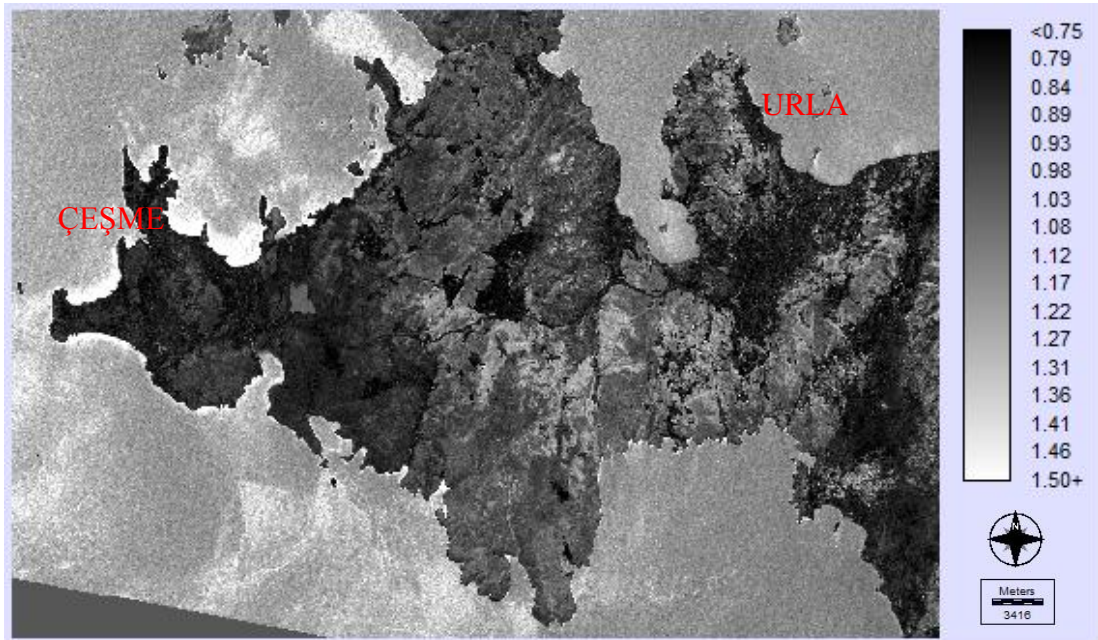


Figure 4.37 Ratio image obtained using band ratio 2/3

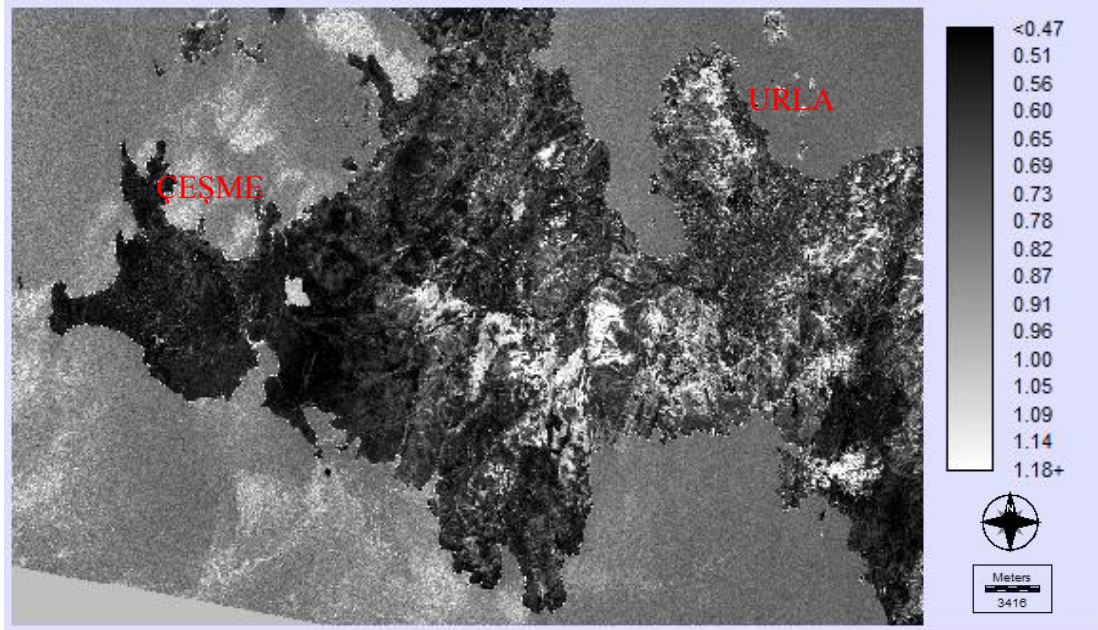


Figure 4.38 Ratio image obtained using band ratio 4/5

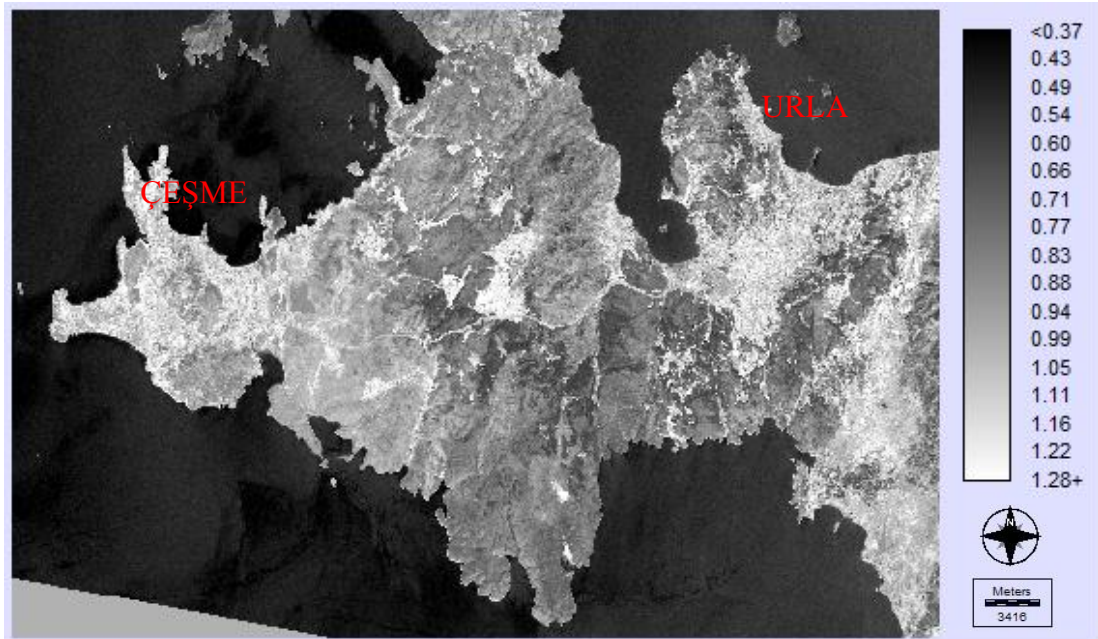


Figure 4.39 Ratio image obtained using band ratio 3/1

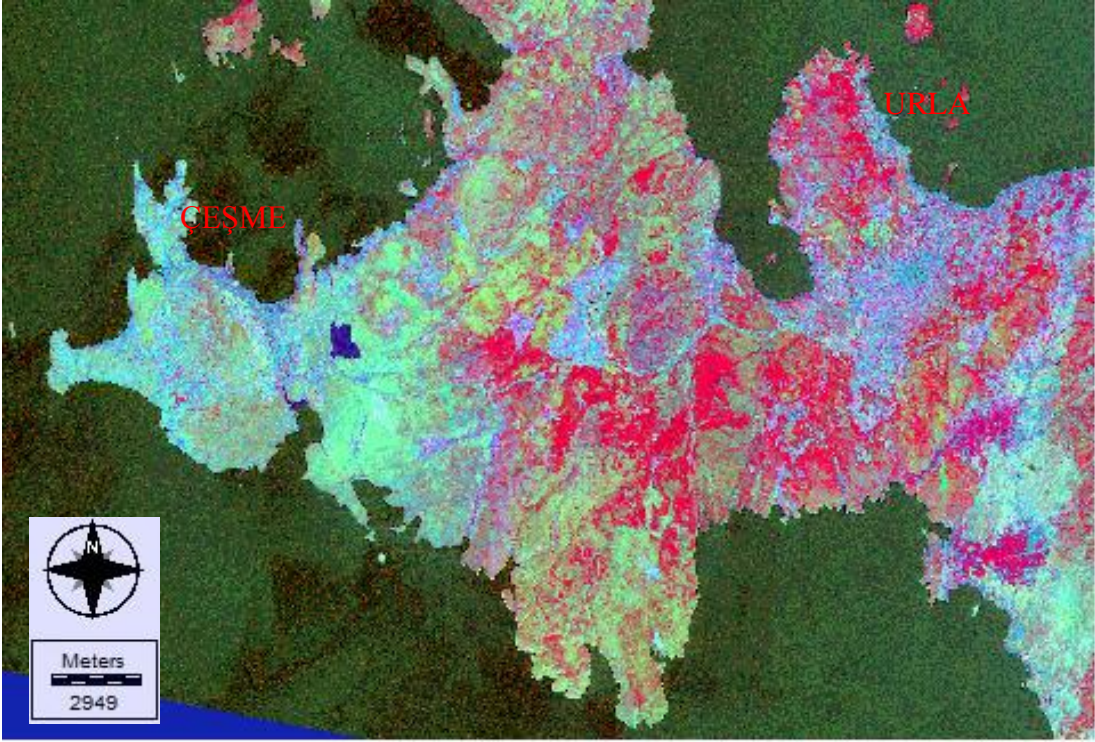


Figure 4.40 RGB image combination of respectively (5/7), (5/4), (3/1)

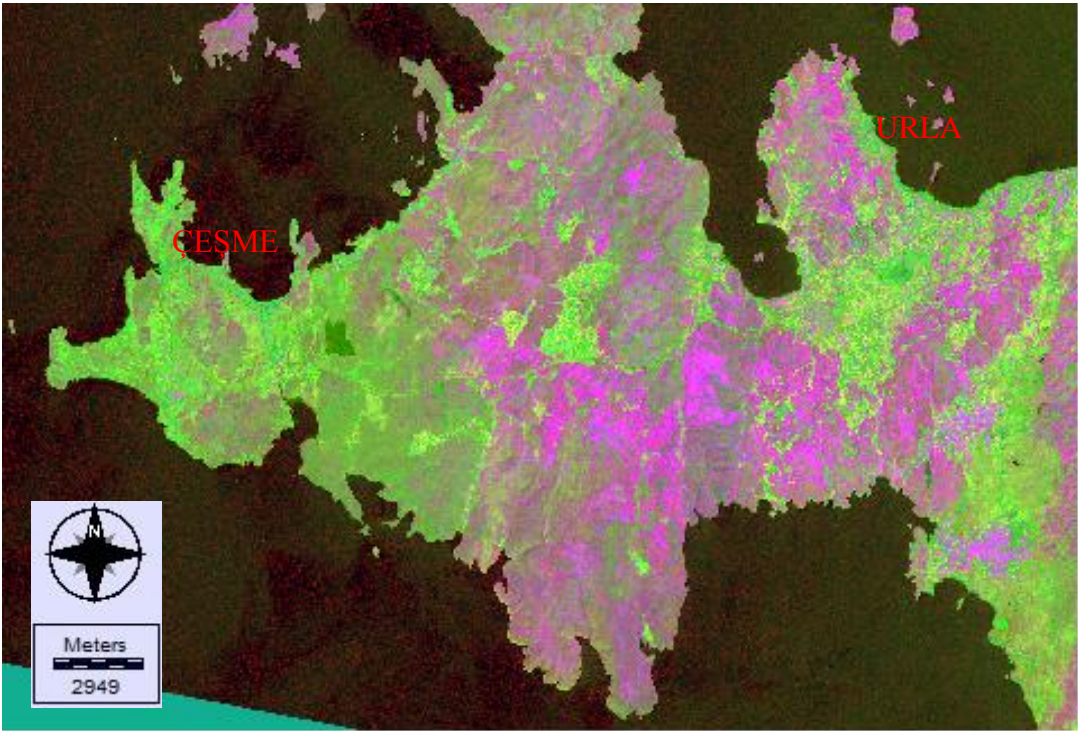


Figure 4.41 RGB image combination of respectively (5/7), (3/1), (4/3)

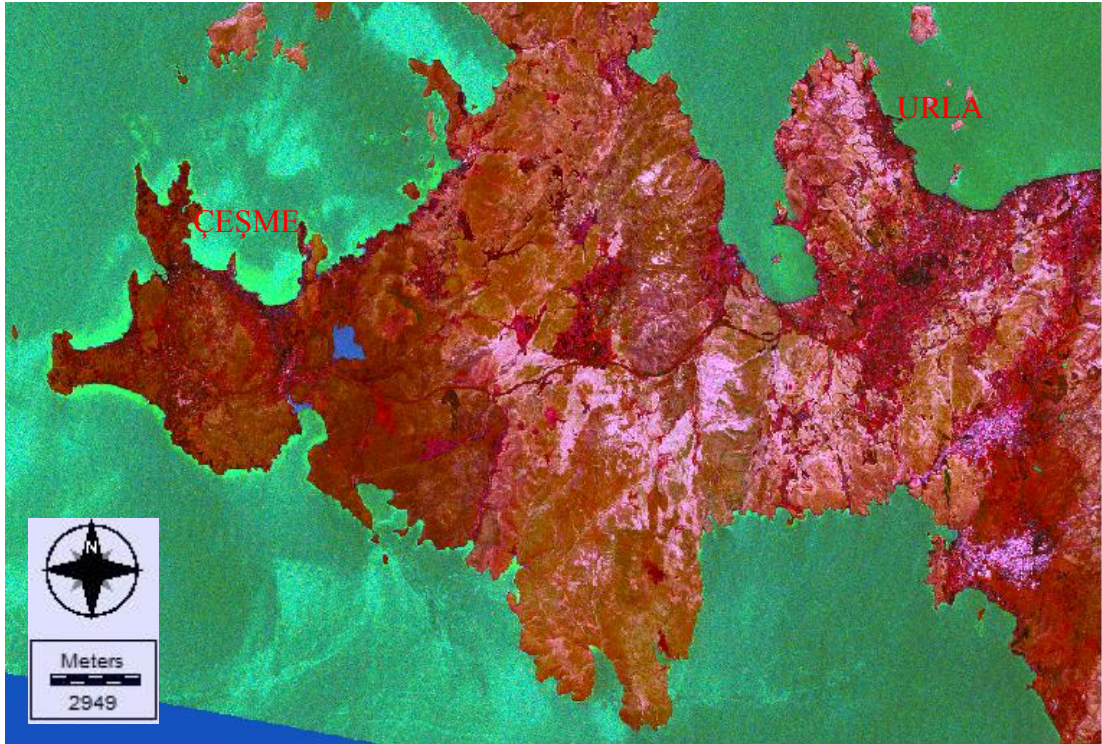


Figure 4.42 RGB image combination of respectively (5/7), (2/3), (4/5)

4.2.6 Determination Of The Thermal Anomalies

Thermal anomalies were determined by calculating the surface temperatures. Surface temperature calculations are made by the radiance values. To perform this calculation DN values of the raster data must be converted to radiance values (Çapar, 2009). The following formulas are used to convert the DN values to radiance values.

$$L_{\lambda} = L_{\min} + \left(\frac{L_{\max} - L_{\min}}{Q_{cal\ max}} \right) Q_{cal}$$

$$L = \text{Offset} + (\text{Gain} * \text{DN}) \quad \text{Offset} = L_{\min} \quad \text{Gain} = \frac{L_{\max} - L_{\min}}{255}$$

L_{λ} is the radiance, L_{\max} is the highest radiance that the sensor can detect, L_{\min} is the lowest radiance that the sensor can detect, $Q_{cal\ max}$ is the maximum DN value of the image and Q_{cal} is the DN value of the examined pixel. L_{\max} and L_{\min} values are

different for each band and they exist in the metadata file of the satellite image (Table 4.2).

Table 4.2 Radiance values of the thermal bands that used in the study

Landsat 7 ETM+	Lmax	Lmin	Qcalmax	Qcalmin	Offset	Gain
Band 6_1	17.040	0.000	255.0	1.0	0	3.200
Band 6_2	12.650	3.200	255.0	1.0	0.0668235	0.0370588

Emissivity values of the materials vary, depending on the geometric position and the wavelength of their emission. The emissivity values in Table 4.3 can be used to find the kinetic temperature.

Table 4.3 Emissivities of various common materials (Lillesand and Keifer, 1994)

Material	Typical Average Emissivity Over 8-14 microns
Clear water	0.98-0.99
Wet snow	0.98-0.99
Human skin	0.97-0.99
Rough ice	0.97-0.98
Healthy green vegetation	0.96-0.99
Wet soil	0.95-0.98
Asphaltic concrete	0.94-0.97
Brick	0.93-0.94
Wood	0.93-0.96
Basaltic rock	0.92-0.94
Dry mineral soil	0.92-0.94
Portland cement concrete	0.92-0.94
Paint	0.90-0.96
Dry vegetation	0.88-0.94
Dry snow	0.85-0.90
Granitic rock	0.83-0.87
Glass	0.77-0.81
Sheet iron (rusted)	0.63-0.70
Polished metals	0.16-0.21
Aluminum foil	0.03-0.07
Highly polished gold	0.02-0.03

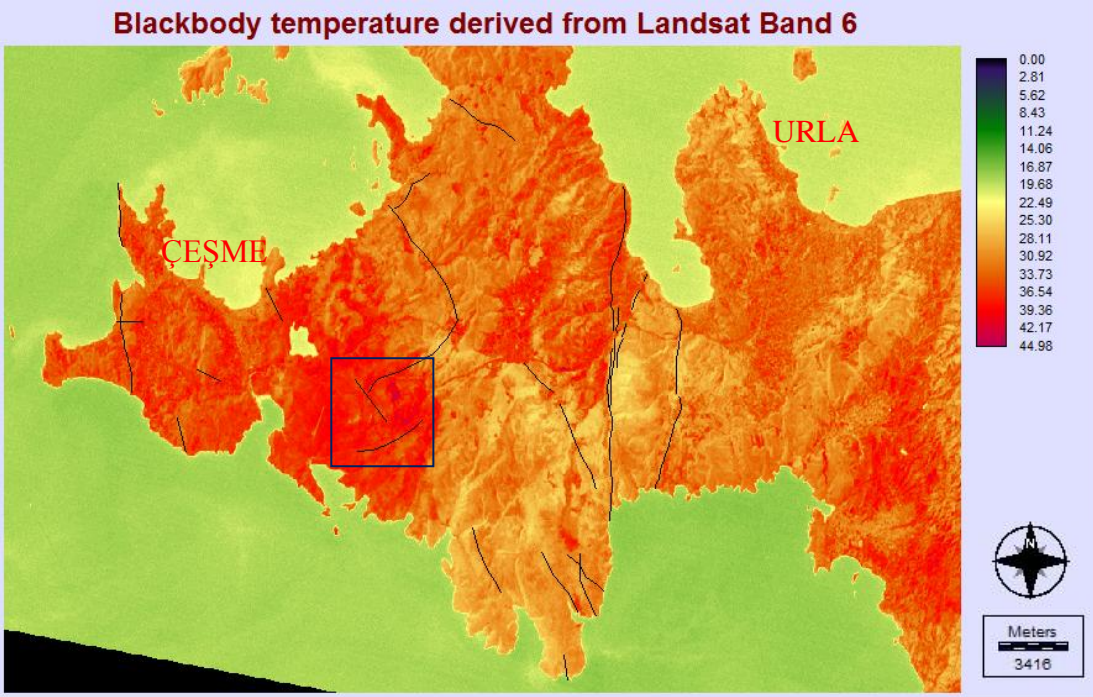


Figure 4.43 Blackbody temperature map of the study area and the active faults, square box shows the region with high temperature

CHAPTER FIVE

CONCLUSIONS

Within the scope of this thesis, ArcGis10 and MapInfo Professional11 softwares were used in the digitizing processes and also IDRISI Selva Edition software was used for the remote sensing applications.

First, the geological map and the active fault map of the study area were digitized and examined. As a result; the trending fault lines of the area run to the NE-SW and NW-SE directions. A thematic map that shows geological units was created.

Filtering, classification, digital elevation model, principal components analysis, band ratioing and determination of thermal anomalies were assigned to the remote sensing applications.

Processing the filtering method, NW, SW, NE and SE directional filters were chosen according to the directions of the fault lines. Also, high-pass and laplacian filters were used (Appendix-1).

ASTER GDEmv2 model was used to create a digital elevation model. Fault lines and formation boundaries were determined by shading the DEM (Appendix-2).

As a result of principal components analysis, RGB images with 6 components were created by gathering information from 7 different bands. Formation boundaries were determined by comparing the images obtained with the geological map.

Band ratioing application was carried out with reference to the previous works. Bands were proportioned with different band combinations and displayed in greyscale and different RGB combinations.

Finally, temperature map of the study area was created to determine the thermal regions. DN values of the images were converted to radiance values and then radiance values were converted to blackbody temperatures.

In comparison of the obtained image processing images, the geological map and the active fault map, the results were largely parallel to each other (Appendix-3). Any geothermal sources that had not been detected before, could not be determined

in the study area. Existing resources were determined with the help of the temperature map and the composite images.

Geographical information systems and remote sensing make it possible to obtain data, analyse the data and create meaningful data in many areas with the help of developing technology.

Geothermal explorations can be performed by geological and hydrological techniques, geophysical techniques, geochemical techniques, drillings, geographical information systems and remote sensing techniques. The maximum benefit is achieved by geographical information systems and remote sensing technique. The digital information of the world can be obtained from the satellites observing the Earth. Also, the temperature detection which is a feature of satellite sensors work on geothermal explorations to be done.

The most important analysis used for geothermal explorations is determining thermal anomalies and lineaments. These properties can be determined by using methods such as filtering or classification of the images. After this analysis, interpretation about the study area can be made by using geological, structural and temperature maps of the area. Based on the information obtained, it can be defined whether a geothermal energy resource exists and if there is a resource, the temperature of the resource and its characteristics can be determined.

REFERENCES

- Akartuna, M. (1962). *İzmir-Torbali-Seferihisar-Urla bölgesinin jeolojisi hakkında*. İstanbul: İstanbul Üniversitesi.
- Al-Shumaimri, M.S. (2012). Application of digital image processing techniques to geological and geomorphological features of southwest Jordan. State of Kuwait: *Journal of Geography and Geology*, 1 (4).
- Arslan, S., & Darıcı, M., & Karahan., Ç. (2001). *Türkiye'nin jeotermal enerji potansiyeli*, MMO/2001/270. İzmir: Teskon Jeotermal Seminer Kitapları, Retrieved November 10, 2012 from http://geocen.iyte.edu.tr/teskon/2001/teskon2001_02.pdf.
- Başel, E.D.K., & Satman, A., & Serpen, Ü. (2009). *Türkiye jeotermal kaynak potansiyeli*, E/2009. İzmir: Teskon Jeotermal Seminer Kitapları, Retrieved November 19, 2012 from <http://geocen.iyte.edu.tr/teskon/2009/2009JEO-02.pdf>.
- Çapar, N. (2009). *Landsat uydu görüntüleri kullanılarak jeotermal kaynakların araştırılması, Ankara örneği*. İstanbul Teknik Üniversitesi Fen Bilimleri Enstitüsü Yüksek Lisans Tezi.
- Dağıstan, H. (2010). *Yenilenebilir enerji ve jeotermal kaynaklarımız*. Ankara: MTA Genel Müdürlüğü Enerji Dairesi Başkanlığı.
- Demirkesen, A.C. (2005). Landsat-5 TM çok bantlı uydu görüntülerinden fayların yorumlanması. *Deprem Sempozyumu*, Kocaeli.
- Devlet Planlama Teşkilatı (2001). *Sekizinci beş yıllık kalkınma planı enerji hammaddeleri alt komisyonu jeotermal enerji grubu raporu*. Ankara.

- Devlet Planlama Teşkilatı (2001). *Sekizinci beş yıllık kalkınma planı harita, tapu kadastro, coğrafi bilgi ve uzaktan algılama sistemleri özel ihtisas komisyonu raporu*. Ankara.
- Devlet Planlama Teşkilatı (2009). *Dokuzuncu kalkınma planı madencilik özel ihtisas komisyonu enerji hammaddeleri çalışma grubu raporu*. Ankara.
- Dickson, M.H., & Fanelli, M. (2004). *What is geothermal energy?*. Italy: Istituto di Geoscienze e Georisorse.
- Doğan, A., & Emre, Ö., & Göktaş, F., & Özaksoy, V., & Özalp, S., & Yıldırım, C. (2005). *İzmir yakın çevresinin diri fayları ve deprem potansiyelleri*, 10754. Ankara: Maden Tetkik ve Arama Genel Müdürlüğü.
- Eastman, J.R. (2012). *IDRISI Selva Manual*. Manual Version 17. USA: Clark University.
- Eastman, J.R. (2012). *IDRISI Selva Tutorial*. Manual Version 17. USA: Clark University.
- Erbay, A.Y. (2005). *Uydu görüntüleri rehber kitapçığı*. İstanbul: Nik İnşaat.
- Eronat, A. H., (1999). *Remote sensing applications for physical and ecological state of Turkish coastal waters*. İzmir: Dokuz Eylül University Graduate School of Natural and Applied Sciences, Phd Thesis.
- Gupta, H., & Roy, S. (2006). *Geothermal Energy an Alternative Resource for the 21st Century*. Netherlands: Elsevier.
- Gupta, R.P., (2003). *Remote sensing geology (2nd ed.)*. Germany: Springer.

Güneş, S.T. (2006). *Jeotermal enerji ve çevre*. İzmir: TMMOB Çevre Mühendisleri Odası.

İşlem Şirketler Grubu (2002). *Uzaktan algılama*. Ankara.

Jeotermal Kaynaklar ve Doğal Mineralli Sular Kanunu (2007). Ankara: Resmi Gazete.

Kalafatçioğlu, A. (1962). *Karaburun yarımadasının jeolojisi*. Ankara: MTA.

Kargı, H. (2004). *Uzaktan algılama*. Denizli: Pamukkale Üniversitesi Jeoloji Mühendisliği Bölümü Ders Notları.

Kavzoğlu, T. (2010). *Uzaktan algılama teknolojisi*. Kocaeli: Gebze Yüksek Teknoloji Enstitüsü, Ders notları.

Koç, A. (2005). Çeşme jeotermal projesi hedefi ve uygulaması, E/2005/393-2. İzmir: *Teskon Jeotermal Enerji Semineri Kitabı*, Retrieved April 18, 2011 from http://geocen.iyte.edu.tr/teskon/2005/teskon2005_24.pdf.

Külekçi, Ö.C., (2009). *Yenilenebilir enerji kaynakları arasında jeotermal enerjinin yeri ve Türkiye açısından önemi*. Ankara: Ankara Üniversitesi Ziraat Fakültesi Peyzaj Mimarlığı Bölümü.

National Aeronautics and Space Administration (2011). *Tour of the electromagnetic spectrum*. Retrieved December 15, 2012 from <http://missionscience.nasa.gov/ems/index.html>.

Özdemir, A. (2010). *Jeotermal enerji ve elektrik üretimi*. Retrieved November 10, 2012 from http://www.adilozdemir.com/dosyalar/1278920580_60.pdf.

Özdemir, A. (2010). Türkiye'nin jeotermal enerji potansiyeli. Retrieved May 15, 2011 from http://www.adilozdemir.com/dosyalar/1308123491_3._SAYI_AD%C2%A6-L_+%C3%BBZDEM%C2%A6-R.pdf.

Pratt, W.K. (2001). *Digital image processing*. New York: Jhon Wiley and Sons, Inc.

Tecim, V. (2008). *Coğrafi bilgi sistemleri harita tabanlı bilgi yönetimi*. Ankara: Renk Form Ofset Matbaacılık.

Toka, B. (2004). *Jeotermal enerji*. Retrieved November 10, 2012, from http://www.maden.org.tr/resimler/ekler/20ad4d76fe97759_ek.pdf?tipi=23&tu ru=X&sube=0.

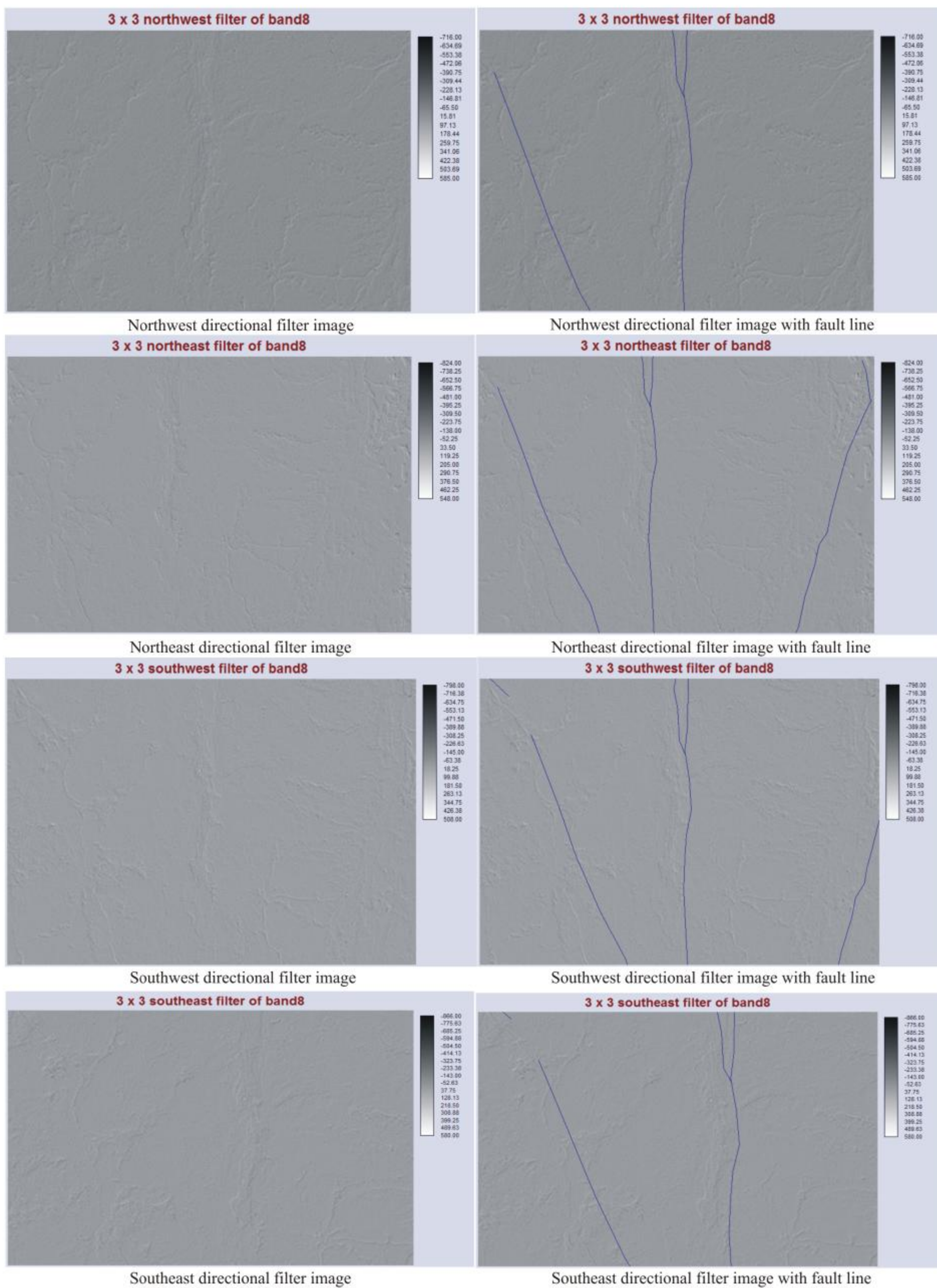
Uysal, K. (2004). *Uzaktan algılamada Landsat MSS ve Spot XS uydu verilerinin kullanımı ile ayrıntılı jeolojik harita alımı ve yorumu; Dereboğazı(Isparta) ve çevresi örneği*. Isparta: Süleyman Demirel Üniversitesi Fen Bilimleri Enstitüsü, Yüksek Lisans Tezi.

Yılmaz, S. (2009). Batı Anadolu'nun olası jeotermal potansiyelinin belirlenmesi. *Türkiye 11. Enerji Kongresi*, İzmir.

Yılmaz, S. (2009). Kentimizde jeotermal enerjinin anlamı ve değerlendirilmesi. *TMMOB Kent Sempozyumu*, İzmir.

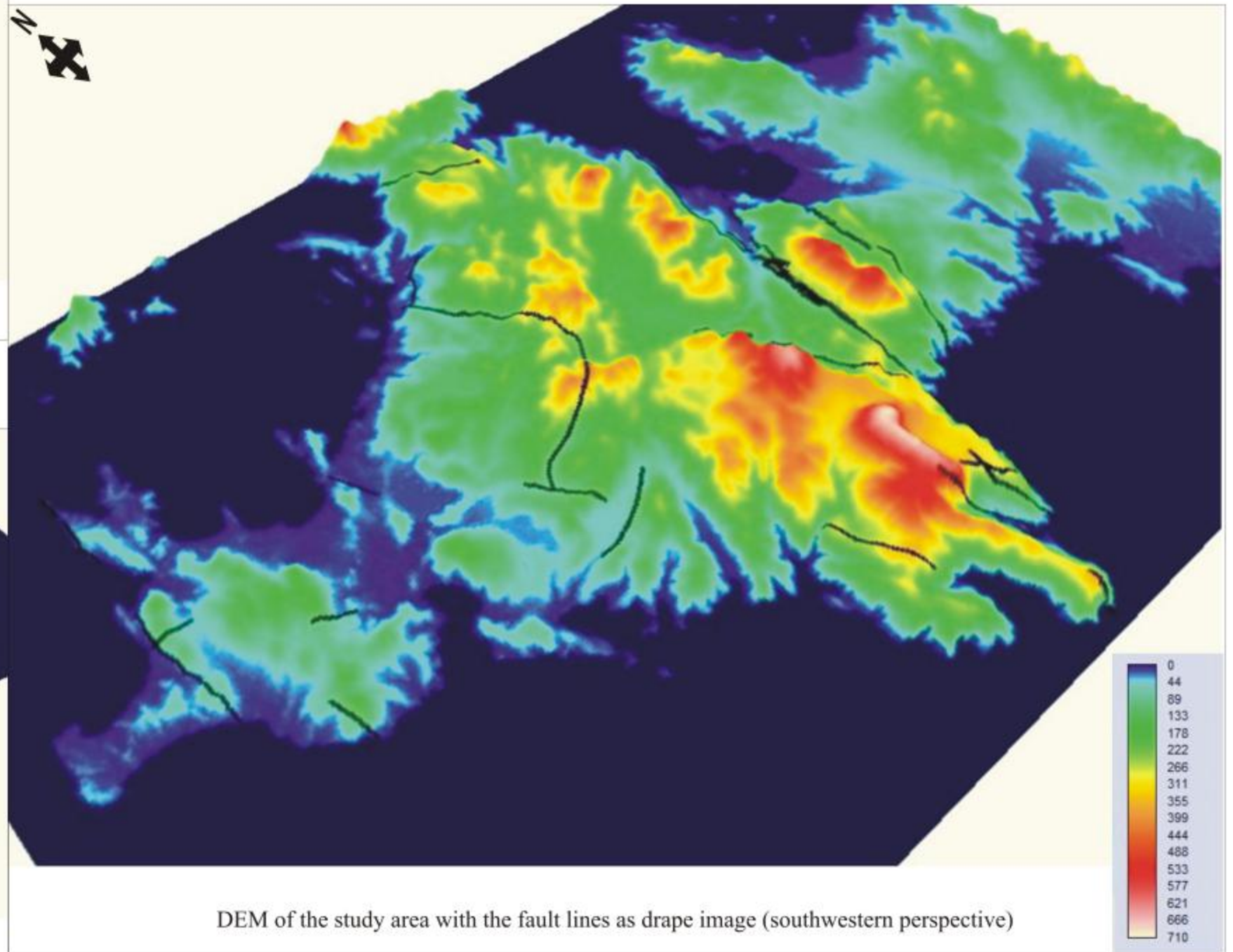
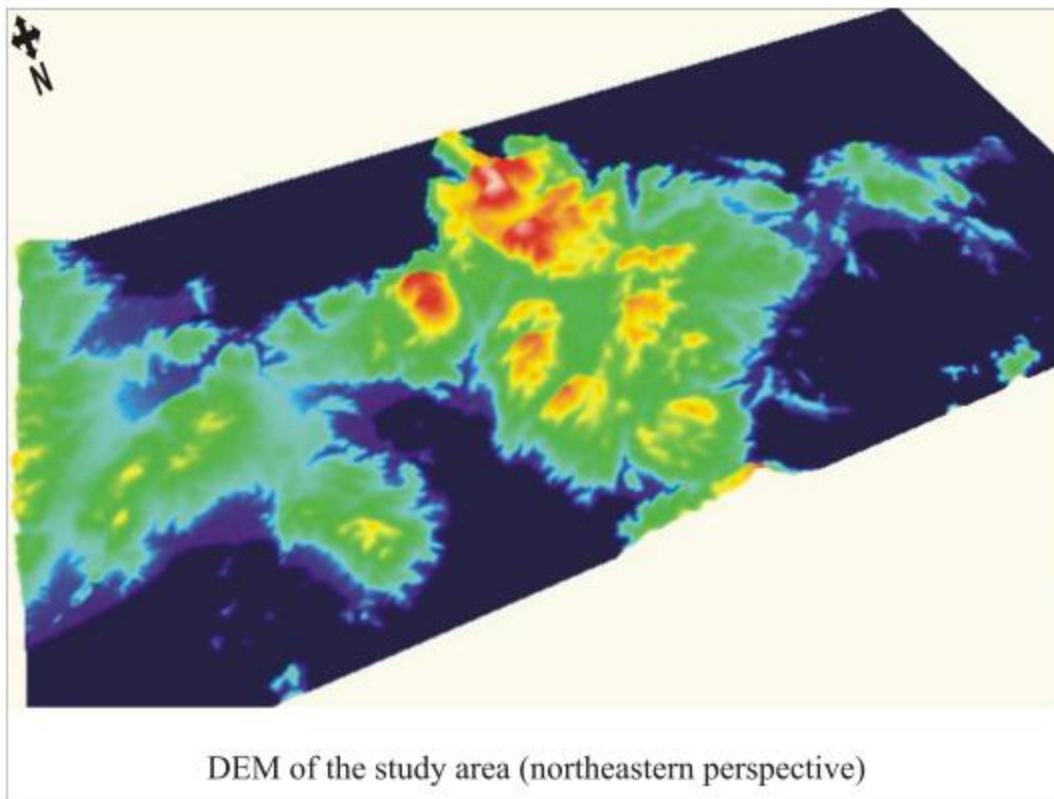
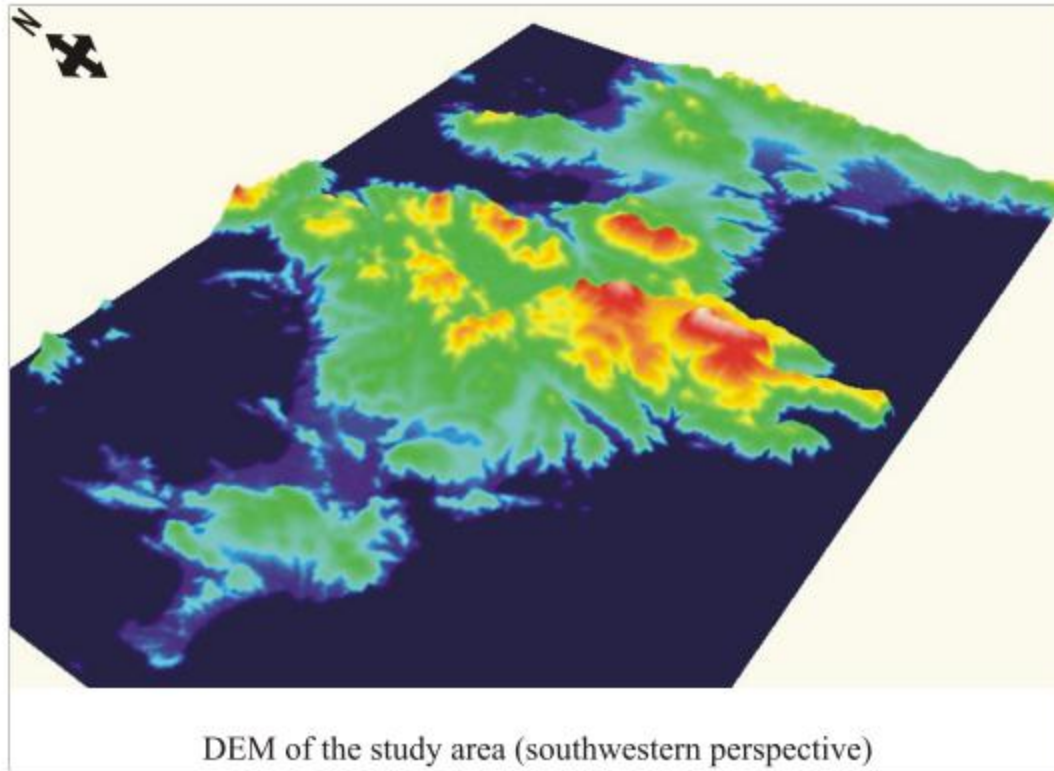
APPENDIX-1

Comparison of the directional filters with the Gülbahçe Fault



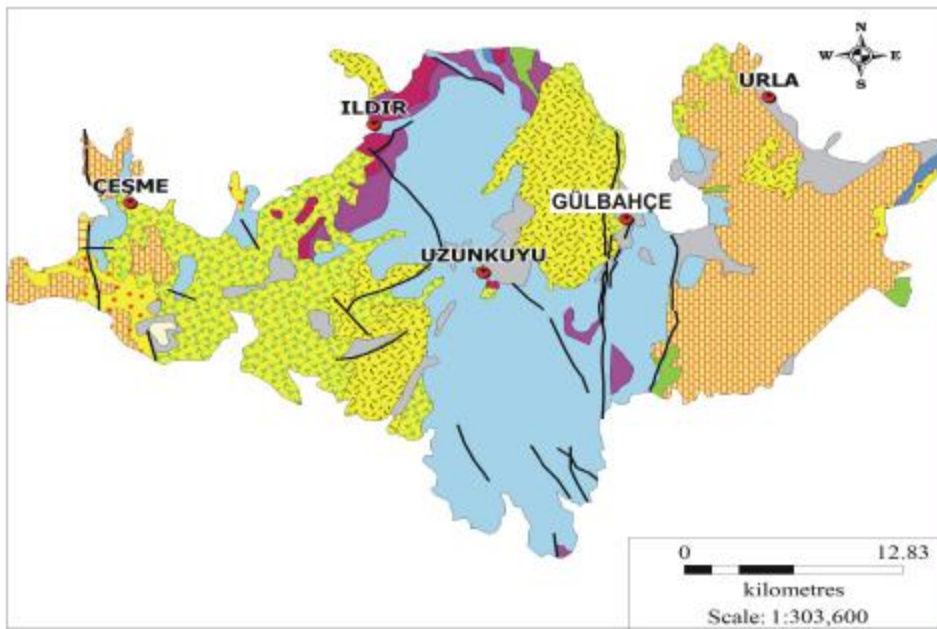
APPENDIX-2

Digital Elevation Model of the study area

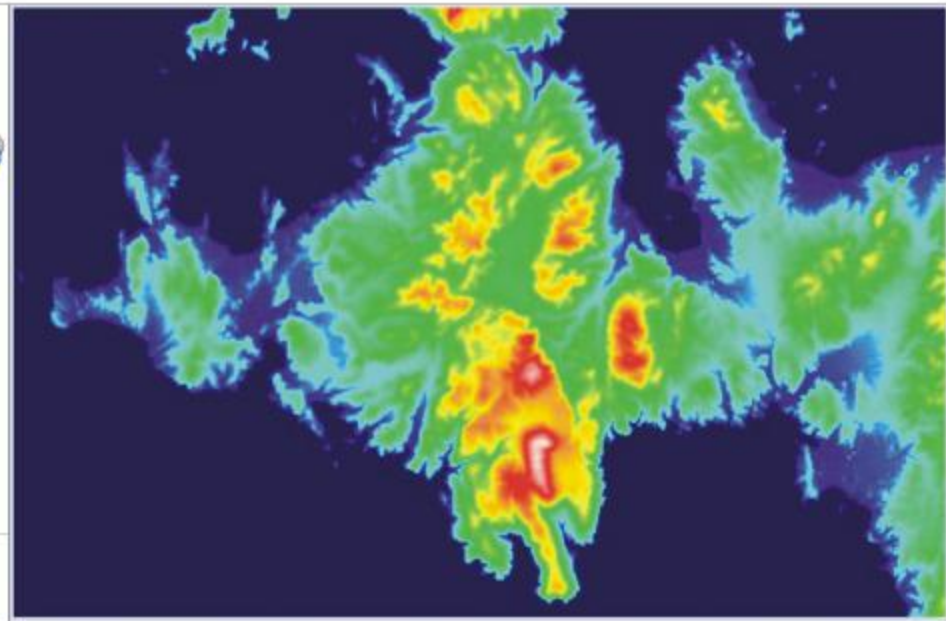


APPENDIX-3

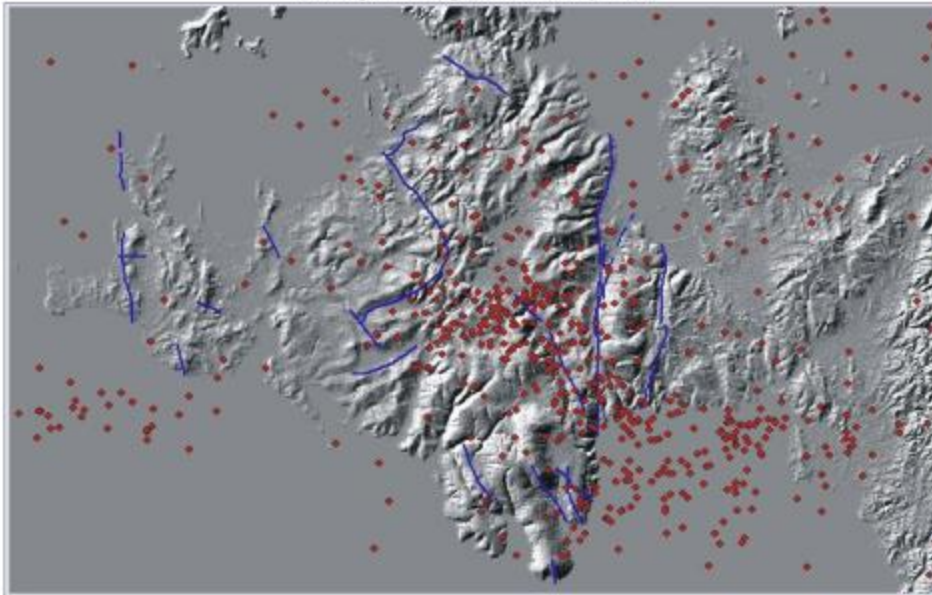
Comparison of geological map of the study area and the obtained Landsat images by image processing techniques



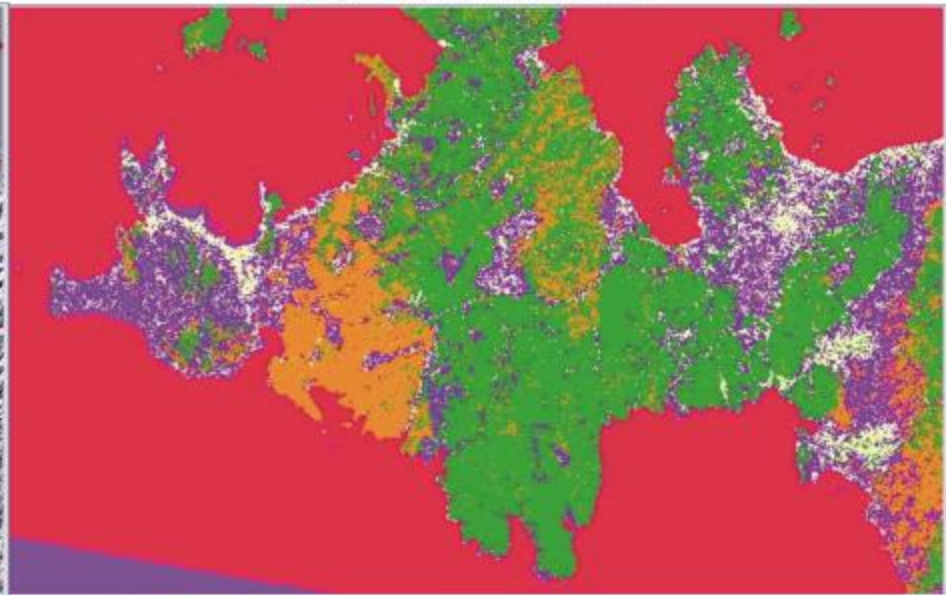
Geological map of the study area



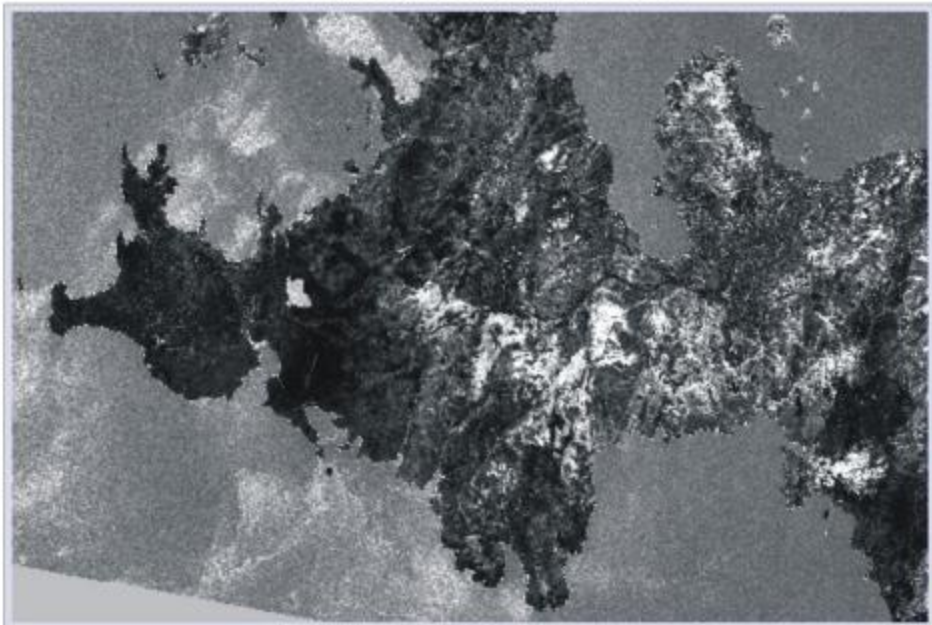
Digital elevation model (DEM)



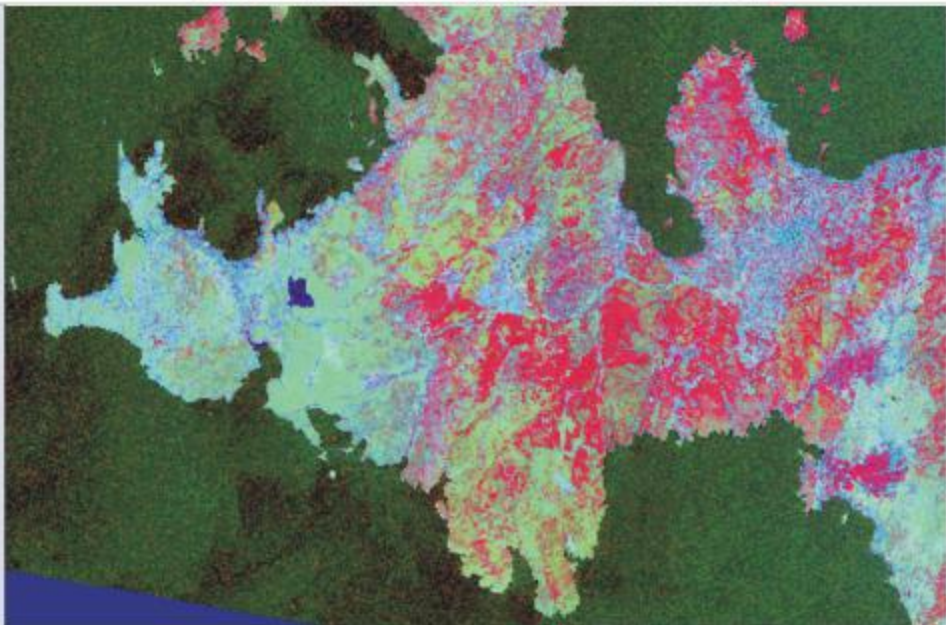
Earthquake epicenters and faults lines



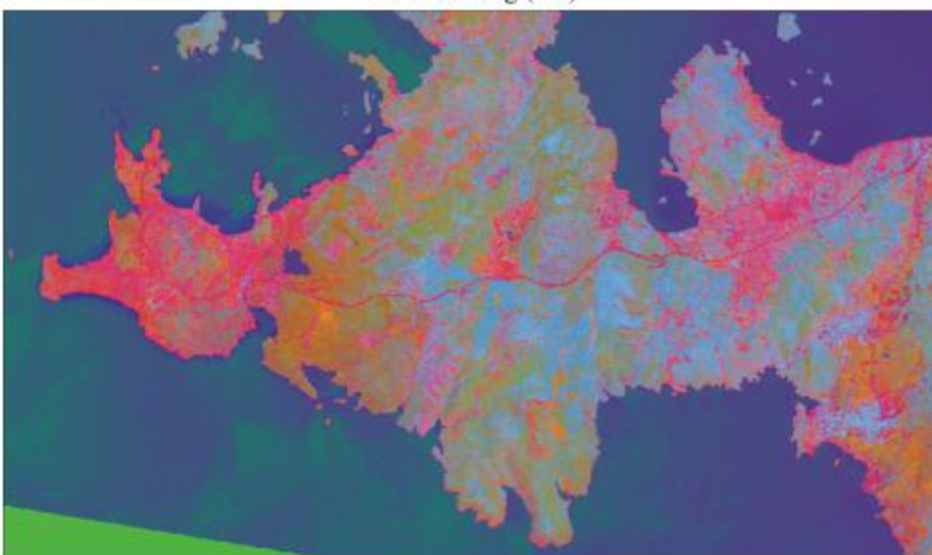
Supervised classification (Max. Likelihood method)



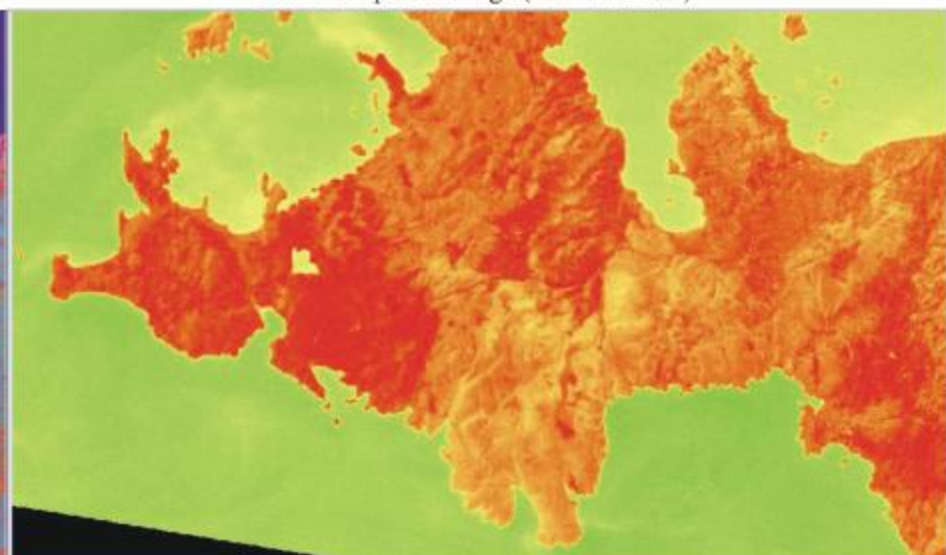
Band ratioing (4/5)



RGB composite image (5/7 - 5/4 - 3/1)



Principal Components Analysis (PCA) RGB image (1 - 2 - 3)



Blackbody temperature map